九州大学学術情報リポジトリ
Kyushu University Institutional Repository

# Estimation of a time-inhomogeneous Ornstein-Uhlenbeck process

ゲトゥート, プラメスティ

https://hdl.handle.net/2324/6787424

出版情報：Kyushu University, 2022, 博士（数理学）, 課程博士
バージョン：
権利関係：

KYUSHU UNIVERSITY

# Estimation of a time-inhomogeneous Ornstein–Uhlenbeck process

Ph.D. thesis

Getut Pramesti

Supervisor: Professor Hiroki Masuda

Graduate School of Mathematics
Kyushu University
January 2023

# Estimation of a time-inhomogeneous Ornstein–Uhlenbeck process

Ph.D. thesis

**Getut Pramesti**
Department of Mathematical Sciences
Faculty of Mathematics
Kyushu University

Thesis advisor: Professor Hiroki Masuda, Kyushu University
Thesis committee:
Professor Shuichi Kawano, Kyushu University
Professor Kei Hirose, Kyushu University
Associate Professor Koji Tsukuda, Kyushu University

# Preface

This Ph.D. thesis contains the result of time-inhomogeneous Gaussian Ornstein–Uhlenbeck regression, undertaken at the Graduate School of Mathematics, Kyushu University, from April 2019. I noticed during these four years that I was stepping outside my comfort zone. However, Ornstein–Uhlenbeck process makes me motivated and challenged to study it more deeply in the future. Periodic time-inhomogeneous Ornstein–Uhlenbeck process can be considered as a potential field for stochastic models of observational series from a wide range of fields since periodicity phenomena are very close to human lives, and we can analyze these phenomena using signal processing models. To be triggered by this periodicity phenomena, this thesis could be a starting point to introduce a periodic time-inhomogeneous Ornstein–Uhlenbeck process using signal processing models which can be used to identify the seasonal behavior of any system in the all-time horizon forecast.

The thesis is structured as follows. The thesis contains a brief introduction in Chapter 1. Chapter 2 contains the notation and model setup. Theoretical results on weak consistency are presented in Chapter 3, followed by the asymptotic properties of the least-square estimators. Chapter 4 confirms our theoretical findings through a simulation study, and also the use of the proposed model in the fitting of electricity load from Tokyo electric power company (TEPCO), the energy use of light fixtures in one Belgium household, France household electric power, and a case study of Tetouan city's power consumption. The summary and future work of the thesis are finally drawn in Chapter 5. An Appendix contains some proofs of our technical discussions.

# Abstract

We address the least-squares estimation of the drift coefficient parameter $\theta = (\lambda, A, B, \delta)$ of a time-inhomogeneous Ornstein–Uhlenbeck process with sinusoidal signal processing. We concentrate on a discrete-time observation scheme, that is, the process is observed at a high-frequency sampling setting, in which the discretized step size $h$ satisfies $h \to 0$.

In this thesis, under the conditions $nh \to \infty$ and $nh^2 \to 0$, we prove the consistency and the asymptotic normality of the estimators. We obtain the convergence of the parameters at rate $\sqrt{nh}$, except for $\delta$ at $\sqrt{n^3h^3}$.

To verify our theoretical findings, we do a simulation study. We then illustrate the use of the proposed model in the fitting of electricity load from Tokyo Electric Power Company (TEPCO), the energy use of light fixtures in one Belgium household, France household electric power, and a case study of Tetouan city's power consumption. In an empirical study, we can show the use of a time-inhomogeneous Ornstein–Uhlenbeck process with periodic sinusoidal signal processing leads to capturing the seasonal variation in very short to medium-term forecasts in electric power and energy systems.

# Acknowledgements

I would like to express my sincere gratitude to my supervisor Professor Hiroki Masuda for his encouragement and numerous valuable suggestions during my study. I can not thank him enough for his infinite patience. Many thanks for your support and belief, in everything you have done for me. Additionally, I would like to express my deepest gratitude to Professor Kei Hirose for his fresh advice and suggestion in my thesis. I would like also to express my appreciation to Professor Shuichi Kawano and Associate Professor Koji Tsukuda for their valuable encouragement and helpful input in creating this thesis.

The financial support of Bantuan Studi Lanjut from Universitas Sebelas Maret (UNS) Indonesia is appreciated. And also LPPM UNS for the grant of the research. Many thanks are due to Cheng Yuzhong and Keith Ho, for the discussion.

Finally, I dedicated this thesis to my family, Ristu and Hamara, also Mapa. My appreciation for their endless support and unconditional love could never be fully expressed in words.

Getut Pramesti

Fukuoka, January 2023

# Contents

# Chapter 1

# Introduction

The Stochastic differential equation (SDE) has a wide range of applications. See, for example, electric power system [El-Hawary, 2017], stock exchange [Heston and Sadka, 2008], agricultural [Ghosh et al., 2018], health [Gutiérrez et al., 2012] and references therein. The mean-reversion model can describe a wide range of behaviors, particularly in electric power systems. The mean-reversion process tends to oscillate around a few mean levels. The Ornstein–Uhlenbeck process is a well-known stochastic process that represents the characteristic of the process to drift towards the mean. Mean-reversion is the term for this phenomenon. The trend, seasonal dynamics and possible irregular effects of time series phenomena are represented by a function of time in the drift in a time-inhomogeneous Ornstein–Uhlenbeck model, see [Pérez Monsalve and Marín Sanchez, 2017] and [Chen et al., 2017] for results about the periodic functional tendency.

Let us consider the SDE

$$dY_t = a(\theta, Y_t, t)dt + \sigma dw_t, \quad t \geq 0, \quad Y_0 = y_0, \tag{1.1}$$

where $\theta \in \Theta$ is a finite-dimensional unknown parameter; $a : \Theta \times \mathbb{R} \times [0,\infty) \to \mathbb{R}$, $\sigma > 0$; $w$ is the standard Wiener process. We assume that

$$a(\theta, Y_t, t) = -\lambda Y_t + h_t(\beta),$$

where $\lambda > 0$, $\theta = (\lambda, \beta)$, and

$$h_t(\beta) = \sum_{k=1}^{K} [A_k \cos(\omega_k t) + B_k \sin(\omega_k t)], \tag{1.2}$$

with $\beta = (A, B, \omega), A = (A_k)_{k=1}^K, B = (B_k)_{k=1}^K, \omega = (\omega_k)_{k=1}^K$, and a fixed $K \in \mathbb{N}$. Moreover, $\lambda$ is known as the rate of reversion and $\frac{h_t(\beta)}{\lambda}$ is a time-inhomogeneous mean reversion level, which is a deterministic function that captures the trend of the process. Note that if $Y_t > \frac{h_t(\beta)}{\lambda}$ then the trend term $a(\theta, Y_t, t) < 0$, which implies $Y_t$, tends to decrease. Conversely, if $a(\theta, Y_t, t) > 0$, then $Y_t$ tends to increase. The time-dependent signal processing function (1.2) can also be decomposed into a form

$$h_t(\beta) = \sum_{k=1}^{K} \sqrt{A_k^2 + B_k^2} \cos(\omega_k t + \vartheta_k), \tag{1.3}$$

for some $k \in \mathbb{N}$,

- $A_k, B_k \in \mathbb{R} \setminus \{0\}$, $\sqrt{A_k^2 + B_k^2}$ is the amplitude of the $k$th sinusoidal signal that represents the maximum values between the horizontal axis and vertical position of the $k$th signal;
- $\vartheta_k$ represents a phase of the $k$th sinusoidal signal, where $\vartheta_k = -\arctan\left(\frac{B_k}{A_k}\right)$;
- $\omega_k \in (0, \infty)$ is an unknown frequency of the $k$th sinusoidal signal.

Since (1.2) is a continuous-time sinusoidal signal, then its periodicity can be modeled by assuming that the $k$th harmonic of the components $\cos(\omega_k t)$ and $\sin(\omega_k t)$ has the same periodicity for

$$\omega_k \equiv 2\pi k \delta, \tag{1.4}$$

for all $k \in \mathbb{N}$ and $\delta > 0$ is the unknown fundamental frequency of $h_t(\beta)$ (See [Oppenheim et al., 1997, Cariolaro, 2011b] for references). Hence, there exists $T > 0$ such that

$$h_t(\beta) = h_{t+T}(\beta). \tag{1.5}$$

From the properties of (1.4) and (1.5), $h_t(\beta)$ ((1.2) or (1.3)) is a continuous-time periodic sinusoidal signal, whereas $T$ is called a fundamental signal's period. Therefore, we recall $\theta$ as

$$\theta := (\lambda, A, B, \delta). \tag{1.6}$$

The sinusoidal processing model can be seen as a random signal, which has been used in analyzing periodic phenomena[Kundu and Nandi, 2012]. A repeating pattern within any fixed period is known as seasonal variation ([Metcalfe and Cowpertwait, 2009]), while a periodicity is a pattern in a time series that occurs at regular time intervals ([Puech et al., 2019]). Hence, the seasonal variation can be used in analyzing seasonal phenomena with $k$th periodic signal.

An observed seasonal time series can be meaningfully divided into several unobserved components, e.g., a seasonal component. The seasonal variation has implications in an economic structure [Plosser, 1978]. [Buonocore et al., 2022] managed the seasonal fluctuation in electricity demand of electrified buildings to be employed renewable energy and seasonal energy storage. The seasonality of coronaviruses from 2012 to 2019 to daily average weather parameters has been compared to show coronavirus infections had a similar distribution to influenza A and bocavirus [Nichols et al., 2021]. A warning against over-interpretation of seasonal signals measured by the Global Navigation Satellite System (GNSS) [Chanard et al., 2020]. Application of seasonal time series model in the precipitation forecast found in [Wang et al., 2013]. The characteristic of the process mentioned in the references that follow to Ornstein–Uhlenbeck process would be interesting for future issues in terms of identifying seasonal variations.

The statistical inference of sinusoidal signals for continuous observation is given (see e.g., [Song and Li, 2011, Kundu, 1997]). For continuously observed diffusion process, see [Gutiérrez et al., 2006, Román-Román et al., 2018, Giorno et al., 2017]. However, for the mentioned models, the sinusoidal signal processing model in a time-inhomogeneous Ornstein–Uhlenbeck process (1.1) observed at high frequency, which motivated our current study, seems to be far from being well-developed especially for the frequency parameter $\delta$. Some of the results of frequency components of diffusion processes are given in [Ibragimov and Hasâ€™minskii, 1981] and [Kundu, 1993]. The anomalous behavior of the angular component has been shown by [Whittle, 1952], that is, the result cannot test for the presence of the harmonic term in the same way as that of most statistical parameters.

In this thesis, we apply least-squares estimation (LSE) for the drift parameters of (1.1) based on discrete time observations, that is, we concentrate on the situation where the diffusion process is observed at discrete times $0 \equiv t_0 < t_1 < \cdots < t_n$, where $t_j^n = t_j = jh$, with $j \leq n$ and for some nonrandom sampling time step $h := h_n$,

$$h \to 0, \tag{1.7}$$

such that for $n \to \infty$,

$$T_n := nh, \quad T_n \to \infty, \tag{1.8}$$

$$nh^2 \to 0. \tag{1.9}$$

Under a high-frequency sampling setting, [Prakasa Rao, 1983] made an important assumption, that is, the rate $nh^2 \to 0$ as the rapidly increasing experimental design in the study of the LSE. Whereas [Yoshida, 1992] assumed $nh^3 \to 0$ in the study of the MLE; [Kessler, 1997] proved that the derived estimator is asymptotic efficient under the rate $nh^p \to 0$ for an arbitrary integer $p$.

The LSE only infers the estimators of the drift, therefore, one can extend the procedure proposed by [Katsamaki and Skiadas, 1995] to estimate the parameters of the diffusion. Further, in the context of the LSE for a model driven by the Wiener process, the estimation of the parameters has been proposed in [Rao and Rubin, 1979] and [Prakasa Rao, 1983]. The literature has mainly concentrated on the estimation of the parameter based on the likelihood approach; see [Billingsley, 2013, Dacunha-Castelle and Florens-Zmirou, 1986, Florens-Zmirou, 1993, Aït-Sahalia, 2002] and references therein.

As far as the author is aware, no results are known regarding the asymptotic property of frequency components of a time-inhomogeneous Ornstein–Uhlenbeck process. Therefore, our aim in this research is to be the first in providing the asymptotic property of frequency components of a time-inhomogeneous Ornstein–Uhlenbeck process under conditions of (1.7)-(1.9) using LSE.

The present research attempts to address, in doing so makes important contributions.

- No previous study to the best of the author's knowledge on the asymptotic property of the frequency components and its impact on life practices. Our study is to provide the theory of an asymptotic property of the frequency components of a time-inhomogeneous

Ornstein–Uhlenbeck process at a high-frequency scheme. The high-frequency sampling scheme has the potential to handle possible non-linear coefficient cases in a unified way. The theoretical considerations would be interesting for future issues.

- We proposed a model of a time-inhomogeneous Ornstein–Uhlenbeck process (1.1).
- Identifying seasonal effects is a critically important aspect of accurately predicting the development of systems. The periodic continuous-time sinusoidal signal processing model (1.2) in the drift of (1.1) can be used in identifying the seasonal variation in very short to medium-term electric power and energy system forecasting problems.

# Chapter 2

# Notation and model setting

## 2.1 Notation

Unless otherwise mentioned, the following basic notation is used in the rest of the paper:

- $\partial_\theta^m$ stands for the $m$th partial differential operator with respect to $\theta$, $\theta = \{\theta_i\}_i$; we write $\partial_\theta := \left\{\frac{\partial}{\partial_{\theta_i}}\right\}_i$, $\partial_\theta^2 := \left\{\frac{\partial^2}{\partial_{\theta_i}\partial_{\theta_l}}\right\}_{i,l}$;
- $a_j(\theta) = a(\theta, Y_{t_j}, t_j)$; $h_j(\beta) = h_{t_j}(\beta)$;
- we abbreviate $\int_{t_{j-1}}^{t_j}$ as $\int_j$;
- $C$ denotes a positive constant independent of $n$; we write $z_n \lesssim s_n$ if there exists $N$ such that for all $n > N$, $z_n \leq C s_n$;
- $\top$ denotes the transpose;
- the symbol $\xrightarrow{p}$ stands for the convergence in $\mathbb{P}_{\theta_0}$ probability, while $\xrightarrow{\mathcal{L}}$ denotes the weak convergence in law under $\mathbb{P}_{\theta_0}$, where $\mathbb{P}_\theta$ denotes the image measure of a solution process $Y$ associated with the parameter value $\theta$ and $\mathbb{P}_{\theta_0}$ denotes the true image measure;
- the notation $\mathbb{I}_K$ is used for the $K \times K$-identity matrix.

## 2.2 Model Setting

Suppose $Y = (Y_t)_{t\in\mathbb{R}_+}$ in (1.1) is a real-valued process that is a solution to the following equation:

$$Y_t = y_0 + \int_0^t \left(-\lambda Y_s + \sum_{k=1}^K [A_k \cos(\omega_k s) + B_k \sin(\omega_k s)]\right) ds + \sigma w_t, \tag{2.1}$$

defined on an underlying complete filtered probability space $(\Omega, \mathcal{F}, (\mathcal{F}_t)_{t\in\mathbb{R}_+}, \mathbb{P})$ with $\mathcal{F}_t = \sigma(w_s : s \leq t)$ such that $\{w_t - w_s\}$ is independent of $\mathcal{F}_s$, where the ingredients involved are as follows:

- $y_0$ is an $\mathcal{F}_0$-measurable real-valued random variable that is independent of the $w = \{w_t\}_{t\in\mathbb{R}_+}$, and fulfills that $\mathbb{E}_0\left[|y_0^2|\right] < \infty$; here and in the sequel, $\mathbb{E}_0$ denotes the expectation operator with respect to $\mathbb{P}_{\theta_0}$;

- $\theta \in \Theta$ (1.6) is an unknown finite-dimensional parameter, where
  - the parameter spaces $\Theta_\lambda \subset (0,\infty)$, $\Theta_A \subset (\mathbb{R}\setminus\{0\})^K$, $\Theta_B \subset (\mathbb{R}\setminus\{0\})^K$, $\Theta_\delta \subset (0,\infty)$ are bounded convex domains,
  - $K$ is assumed to be known,
  - $\Theta := \Theta_\lambda \times \Theta_A \times \Theta_B \times \Theta_\delta$;
- the true parameter value is denoted by $\theta_0 = (\lambda_0, A_0, B_0, \delta_0) \in \Theta$, where $A_0 = (A_{0,k})_{k=1}^K$, $B_0 = (B_{0,k})_{k=1}^K$, and we suppose that $\theta_0 \in \Theta$ does exist.

Due to the drift coefficients, $a_t(\theta)$ with (1.2), the solution of equation (2.1) exists and is unique. Using integration by parts, an explicit expression for the solution of the SDE (2.1) can be obtained as

$$Y_t = e^{-\lambda t} y_0 + \int_0^t e^{-\lambda(t-\tau)} h_\tau(\beta) d\tau + \sigma \int_0^t e^{-\lambda(t-\tau)} dw_\tau. \tag{2.2}$$

Here and for later use, the notation $\mathbb{E}_\theta[.|y_0]$, and $\mathrm{var}_\theta(.|y_0)$ denote the expectation and variance operator under $\mathbb{P}_\theta$ conditional on $y_0$, respectively. Note that, since we have (2.2), then we can find

$$\mathbb{E}_\theta[Y_t|y_0] = e^{-\lambda t} y_0 + \mu_t(\theta), \tag{2.3}$$

where

$$\mu_t(\theta) = \sum_{k=1}^K \left[\frac{\omega_k}{\omega_k^2 + \lambda^2}\right] \left\{ \sin(\omega_k t) \left[\frac{\lambda B_k}{\omega_k} + A_k\right] + \cos(\omega_k t) \left[\frac{\lambda A_k}{\omega_k} - B_k\right] - e^{-\lambda t} \left[\frac{\lambda A_k}{\omega_k} - B_k\right] \right\}. \tag{2.4}$$

Making use of the fact that, for the random variable,

$$\int_0^t e^{\lambda \tau} dw_\tau \sim \mathcal{N}\left(0, \int_0^t e^{2\lambda s} ds\right),$$

we obtain the conditional variance,

$$\mathrm{var}_\theta(Y_t|y_0) = \mathbb{E}_\theta\left[\int_0^t \sigma e^{-\lambda(t-\tau)} dw_\tau\right]^2 = \sigma^2 \mathbb{E}_\theta\left[\int_0^t e^{-2\lambda(t-u)} du\right] = \frac{\sigma^2}{2\lambda}\left(1 - \frac{1}{e^{2\lambda t}}\right). \tag{2.5}$$

Equations (2.3) and (2.5) help to develop the intuition for the process of $Y$. The mean value of the process $[\mathbb{E}_\theta[Y_t|y_0] - \mu_t(\theta)] \to 0$ in the long run, given its value at $y_0$; the variance of the process has a finite limit as $t \to \infty$.

Given (2.2), $Y$ is not stationary. Further, we will look for $\{\tilde{Y}_t, t \in \mathbb{R}\}$ as a stationary solution of (2.2). Following the route of Lemma 4.3 and Lemma 4.4 of [Dehling et al., 2010]; with the periodicity of $h_t(\beta)$ (see (1.2) and (1.4)), for our problem, we derive Lemma 2.1 and Lemma 2.2 (see Appendix A for details).

**Lemma 2.1.** *The sequence of* $\{\tilde{Y}_{s-1+t}\}_{t\in[0,T], s\in\mathbb{N}}$ *is stationary and ergodic, with* $T$ *defined as in* (1.5).

**Lemma 2.2.** *We have*

$$|\tilde{Y}_t - Y_t| \xrightarrow{a.s.} 0, \quad as \quad t \to \infty.$$

It follows from Lemma 2.1 and Lemma 2.2 that, for any continuous real-valued function $\phi(.)$ with polynomial growth that satisfies $\mathbb{E}_0[|\phi(y_0)|] < \infty$,

$$\frac{1}{n}\sum_{j=1}^{n}\phi(Y_{t_j}) \xrightarrow{p} \mathbb{E}_0[\phi(y_0)]. \tag{2.6}$$

Lemma 2.1 is the original finding of this thesis. The difference with one provided in [Dehling et al., 2010] is shown by the sinusoidal signal processing $h_t(\beta)$ in the drift $a_t(\theta)$. Under a high-frequency sampling setting, this signal cause the difficulty in showing the stationarity condition of $\{\tilde{q}_t, t \in \mathbb{R}\}$, i.e., application of the concept of analog/digital (A/D) signal conversion to treat the continuous-time sinusoidal signal processing; application of the periodic continuous-time sinusoidal signal processing.

# Chapter 3

# Theoretical Results

The Euler–Maruyama discretization for the underlying SDE model (2.1) under $\mathbb{P}_\theta$ is given by

$$Y_{t_j} \stackrel{\mathbb{P}_\theta}{=} Y_{t_{j-1}} + \int_j a_s(\theta) ds + \sigma \int_j dw_s \approx Y_{t_{j-1}} + a_{j-1}(\theta) h + \sigma \Delta_j w, \tag{3.1}$$

where

$$a_{j-1}(\theta) = -\lambda Y_{t_{j-1}} + h_{j-1}(\beta) \tag{3.2}$$

and $\Delta_j w$ is the $j$th increment of the Wiener process $w$. Here, we used the notation $\Delta_j \zeta := \zeta_{t_j} - \zeta_{t_{j-1}}$ as the $j$th increment of the process $\zeta$. Then, we have

$$\Delta_j Y \stackrel{\mathbb{P}_{\theta_0}}{=} \int_j a_s(\theta_0) ds + \sigma \Delta_j w \approx a_{j-1}(\theta_0) h + \sigma \Delta_j w, \tag{3.3}$$

and introduce the function

$$\mathbb{Q}_n(\theta) := \sum_{j=1}^{n} \frac{1}{h} [\Delta_j Y - a_{j-1}(\theta) h]^2. \tag{3.4}$$

The LSE of $\theta$ is defined by

$$\hat{\theta}_n \in \underset{\theta \in \overline{\Theta}}{\operatorname{argmin}} \, \mathbb{Q}_n(\theta), \tag{3.5}$$

where $\overline{\Theta}$ denotes the closure of $\Theta$. In the following, we discuss the consistency of the least squares of $(\lambda, A, B)$ and $\delta$ separately.

## 3.1 The consistency of the LSE of $(\lambda, A, B)$

Let us introduce the function

$$f_n(\theta) := \frac{1}{nh} [\mathbb{Q}_n(\theta) - \mathbb{Q}_n(\theta_0)], \tag{3.6}$$

and we will look at the asymptotic behavior of (3.6). Observe that

$$\mathbb{Q}_n(\theta)-\mathbb{Q}_n(\theta_0)=\sum_{j=1}^{n}\frac{1}{h}\left\{\left(\int_j[a_s(\theta_0)-a_{j-1}(\theta)]ds+\sigma\Delta_j w\right)^2-\left(\int_j[a_s(\theta_0)-a_{j-1}(\theta_0)]ds+\sigma\Delta_j w\right)^2\right\}. \tag{3.7}$$

Now, we proceed to the first term of the right-hand side of (3.7). We have

$$\begin{aligned}&\sum_{j=1}^{n}\frac{1}{h}\left(\int_j[a_s(\theta_0)-a_{j-1}(\theta)]ds+\sigma\Delta_j w\right)^2\\ &=\sum_{j=1}^{n}\frac{1}{h}\left\{\left(\int_j[a_s(\theta_0)-a_{j-1}(\theta)]ds\right)^2+2\sigma\int_j\Delta_j w[a_s(\theta_0)-a_{j-1}(\theta)]ds+\sigma^2\Delta_j^2 w\right\}\end{aligned} \tag{3.8}$$

together with the second term of the right-hand side of (3.7) which is can be found similarly to (3.8), we obtain

$$\begin{aligned}\mathbb{Q}_n(\theta)-\mathbb{Q}_n(\theta_0) &= h\sum_{j=1}^{n}[a_{j-1}(\theta_0)-a_{j-1}(\theta)]^2+2\sum_{j=1}^{n}[a_{j-1}(\theta_0)-a_{j-1}(\theta)]\int_j[a_s(\theta_0)-a_{j-1}(\theta_0)]ds\\ &+ 2\sigma\sum_{j=1}^{n}[a_{j-1}(\theta_0)-a_{j-1}(\theta)]\Delta_j w\end{aligned} \tag{3.9}$$

Now, we observe the second term of the right-hand side of (3.9). There exists $C_1>0$ such that

$$\left|\int_j[a_s(\theta_0)-a_{j-1}(\theta_0)]ds\right| \leq C_1\int_j\left|Y_s-Y_{t_{j-1}}\right|ds\lesssim\left(1+|Y_{t_{j-1}}|\right)h^2+\sigma h\Delta_j w. \tag{3.10}$$

To proceed further, we begin with the following Lemmas.

**Lemma 3.1.** *We have*

$$\frac{1}{n}\sum_{j=1}^{n}\sin^2(\omega t_j)=\frac{1}{2}+o\left(\frac{1}{T_n}\right), \tag{3.11}$$

$$\frac{1}{n^2h}\sum_{j=1}^{n}\sin(\omega t_j)\cos(\omega t_j)=o\left(\frac{1}{T_n^2}\right), \tag{3.12}$$

$$\frac{1}{n^2h}\sum_{j=1}^{n}\cos(\omega t_j)\cos(\omega_0 t_j)=o\left(\frac{1}{T_n^2}\right),\quad \omega\neq\omega_0. \tag{3.13}$$

*Proof.* To provide the proof, we use a quantization scheme to process a continuous-time sinusoidal signal into a sequence of numbers. Quantization is the process of converting a continuous-time signal by expressing each sample value as a finite (instead of an infinite) number of digits ([Proakis, 2001]). Observe that

$$\sum_{j=1}^{n}\sin^2(\omega t_j)=\sum_{j=1}^{n}\frac{1}{2}[1-\cos(2\omega t_j)]=\frac{n}{2}-\frac{1}{2}\sum_{j=1}^{n}\cos(2\omega t_j). \tag{3.14}$$

We observe the second term of the right-hand side of (3.14). Let us denote $2\omega=\nu$,

$$\begin{aligned}\sum_{j=1}^{n}\cos(\nu t_j) &= \cos(\nu h)+\cos(\nu h+\nu h)+\cos(\nu h+2\nu h)+\cdots+\cos(\nu h+\nu nh-\nu h)\\ &= \frac{1}{2}\left\{\frac{\sin\left(n\nu h+\frac{1}{2}\nu h\right)}{\sin\left(\frac{\nu h}{2}\right)}-1\right\}=-\frac{1}{2}+\frac{\sin\left(\nu h[n+\frac{1}{2}]\right)}{2\sin\left(\frac{\nu h}{2}\right)}. \end{aligned} \tag{3.15}$$

Plugging the result of (3.15) to (3.14), we get (3.11). The result is true for the cosine function. We will prove (3.12) next,

$$\frac{h}{2T_n^2}\sum_{j=1}^{n}\sin(2\omega t_j)=\frac{h}{T_n^2}\sum_{j=1}^{n}\sin(\omega t_j)\cos(\omega t_j), \tag{3.16}$$

then

$$\sum_{j=1}^{n}\sin(\nu t_j) = \frac{\sin\left(\nu h+(\frac{n-1}{2})\nu h\right)\sin\left(\frac{n\nu h}{2}\right)}{\frac{\sin(\nu h)}{2}}=\frac{1}{2}\left\{\frac{\cos\left(\frac{\nu h}{2}\right)-\cos\left(n\nu h+\frac{\nu h}{2}\right)}{\sin\left(\frac{\nu h}{2}\right)}\right\}. \tag{3.17}$$

Plugging (3.17) to (3.16), we obtain (3.12). We turn to (3.13).

$$\begin{aligned}\frac{1}{n}\sum_{j=1}^{n}\cos(\omega t_j)\cos(\omega_0 t_j) &= \frac{1}{n}\frac{1}{2}\sum_{j=1}^{n}[\cos([\omega-\omega_0]t_j)+\cos([\omega+\omega_0]t_j)]\\ &= \frac{1}{2}\left\{-\frac{1}{2n}+\frac{\sin\left([\omega-\omega_0]h[n+\frac{1}{2}]\right)}{2n\sin\left(\frac{[\omega-\omega_0]h}{2}\right)}\right\}+\frac{1}{2}\left\{-\frac{1}{2n}+\frac{\sin\left([\omega+\omega_0]h[n+\frac{1}{2}]\right)}{2n\sin\left(\frac{[\omega+\omega_0]h}{2}\right)}\right\}\\ &= -\frac{1}{2n}+\frac{\sin\left([\omega-\omega_0]h[n+\frac{1}{2}]\right)}{4n\sin\left(\frac{[\omega-\omega_0]h}{2}\right)}+\frac{\sin\left([\omega+\omega_0]h[n+\frac{1}{2}]\right)}{4n\sin\left(\frac{[\omega+\omega_0]h}{2}\right)}=o\left(\frac{1}{T_n}\right),\end{aligned}$$

and this implies (3.13). The result is also true for the sine function. □

**Corollary 3.2.** *For $m\in\mathbb{N}_0$,*

$$\frac{h}{T_n^{m+2}}\sum_{j=1}^{n}t_j^m\cos(\omega t_j)=o\left(\frac{1}{T_n^2}\right), \tag{3.18}$$

$$\frac{h}{T_n^{m+2}}\sum_{j=1}^{n}t_j^m\sin(\omega t_j)\cos(\omega t_j)=o\left(\frac{1}{T_n^2}\right), \tag{3.19}$$

$$\frac{h}{T_n^{m+2}}\sum_{j=1}^{n}t_j^m\cos(\omega t_j)\cos(\omega_0 t_j)=o\left(\frac{1}{T_n^2}\right), \tag{3.20}$$

*Proof.* We will prove (3.18) using mathematical induction. For $m\in\mathbb{N}_0$,

$$\frac{h}{T_n^{m+2}}\sum_{j=1}^{n}t_j^m\cos(\omega t_j)=o\left(\frac{1}{T_n^2}\right).$$

The statement $P_0$ says that

$$\frac{h}{T_n^2}\sum_{j=1}^{n}\cos(\omega t_j)=o\left(\frac{1}{T_n^2}\right),$$

is true by Lemma 3.1, that is,

$$\frac{h}{T_n^2}\sum_{j=1}^{n}\cos(\omega t_j)=\frac{h}{nh^2}\frac{1}{n}\sum_{j=1}^{n}\cos(\omega t_j)=o\left(\frac{1}{T_n^2}\right).$$

Now, suppose that $P_L$ holds for $L\in\mathbb{N}_0$, that is,

$$\frac{h}{T_n^{L+2}}\sum_{j=1}^{n}t_j^L\cos(\omega t_j)=o\left(\frac{1}{T_n^2}\right). \tag{3.21}$$

Since (3.21) then $\left|\frac{h}{T_n^{(L+1)+2}}\sum_{j=1}^{n}t_j^{L+1}\cos(\omega t_j)\right|\to 0$. This result implies the truth of (3.18). Similar way on the proof of (3.19) and (3.20).

$\square$

**Lemma 3.3.** *We have*

$$\sup_{\omega}\left|\frac{1}{n}\sum_{j=1}^{n}Y_{t_j}\cos(\omega t_j)\right|\xrightarrow{p}0 \quad as \quad n\to\infty.$$

*Proof.* Observe that

$$\begin{aligned}\mathbb{E}_0\left[\sup_{\omega}\left|\frac{1}{n}\sum_{j=1}^{n}Y_{t_j}\cos(\omega t_j)\right|\right] &\leq \frac{1}{n}\left\{\mathbb{E}_0\left[\sup_{\omega}\left|\sum_{j=1}^{n}Y_{t_j}e^{i\omega t_j}\right|^2\right]\right\}^{\frac{1}{2}}\\ &= \frac{1}{n}\left\{\mathbb{E}_0\left[\sum_{j=1}^{n}Y_{t_j}^2+2\left(\sum_{j=1}^{n-1}Y_{t_j}Y_{t_{j+1}}+\sum_{j=1}^{n-2}Y_{t_j}Y_{t_{j+2}}+\cdots+\sum_{j=1}^{n-r}Y_{t_j}Y_{t_{j+r}}\right)\right]\right\}^{\frac{1}{2}}.\end{aligned}$$

By Lemma 2.1 and Lemma 2.2, there exists $\vartheta(Y_{t_j})=Y_{t_j}Y_{t_{j+r}}$ satisfying $\mathbb{E}_0[|\vartheta(y_0)|]<\infty$, such that, for $r$ an arbitrary element of $\mathbb{N}$ with $r<n$,

$$\frac{1}{n-r}\sum_{j=1}^{n-r}\vartheta(Y_{t_j})\xrightarrow{p}\mathbb{E}_0[\vartheta(y_0)].$$

Hence

$$\mathbb{E}_0\left[\sup_{\omega}\left|\frac{1}{n}\sum_{j=1}^{n}Y_{t_j}\cos(\omega t_j)\right|\right]\leq\frac{1}{n}\left\{O(\max(n,n-1,n-2,\ldots,n-r))\right\}^{\frac{1}{2}}=O\left(\frac{1}{\sqrt{n}}\right).$$

The result above is true for the sine function. $\square$

**Lemma 3.4.** *For* $l=1,2,\ldots,$

$$\sup_{\omega}\left|\frac{1}{n}\sum_{j=1}^{n}Y_{t_j}^{l}\cos(\omega t_j)\right|\xrightarrow{p}0 \quad as \quad n\to\infty.$$

Lemma 3.4 also holds with a proof similar to the one of Lemma 3.3.

**Corollary 3.5.** *For $l=1,2,...$ and $m\in\mathbb{N}_0$,*

$$\sup_{\omega}\left|\frac{h}{T_n^{m+1}}\sum_{j=1}^{n}Y_{t_j}^{l}t_j^{m}\cos(\omega t_j)\right|\xrightarrow{p}0 \quad as \quad n\to\infty, \quad T_n\to\infty, \quad h\to 0.$$

*Proof.* We will prove

$$\sup_{\omega}\left|\frac{h}{T_n^{m+1}}\sum_{j=1}^{n}Y_{t_j}^{l}t_j^{m}\cos(\omega t_j)\right|\xrightarrow{p}0,$$

using mathematical induction. For $m\in\mathbb{N}_0$, the statement $P_0$ says that

$$\sup_{\omega}\left|\frac{h}{T_n}\sum_{j=1}^{n}Y_{t_j}^{l}\cos(\omega t_j)\right|\xrightarrow{p}0,$$

is true by Lemma 3.4. Now, suppose that $P_L$ holds, that is,

$$\sup_{\omega}\left|\frac{h}{T_n^{L+1}}\sum_{j=1}^{n}Y_{t_j}^{l}t_j^{L}\cos(\omega t_j)\right|\xrightarrow{p}0, \tag{3.22}$$

with $L\in\mathbb{N}_0$. It remains to show that $P_{L+1}$ holds, that is,

$$\sup_{\omega}\left|\frac{h}{T_n^{(L+1)+1}}\sum_{j=1}^{n}Y_{t_j}^{l}t_j^{L+1}\cos(\omega t_j)\right|\xrightarrow{p}0.$$

Using (3.22) we have

$$\mathbb{E}_0\left[\sup_{\omega}\left|\frac{h}{T_n^{(L+1)+1}}\sum_{j=1}^{n}Y_{t_j}^{l}t_j^{L+1}\cos(\omega t_j)\right|\right] \quad \leq \quad O\Big(\max\Big(\frac{1}{\sqrt{n}},\frac{1}{n\sqrt{n}}\Big)\Big).$$

The result above is true for the sine function. □

**Lemma 3.6.** *We have*

$$\left|\frac{1}{T_n}\sum_{j=1}^{n}Y_{t_{j-1}}\Delta_j w\right|\xrightarrow{p}0 \quad as \quad T_n\to\infty.$$

*Proof.* Observe that

$$\mathbb{E}_0\left[\left|\frac{1}{T_n}\sum_{j=1}^{n}Y_{t_{j-1}}\Delta_j w\right|\right]$$

$$\leq \frac{1}{T_n}\left\{\mathbb{E}_0\left[\sum_{j=1}^{n} Y_{t_{j-1}}^2 \Delta_j^2 w + 2\left(\sum_{j=1}^{n-1} Y_{t_j}\Delta_{j+1} w Y_{t_{j-1}}\Delta_j w + \cdots + \sum_{j=1}^{n-r} Y_{t_{j+r-1}}\Delta_{j+r} w Y_{t_{j-1}}\Delta_j w\right)\right]\right\}^{\frac{1}{2}},$$

where $r$ is an arbitrary element of $\mathbb{N}$ with $r<n$. It follows that

$$\mathbb{E}_0\left[\left|\frac{1}{T_n}\sum_{j=1}^{n} Y_{t_{j-1}}\Delta_j w\right|\right] \leq O\left(\frac{1}{\sqrt{T_n}}\right).$$

□

**Lemma 3.7.** *For $l=1,2,\ldots,$*

$$\left|\frac{1}{T_n}\sum_{j=1}^{n} Y_{t_{j-1}}^{l}\Delta_j w\right| \xrightarrow{p} 0 \quad as \quad T_n \to \infty.$$

The proof of Lemma 3.7 can be provided similarly to the proof of Lemma 3.6.

**Lemma 3.8.** *We have*

$$\sup_{\omega}\left|\frac{1}{T_n}\sum_{j=1}^{n}\cos(\omega t_{j-1})\Delta_j w\right| \xrightarrow{p} 0 \quad as \quad T_n \to \infty.$$

*Proof.* Observe that

$$\begin{aligned}
&\mathbb{E}_0\left[\sup_{\omega}\left|\frac{1}{T_n}\sum_{j=1}^{n}\cos(\omega t_{j-1})\Delta_j w\right|\right]\\
&\leq \frac{1}{T_n}\left\{\mathbb{E}_0\left[\sup_{\omega}\left|\sum_{j=1}^{n} e^{i\omega t_{j-1}}\Delta_j w\right|^2\right]\right\}^{\frac{1}{2}}\\
&= \frac{1}{T_n}\left\{\mathbb{E}_0\left[\sum_{j=1}^{n}\Delta_j^2 w + 2\left(\sum_{j=1}^{n-1}\Delta_j w\Delta_{j+1} w + \sum_{j=1}^{n-2}\Delta_j w\Delta_{j+2} w + \cdots + \sum_{j=1}^{n-r}\Delta_j w\Delta_{j+r} w\right)\right]\right\}^{\frac{1}{2}},
\end{aligned}$$

where $r$ is an arbitrary element of $\mathbb{N}$ with $r<n$. Therefore

$$\mathbb{E}_0\left[\sup_{\omega}\left|\frac{1}{T_n}\sum_{j=1}^{n}\cos(\omega t_{j-1})\Delta_j w\right|\right] \leq o\left(\frac{1}{\sqrt{T_n}}\right).$$

The result is true for the sine function.

□

**Corollary 3.9.** *For $m \in \mathbb{N}_0$,*

$$\sup_{\omega}\left|\frac{1}{T_n^{m+1}}\sum_{j=1}^{n} t_{j-1}^{m}\cos(\omega t_{j-1})\Delta_j w\right| \xrightarrow{p} 0 \quad as \quad T_n \to \infty.$$

*Proof.* We provide the proof of Corollary 3.9 in a similar way to the proof of Corollary 3.5.

The statement $P_0$ says that

$$\sup_{\omega}\left|\frac{1}{T_n}\sum_{j=1}^{n}\cos(\omega t_{j-1})\Delta_j w\right|\xrightarrow{p}0,$$

is true by Lemma 3.8. Now, suppose that $P_L$ holds, that is,

$$\sup_{\omega}\left|\frac{1}{T_n^{L+1}}\sum_{j=1}^{n}t_{j-1}^{L}\cos(\omega t_{j-1})\Delta_j w\right|\xrightarrow{p}0, \tag{3.23}$$

with $L\in\mathbb{N}_0$. It remains to show that $P_{L+1}$ holds. By (3.23) we find that

$$\mathbb{E}_0\left[\sup_{\omega}\left|\frac{1}{T_n^{(L+1)+1}}\sum_{j=1}^{n}t_{j-1}^{L+1}\cos(\omega t_{j-1})\Delta_j w\right|\right] \leq O\left(\max\left(\frac{1}{\sqrt{T_n}},\frac{1}{n\sqrt{T_n}}\right)\right).$$

The result above is true for the sine function. □

**Lemma 3.10.** *For* $l=1,2,\ldots,$

$$\sup_{\omega}\left|\frac{1}{T_n}\sum_{j=1}^{n}Y_{t_{j-1}}^{l}\Delta_j w\cos(\omega t_{j-1})\right|\xrightarrow{p}0 \quad \textit{as} \quad T_n\to\infty.$$

*Proof.* Observe that

$$\begin{aligned}
&\frac{1}{T_n}\mathbb{E}_0\left[\sup_{\omega}\left|\sum_{j=1}^{n}Y_{t_{j-1}}^{l}\cos(\omega t_{j-1})\Delta_j w\right|\right]\\
&\leq\frac{1}{T_n}\left\{\mathbb{E}_0\left[\sup_{\omega}\left|\sum_{j=1}^{n}Y_{t_{j-1}}^{l}e^{i\omega t_{j-1}}\Delta_j w\right|^2\right]\right\}^{\frac{1}{2}}\\
&=\frac{1}{T_n}\left\{\mathbb{E}_0\left[\sum_{j=1}^{n}Y_{t_{j-1}}^{2l}\Delta_j^2 w+2\left(\sum_{j=1}^{n-1}Y_{t_j}^{l}\Delta_{j+1}wY_{t_{j-1}}^{l}\Delta_j w+\cdots+\sum_{j=1}^{n-r}Y_{t_{j+r-1}}^{l}\Delta_{j+r}wY_{t_{j-1}}^{l}\Delta_j w\right)\right]\right\}^{\frac{1}{2}}\\
&=O\left(\frac{1}{\sqrt{T_n}}\right),
\end{aligned}$$

where $r$ is an arbitrary element of $\mathbb{N}$ with $r<n$. The result is true for the sine function. □

Putting (3.10) to (3.9). Since $\mathbb{E}_0[|g(y_0)|]<\infty$,

$$\frac{1}{n}\sum_{j=1}^{n}g(Y_{t_j})(1+|Y_{t_j}|)\xrightarrow{p}\mathbb{E}_0[g(y_0)(1+|y_0|)],$$

and by applying Lemma 3.6, then, we can write expression (3.6) as

$$f_n(\theta)=\frac{1}{n}\sum_{j=1}^{n}[a_{j-1}(\theta_0)-a_{j-1}(\theta)]^2+\frac{2\sigma}{nh}\sum_{j=1}^{n}[a_{j-1}(\theta_0)-a_{j-1}(\theta)]\Delta_j w+o_p(h). \tag{3.24}$$

Recall (3.2),

$$\begin{aligned}&\frac{1}{n}\sum_{j=1}^{n}[a_{j-1}(\theta_0)-a_{j-1}(\theta)]^2\\&=(\lambda-\lambda_0)^2\frac{1}{n}\sum_{j=1}^{n}Y_{t_{j-1}}^2+2(\lambda-\lambda_0)\frac{1}{n}\sum_{j=1}^{n}Y_{t_{j-1}}[h_{j-1}(\beta_0)-h_{j-1}(\beta)]+\frac{1}{n}\sum_{j=1}^{n}[h_{j-1}(\beta_0)-h_{j-1}(\beta)]^2.\end{aligned} \tag{3.25}$$

By applying Lemma 3.3 to the second term of the right-hand side of (3.25), then

$$\begin{aligned}\frac{1}{n}\sum_{j=1}^{n}[a_{j-1}(\theta_0)-a_{j-1}(\theta)]^2 &= (\lambda-\lambda_0)^2\frac{1}{n}\sum_{j=1}^{n}Y_{t_{j-1}}^2+\frac{1}{n}\sum_{j=1}^{n}\sum_{k=1}^{K}\Big\{[A_{0,k}\cos(\omega_k t_{j-1})-A_k\cos(\omega_k t_{j-1})]^2\\&+ [B_{0,k}\sin(\omega_k t_{j-1})-B_k\sin(\omega_k t_{j-1})]^2\Big\}+o_p\Big(\frac{1}{\sqrt{n}}\Big)+o_p\Big(\frac{1}{T_n}\Big).\end{aligned} \tag{3.26}$$

We will observe the second term of the right-hand side of (3.26), for the term of cosine. Using Lemma 3.1,

$$\frac{1}{2}\sum_{k=1}^{K}\{(A_{0,k}-A_k)^2+2A_{0,k}A_k\}\frac{1}{n}\sum_{j=1}^{n}[\cos(\omega_k t_j)-\cos(\omega_{0,k}t_j)]^2=\frac{1}{2}\sum_{k=1}^{K}(A_{0,k}-A_k)^2+\sum_{k=1}^{K}A_{0,k}A_k+o\Big(\frac{1}{T_n}\Big), \tag{3.27}$$

and

$$\sum_{k=1}^{K}(A_{0,k}-A_k)^2\frac{1}{n}\sum_{j=1}^{n}\cos^2([\omega_{0,k}-\omega_k]t_j)=\frac{1}{2}\sum_{k=1}^{K}(A_{0,k}^2+A_k^2)-\sum_{k=1}^{K}A_{0,k}A_k+o\Big(\frac{1}{T_n}\Big). \tag{3.28}$$

The expression of sine can be found similarly to (3.27) and (3.28). Further, from (3.24), (3.26)-(3.28), and by using Lemma 3.6, and Lemma 3.8, we have

$$f_n(\theta)=\sum_{j=1}^{n}\Big\{v_{1,j}^n(\theta)+v_{2,j}^n(\theta)\Big\}+q^K(A,B)+o_p\Big(\frac{1}{T_n}\Big)+o_p(h), \tag{3.29}$$

where

$$v_{1,j}^n(\theta)=\frac{1}{n}(\lambda-\lambda_0)^2Y_{t_{j-1}}^2, \tag{3.30}$$

$$v_{2,j}^n(\theta)=\frac{2\sigma}{T_n}\Big\{(\lambda-\lambda_0)Y_{t_{j-1}}+q_j(\beta)\Big\}\Delta_j w, \tag{3.31}$$

$$q_j(\beta)=h_{j-1}(\beta_0)-h_{j-1}(\beta), \tag{3.32}$$

$$q^K(A,B)=\frac{1}{2}\sum_{k=1}^{K}\Big[(A_k-A_{0,k})^2+(B_k-B_{0,k})^2\Big]. \tag{3.33}$$

Next, we will show the consistency of the estimates. The consistency follows on showing that there exists $f_0(\theta)$ such that

$$\sup_{\theta\in\Theta}|f_n(\theta)-f_0(\theta)|\xrightarrow{p}0 \quad as \quad n\to\infty. \tag{3.34}$$

Let the notation $\mathbb{E}_0^{j-1}$ denotes the expectation operator under $\mathbb{P}_{\theta_0}$ conditional on $\mathcal{F}_{t_{j-1}}$. Applying Lemma 9 of [Genon-Catalot and Jacod, 1993], first of all, we will compute for $\sum_{j=1}^{n}\mathbb{E}_0^{j-1}\Big[v_{1,j}^n(\theta)+v_{2,j}^n(\theta)\Big]$. Note the following observations.

- Recalling (3.30), we have

$$\sum_{j=1}^{n}\mathbb{E}_0^{j-1}\Big[v_{1,j}^n(\theta)\Big]=(\lambda-\lambda_0)^2\frac{1}{n}\sum_{j=1}^{n}Y_{t_{j-1}}^2.$$

Since $\mathbb{E}_0[|y_0^2|]<\infty$,

$$\frac{1}{n}\sum_{j=1}^{n}Y_{t_j}^2\xrightarrow{p}\mathbb{E}_0\Big[y_0^2\Big], \tag{3.35}$$

where

$$\mathbb{E}_0\Big[y_0^2\Big]=C, \tag{3.36}$$

and then

$$\sum_{j=1}^{n}\mathbb{E}_0^{j-1}\Big[v_{1,j}^n(\theta)\Big]\xrightarrow{p}(\lambda-\lambda_0)^2C. \tag{3.37}$$

- We can obtain

$$\sum_{j=1}^{n}\mathbb{E}_0^{j-1}\Big[v_{2,j}^n(\theta)\Big]\xrightarrow{p}0. \tag{3.38}$$

Next, it is easy to show $\sum_{j=1}^{n}\mathbb{E}_0^{j-1}\Big[\Big(v_{1,j}^n(\theta)+v_{2,j}^n(\theta)\Big)^2\Big]\xrightarrow{p}0$: indeed,

$$\begin{aligned}\sum_{j=1}^{n}\mathbb{E}_0^{j-1}\Big[\Big(v_{1,j}^n(\theta)+v_{2,j}^n(\theta)\Big)^2\Big] &= \sum_{j=1}^{n}\mathbb{E}_0^{j-1}\Bigg[\Bigg((\lambda-\lambda_0)^2\frac{1}{n}Y_{t_{j-1}}^2+\frac{2\sigma}{T_n}\Big\{(\lambda-\lambda_0)Y_{t_{j-1}}+q_j(\beta)\Big\}\Delta_j w\Bigg)^2\Bigg]\\ &= \sum_{j=1}^{n}\mathbb{E}_0^{j-1}\Big[u_{1,j}^n+u_{2,j}^n+u_{3,j}^n\Big],\end{aligned}$$

where

$$u_{1,j}^n=(\lambda-\lambda_0)^4\frac{Y_{t_{j-1}}^4}{n^2}, \tag{3.39}$$

$$u_{2,j}^n=\frac{4\sigma^2}{T_n^2}\Big\{(\lambda-\lambda_0)Y_{t_{j-1}}+q_j(\beta)\Big\}^2\Delta_j^2 w, \tag{3.40}$$

$$u_{3,j}^n = \frac{4\sigma(\lambda-\lambda_0)^2}{n^2 h} Y_{t_{j-1}}^2 \Big\{ (\lambda-\lambda_0) Y_{t_{j-1}} + q_j(\beta) \Big\} \Delta_j w. \tag{3.41}$$

We observe (3.39) first. It follows that

$$\sum_{j=1}^n \mathbb{E}_0^{j-1} \Big[ u_{1,j}^n \Big] = \frac{(\lambda-\lambda_0)^4}{n} \frac{1}{n} \sum_{j=1}^n Y_{t_{j-1}}^4,$$

and $\mathbb{E}_0 [|y_0^4|] < \infty$,

$$\frac{1}{n} \sum_{j=1}^n Y_{t_j}^4 \xrightarrow{p} \mathbb{E}_0 \Big[ y_0^4 \Big], \tag{3.42}$$

thus

$$\sum_{j=1}^n \mathbb{E}_0^{j-1} \Big[ u_{1,j}^n \Big] \xrightarrow{p} 0. \tag{3.43}$$

Now, we move to (3.40),

$$\begin{aligned}
&\sum_{j=1}^n \mathbb{E}_0^{j-1} \Big[ u_{2,j}^n \Big] \\
&= \frac{4\sigma^2}{T_n^2} \sum_{j=1}^n \Big\{ \mathbb{E}_0 \Big[ (\lambda-\lambda_0)^2 Y_{t_{j-1}}^2 \Delta_j^2 w | \mathcal{F}_{t_{j-1}} \Big] + \mathbb{E}_0 \Big[ 2(\lambda-\lambda_0) Y_{t_{j-1}} q_j(\beta) \Delta_j^2 w | \mathcal{F}_{t_{j-1}} \Big] + \mathbb{E}_0 \Big[ q_j^2(\beta) \Delta_j^2 w | \mathcal{F}_{t_{j-1}} \Big] \Big\} \\
&= (\lambda-\lambda_0)^2 \frac{\sigma^2}{T_n} \frac{1}{n} \sum_{j=1}^n Y_{t_{j-1}}^2 + \frac{8\sigma^2(\lambda-\lambda_0)}{T_n} \frac{1}{n} \sum_{j=1}^n Y_{t_{j-1}} q_j(\beta) + \frac{4\sigma^2}{T_n} \frac{1}{n} \sum_{j=1}^n q_j^2(\beta).
\end{aligned} \tag{3.44}$$

Applying (3.35), Lemma 3.3, and (3.33) to the first, the second, and the third term of the right-hand side of (3.44), respectively, and we find that

$$\sum_{j=1}^n \mathbb{E}_0^{j-1} \Big[ u_{2,j}^n \Big] = o\Big(\frac{1}{T_n}\Big) + O\Big(\frac{1}{T_n}\Big) + o\Big(\frac{1}{T_n}\Big). \tag{3.45}$$

It is easy to find

$$\sum_{j=1}^n \mathbb{E}_0^{j-1} \Big[ u_{3,j}^n \Big] \xrightarrow{p} 0. \tag{3.46}$$

From (3.43)-(3.46), we get that

$$\sum_{j=1}^n \mathbb{E}_0^{j-1} \Big[ \Big( v_{1,j}^n(\theta) + v_{2,j}^n(\theta) \Big)^2 \Big] \xrightarrow{p} 0. \tag{3.47}$$

It follows under (3.33), (3.37), (3.38), and (3.47) that

$$|f_n(\theta) - f_0(\theta)| \xrightarrow{p} 0 \quad as \quad n \to \infty, \tag{3.48}$$

where

$$f_0(\theta) = (\lambda-\lambda_0)^2 C + \frac{1}{2} \sum_{k=1}^K \Big[ (A_k - A_{0,k})^2 + (B_k - B_{0,k})^2 \Big], \tag{3.49}$$

with (3.36).

As we can see, the explicit expression of $(\delta-\delta_0)$ does not appear in (3.49). Given that parameter $\delta$ has a different character than $\lambda$,$A$ and $B$, the presence of parameter $\delta$ with other parameters in (2.1) adds to the complexity of providing evidence of consistency. This evidence will be shown in section 3.2. For this complexity, [Kundu and Nandi, 2012] which develops the LSE of $(A,B,\omega)$ shows the consistency of $(A,B,\omega)$ in separate ways; say, Lemma 4.1 for strongly consistency of $(A,B)$, and Lemma 4.3 for $\omega$. However, to show the LSE of $(\lambda,A,B)$ then follows, using Lemma 3.6 and Lemma 3.8 to (3.6), it suffices to show (3.48) holds. Recall (3.24), (3.49), using Lemma 3.6, Lemma 3.8, we will show that

$$\left|(\lambda-\lambda_0)^2\frac{1}{n}\sum_{j=1}^{n}Y_{t_{j-1}}^2-(\lambda-\lambda_0)^2C+g_{1,n}(A,\delta)+g_{2,n}(B,\delta)\right|\xrightarrow{p}0, \tag{3.50}$$

where

$$g_{1,n}(A,\delta)=\frac{1}{n}\sum_{j=1}^{n}\sum_{k=1}^{K}[A_{0,k}\cos(\omega_{0,k}t_{j-1})-A_k\cos(\omega_k t_{j-1})]^2-\frac{1}{2}\sum_{k=1}^{K}(A_k-A_{0,k})^2, \tag{3.51}$$

$$g_{2,n}(B,\delta)=\frac{1}{n}\sum_{j=1}^{n}\sum_{k=1}^{K}[B_{0,k}\sin(\omega_{0,k}t_{j-1})-B_k\sin(\omega_k t_{j-1})]^2-\frac{1}{2}\sum_{k=1}^{K}(B_k-B_{0,k})^2 \tag{3.52}$$

Now, we will observe one of the terms (3.51) or (3.52). Let us rewrite (3.51) as follows:

$$g_{1,n}(A,\delta)=\sum_{k=1}^{K}(A_{0,k}-A_k)^2\frac{1}{n}\sum_{j=1}^{n}\cos^2([\omega_{0,k}-\omega_k]t_{j-1})-\frac{1}{2}\sum_{k=1}^{K}(A_k-A_{0,k})^2. \tag{3.53}$$

Take a look at the first term of the right-hand side of (3.53). Using arguments similar to the proof of Lemma 3.1, we have

$$\frac{1}{n}\sum_{j=1}^{n}\cos^2([\omega_0-\omega]t_{j-1})=\frac{1}{2}+o\left(\frac{1}{T_n}\right). \tag{3.54}$$

We can show (3.52) similarly to (3.51). The consistency of $\lambda$ follows on the first and the second term of the left expression of (3.50), with $C$ (3.36), leaving out the terms (3.51) and (3.52). With (3.53), (3.54) and (3.52), then (3.50) holds.

Now, we will verify condition (3.34). To prove the uniformity of the convergence of $f_n(\theta)$, it suffices to verify the following conditions

$$\sup_n\mathbb{E}_0\left[\sup_\theta|\partial_\lambda f_n(\theta)|\right]<\infty \quad as \quad n\to\infty, \tag{3.55}$$

$$\sup_n\mathbb{E}_0\left[\sup_\theta|\partial_{A_K} f_n(\theta)|\right]<\infty \quad as \quad n\to\infty, \tag{3.56}$$

$$\sup_n\mathbb{E}_0\left[\sup_\theta|\partial_{B_K} f_n(\theta)|\right]<\infty \quad as \quad n\to\infty, \tag{3.57}$$

for any $K\in\mathbb{N}$.

Recalling (3.29), we obtain

$$\begin{aligned}\mathbb{E}_0\left[\sup_\theta|\partial_\lambda f_n(\theta)|\right] &\leq \mathbb{E}_0\left[\sup_\theta\left|\frac{2(\lambda-\lambda_0)}{n}\sum_{j=1}^n Y_{t_{j-1}}^2\right|\right]+\mathbb{E}_0\left[\sup_\theta\left|\frac{2}{n}\sum_{j=1}^n Y_{t_{j-1}}q_j(\beta)\right|\right]\\ &+ \mathbb{E}_0\left[\sup_\theta\left|\frac{2\sigma}{T_n}\sum_{j=1}^n Y_{t_{j-1}}\Delta_j w\right|\right]. \qquad (3.58)\end{aligned}$$

Using (3.35) for the first term, Lemma 3.3 for the second term, and Lemma 3.6 for the third term on the right-hand side of (3.58), respectively, we get

$$\mathbb{E}_0\left[\sup_\theta|\partial_\lambda f_n(\theta)|\right]\leq O(1)+O\left(\frac{1}{\sqrt{n}}\right)+O\left(\frac{1}{\sqrt{T_n}}\right).$$

Hence, (3.55) holds. We now turn to (3.56) and (3.57).

$$\begin{aligned}&\mathbb{E}_0\left[\sup_\theta|\partial_{A_K} f_n(\theta)|\right]\\ &\leq 2\left\{\mathbb{E}_0\left[\sup_\theta\left|(\lambda-\lambda_0)\frac{1}{n}\sum_{j=1}^n Y_{t_{j-1}}\cos(\omega_K t_{j-1})\right|\right]\right.\\ &\left.+\mathbb{E}_0\left[\sup_\theta\left|\frac{1}{n}\sum_{j=1}^n q_j(\beta)\cos(\omega_K t_{j-1})\right|\right]+\sigma\mathbb{E}_0\left[\sup_\theta\left|\frac{1}{T_n}\sum_{j=1}^n\cos(\omega_K t_{j-1})\Delta_j w\right|\right]\right\}. \qquad (3.59)\end{aligned}$$

Using Lemma 3.1, we get

$$\begin{aligned}\mathbb{E}_0\left[\sup_\theta\left|\frac{1}{n}\sum_{j=1}^n q_j(\beta)\cos(\omega_K t_{j-1})\right|\right] &= |A_K|\left(\frac{1}{n}\sum_{j=1}^n\cos^2(\omega_K t_{j-1})\right)+o\left(\frac{1}{T_n}\right)\\ &= |A_K|\left(\frac{1}{2}+o\left(\frac{1}{T_n}\right)\right)+o\left(\frac{1}{T_n}\right), \qquad (3.60)\end{aligned}$$

and together with (3.60), by applying Lemma 3.3 and Lemma 3.8 to the first and third term on the right-hand side of (3.59), respectively, we have

$$\mathbb{E}_0\left[\sup_\theta|\partial_{A_K} f_n(\theta)|\right] \leq O\left(\frac{1}{\sqrt{n}}\right)+|A_K|+o\left(\frac{1}{T_n}\right)+O\left(\frac{1}{\sqrt{T_n}}\right).$$

Therefore, we obtain (3.56). Quite similarly, we find (3.57). Summarizing the computations of above, then we can deduce that $\sup_n\mathbb{E}_0[\sup_\theta|\partial_\theta f_n(\theta)|]<\infty$, yielding the uniformity (3.34).

## 3.2 The consistency of the LSE of $\delta$

The frequency component corresponds to the periodogram's greatest ordinate, and the gauge of this ordinate provides other least-squares estimators. To see this more clearly, let us take a look at (3.4). Following the way of [Whittle, 1952, Rice and Rosenblatt, 1988, Stoica and Moses, 1997, Kundu and Nandi, 2012]) in showing the periodogram, we plug the explicit expression of the least-squares estimators of $(\lambda,A,B)$, and we find that

$$\min_{\delta\in\overline{\Theta}}\mathbb{Q}_n(\hat{\lambda},\hat{A},\hat{B},\delta)=:\mathbb{Q}_n^*(\delta), \tag{3.61}$$

where

$$\mathbb{Q}_n^*(\delta)=\frac{1}{h}\sum_{j=1}^{n}\varphi_{j-1}^2-I_n(\delta), \tag{3.62}$$

$$\varphi_{j-1}=\Delta_j Y+h\hat{\lambda}Y_{t_{j-1}}, \tag{3.63}$$

with (B.3), and

$$I_n(\delta)=\frac{2}{T_n}\sum_{k=1}^{K}\left\{\left[\sum_{j=1}^{n}\varphi_{j-1}\cos(\omega_k t_{j-1})\right]^2+\left[\sum_{j=1}^{n}\varphi_{j-1}\sin(\omega_k t_{j-1})\right]^2\right\}, \tag{3.64}$$

with (1.4). The explicit expressions of the least-squares estimators of $(\lambda,A,B)$ and (3.62) are given in Appendix B.

The complexity in showing the consistency of the estimators occurs when the least-squares estimators of $(\lambda,A,B)$ is obtained by minimizing (3.4). On the other hand, for the frequency components estimator $\delta$, the minimization occurs when the periodogram (3.64) is maximal. Further, the term $(\delta-\delta_0)$ always vanishes in the calibration of (3.6); therefore, we look for the consistency of the LSE of $\delta$ through the periodogram (3.64). Hence, based on (3.62) and (3.64), we can find the least-squares estimators of $\delta$ by minimizing $\mathbb{Q}_n(\hat{\lambda},\hat{A},\hat{B},\delta)$ which can be done by maximizing

$$\mathbb{J}_n(\delta)=\frac{1}{T_n}\sum_{k=1}^{K}\left\{\left[\sum_{j=1}^{n}\varphi_{j-1}\cos(2\pi k\delta t_{j-1})\right]^2+\left[\sum_{j=1}^{n}\varphi_{j-1}\sin(2\pi k\delta t_{j-1})\right]^2\right\}. \tag{3.65}$$

Thus, the LSE of $\delta$ corresponds to the greatest ordinate of periodogram (3.65). In the sequel, unless otherwise mentioned, we used the notation $\omega_k$ to shorten the writing of the term $2\pi k\delta$.

To prove the consistency of the least-squares estimators of $\delta$, we define

$$\tilde{f}_n(\delta):=\frac{1}{n^2}[\mathbb{J}_n(\delta)-\mathbb{J}_n(\delta_0)]. \tag{3.66}$$

Therefore, through (3.66), we will show that there exists $\tilde{f}_0(\delta)$ such that

$$\sup_{\delta\in\Theta_\delta}\left|\tilde{f}_n(\delta)-\tilde{f}_0(\delta)\right|\xrightarrow{p}0 \quad as \quad n\to\infty, \tag{3.67}$$

with

$$\operatorname*{argmax}_{\delta\in\overline{\Theta}}\tilde{f}_0(\delta)=\{\delta_0\}. \tag{3.68}$$

Now, recalling (3.66), (3.65), and (1.4), we have

$$\begin{aligned}\tilde{f}_n(\delta) &= \frac{1}{n^3 h}\sum_{k=1}^{K}\left\{\left[\sum_{j=1}^{n}\varphi_{j-1}\cos(\omega_k t_{j-1})\right]^2 - \left[\sum_{j=1}^{n}\varphi_{0,j-1}\cos(\omega_{0,k} t_{j-1})\right]^2\right. \\ &+ \left.\left[\sum_{j=1}^{n}\varphi_{j-1}\sin(\omega_k t_{j-1})\right]^2 - \left[\sum_{j=1}^{n}\varphi_{0,j-1}\sin(\omega_{0,k} t_{j-1})\right]^2\right\}, \end{aligned} \tag{3.69}$$

where $\varphi_{0,j-1} = \Delta_j Y + h\lambda_0 Y_{t_{j-1}}$.

Take a look for the cosine term, namely

$$\frac{1}{n^3 h}\sum_{k=1}^{K}\left[\sum_{j=1}^{n}\varphi_{j-1}\cos(\omega_k t_{j-1})\right]^2 = \frac{1}{n^3 h}\sum_{k=1}^{K}\sum_{j=1}^{n}\varphi_{j-1}^2\cos^2(\omega_k t_{j-1}) + \varphi_n^*(\omega), \tag{3.70}$$

where

$$\varphi_n^*(\omega) = \frac{2}{n^3 h}\sum_{k=1}^{K}\left\{\sum_{j=1}^{n-1}\psi_j\cos(\omega_k t_j)\cos(\omega_k t_{j-1}) + \cdots + \sum_{j=1}^{n-r}\psi_{j+r-1}\cos(\omega_k t_{j+r-1})\cos(\omega_k t_{j-1})\right\},$$

for $r$ to be an arbitrary element of $\mathbb{N}$ with $r < n$, and $\varphi_i\varphi_{i-1} =: \psi_i$. Together with the sine term that has arguments similar to (3.70), we have $\tilde{f}_n$ as

$$\tilde{f}_n(\delta) = \sum_{j=1}^{n}\left[\tilde{f}_{1,j}^n(\delta) + \tilde{f}_{2,j}^n(\delta)\right] + o_p\left(\frac{1}{nT_n}\right), \tag{3.71}$$

where

$$\tilde{f}_{1,j}^n(\delta) = \frac{1}{n^3 h}\sum_{k=1}^{K}[\varphi_{j-1}\cos(\omega_k t_{j-1}) - \varphi_{0,j-1}\cos(\omega_{0,k} t_{j-1})]^2, \tag{3.72}$$

$$\tilde{f}_{2,j}^n(\delta) = \frac{1}{n^3 h}\sum_{k=1}^{K}[\varphi_{j-1}\sin(\omega_k t_{j-1}) - \varphi_{0,j-1}\sin(\omega_{0,k} t_{j-1})]^2. \tag{3.73}$$

The details of (3.70) and (3.71) are provided in Appendix B. Let us define $\phi_k := \omega_k - \omega_{0,k}$ and $\varphi_i\varphi_{0,i} =: \tilde{\varphi}_i$. Again, using Lemma 9 of [Genon-Catalot and Jacod, 1993], we can deduce that

$$\begin{aligned}\sum_{j=1}^{n}\mathbb{E}_0^{j-1}\left[\tilde{f}_{1,j}^n(\delta) + \tilde{f}_{2,j}^n(\delta)\right] &= \frac{1}{n^3 h}\sum_{k=1}^{K}\sum_{j=1}^{n}\left\{\varphi_{j-1}^2 + \varphi_{0,j-1}^2 - 2\tilde{\varphi}_{j-1}\cos(\phi_k t_{j-1})\right\} \\ &= \frac{-2}{n^3 h}\sum_{k=1}^{K}\sum_{j=1}^{n}\tilde{\varphi}_{j-1}\cos(\phi_k t_{j-1}) + O\left(\frac{1}{nT_n}\right) \\ &= \frac{-2}{n^3 h}\sum_{k=1}^{K}\sum_{j=1}^{n-1}\tilde{\varphi}_j\cos(\phi_k t_j) + O\left(\frac{1}{nT_n}\right).\end{aligned}$$

Using the quantization scheme of [Proakis, 2001], i.e., for some $n$, the sampling analog signal, periodically every $T^*$ seconds to produce a discrete signal, that is, $\cos(\omega n) = \cos(\omega n T^*)$, and the periodicity, we thus obtain

$$\begin{aligned}\sum_{j=1}^{n}\mathbb{E}_0^{j-1}\Big[\tilde{f}_{1,j}^n(\delta)+\tilde{f}_{2,j}^n(\delta)\Big] &= \frac{-2}{n^3h}\sum_{k=1}^{K}\cos(\phi_k)\Big\{\tilde{\varphi}_1+\tilde{\varphi}_2+\cdots+\tilde{\varphi}_{n-1}\Big\}\Big\{h+2h+\cdots+(n-1)h\Big\}+O\Big(\frac{1}{nT_n}\Big)\\ &= -\sum_{k=1}^{K}\cos(\phi_k)\frac{1}{n}\sum_{j=1}^{n-1}\tilde{\varphi}_j+O\Big(\frac{1}{T_n}\Big)+O\Big(\frac{1}{nT_n}\Big).\end{aligned}$$

There exists $\tilde{\varphi}(.)$ that satisfies $\mathbb{E}_0[|\tilde{\varphi}(y_0)|]<\infty$,

$$\frac{1}{n}\sum_{j=1}^{n}\tilde{\varphi}(Y_{t_j})\xrightarrow{p}\mathbb{E}_0[\tilde{\varphi}(y_0)],$$

where

$$\mathbb{E}_0[\tilde{\varphi}(y_0)]=C^*, \tag{3.74}$$

and then

$$\sum_{j=1}^{n}\mathbb{E}_0^{j-1}\Big[\tilde{f}_{1,j}^n(\delta)+\tilde{f}_{2,j}^n(\delta)\Big]=-C^*\sum_{k=1}^{K}\cos(2\pi k(\delta-\delta_0))+O\Big(\frac{1}{T_n}\Big)+O\Big(\frac{1}{nT_n}\Big). \tag{3.75}$$

In a quite similar manner, we can find

$$\sum_{j=1}^{n}\mathbb{E}_0^{j-1}\Big[\Big(\tilde{f}_{1,j}^n(\delta)+\tilde{f}_{2,j}^n(\delta)\Big)^2\Big]\xrightarrow{p}0. \tag{3.76}$$

See Appendix B for detail (3.76). It follows under (3.71), (3.75) and (3.76), that

$$\Big|\tilde{f}_n(\delta)-\tilde{f}_0(\delta)\Big|\xrightarrow{p}0 \quad as \quad n\to\infty \tag{3.77}$$

where

$$\tilde{f}_0(\delta)=-C^*\sum_{k=1}^{K}\cos(2\pi k(\delta-\delta_0)), \tag{3.78}$$

with (3.74) and (3.68). Observe that

$$\begin{aligned}\underset{\delta\in\overline{\Theta}}{\operatorname{argmax}}\,\tilde{f}_0(\delta) &= \underset{\delta\in\overline{\Theta}}{\operatorname{argmax}}\Big\{-C^*\sum_{k=1}^{K}\cos(2\pi k(\delta-\delta_0))\Big\}\\ &= -C^*\underset{\delta\in\overline{\Theta}}{\operatorname{argmax}}\Big\{\cos(2\pi\delta-2\pi\delta_0)+\cos(4\pi\delta-4\pi\delta_0)+\cdots+\cos(2\pi K\delta-2\pi K\delta_0)\Big\}.\end{aligned}$$

Because of the periodicity of $h_t(\beta)$ in (1.2), (1.4), and (1.5), then for any $\delta\in\overline{\Theta}$ there exists $T>0$ such that $T=T(\delta)$. Therefore,

$$\underset{\delta\in\overline{\Theta}}{\operatorname{argmax}}\,\tilde{f}_0(\delta)=-C^*\underset{\delta\in\overline{\Theta}}{\operatorname{argmax}}\left\{\cos\Big(2\pi\frac{1}{T}-2\pi\delta_0\Big)+\cos\Big(2\pi\frac{2}{T}-4\pi\delta_0\Big)+\cdots+\cos\Big(2\pi\frac{K}{T}-2\pi K\delta_0\Big)\right\},$$

and we obtain (3.68).

Now, in order to prove the uniformity of the convergence $\tilde{f}_n(\delta)$, we will show that

$$\sup_n \mathbb{E}_0\left[\sup_\delta \left|\partial_\delta \tilde{f}_n(\delta)\right|\right] < \infty. \tag{3.79}$$

If we denote

$$2\pi k =: \tilde{k}, \quad k = 1,...,K, \tag{3.80}$$

then for any $K \in \mathbb{N}$, we have

$$\partial_\delta \tilde{f}_n(\delta) = \frac{2\tilde{K}}{n^3 h}[\xi_1(\delta) + \xi_2(\delta)], \tag{3.81}$$

where

$$\xi_1(\delta) = \sum_{j=1}^{n}[\varphi_{j-1}\cos(\omega_K t_{j-1}) - \varphi_{0,j-1}\cos(\omega_{0,K} t_{j-1})][-t_{j-1}\sin(\omega_K t_{j-1})\varphi_{j-1}], \tag{3.82}$$

$$\xi_2(\delta) = \sum_{j=1}^{n}[\varphi_{j-1}\sin(\omega_K t_{j-1}) - \varphi_{0,j-1}\sin(\omega_{0,K} t_{j-1})][t_{j-1}\cos(\omega_K t_{j-1})\varphi_{j-1}]. \tag{3.83}$$

We observe the term (3.82). Then

$$\begin{aligned}
&\frac{2\tilde{K}}{n^3 h}\mathbb{E}_0\left[\sup_\delta |\xi_1(\delta)|\right] \\
&= \frac{2\tilde{K}}{n^3 h}\mathbb{E}_0\left[\sup_\delta \left| -\sum_{j=1}^{n} t_{j-1}\varphi_{j-1}\left[\varphi_{j-1}e^{i\omega_K t_{j-1}} - \varphi_{0,j-1}e^{i\omega_{0,K} t_{j-1}}\right]\sin(\omega_K t_{j-1})\right|^2\right] \\
&\leq \frac{2\tilde{K}}{n^3 h}\left\{\mathbb{E}_0\left[\sup_\delta \left| -\sum_{j=1}^{n} t_{j-1}\varphi_{j-1}\left[\varphi_{j-1}e^{i\omega_K t_{j-1}} - \varphi_{0,j-1}e^{i\omega_{0,K} t_{j-1}}\right] i e^{i\omega_K t_{j-1}}\right|^2\right]\right\}^{\frac{1}{2}} \\
&= \frac{2\tilde{K}}{n^3 h}\left\{\mathbb{E}_0\left[\sup_\delta \left(\sum_{j=1}^{n} t_{j-1}^2\varphi_{j-1}^2\left[\varphi_{j-1}e^{i\omega_K t_{j-1}} - \varphi_{0,j-1}e^{i\omega_{0,K} t_{j-1}}\right]^2 + r(\delta)\right)\right]\right\}^{\frac{1}{2}} \\
&= \frac{2\tilde{K}}{n^3 h}\left\{\mathbb{E}_0\left[\sup_\delta \left(\sum_{j=1}^{n} t_{j-1}^2\varphi_{j-1}^2\left(\varphi_{j-1}^2 + \varphi_{0,j-1}^2 - 2\varphi_{j-1}\varphi_{0,j-1}\right) + r(\delta)\right)\right]\right\}^{\frac{1}{2}}
\end{aligned}$$

where

$$\begin{aligned}
r(\delta) \quad = \quad & 2\sum_{j=1}^{n-1} t_j\varphi_j[\varphi_j e^{i\omega_K t_j} - \varphi_{0,j}e^{i\omega_{0,K} t_j}]\left\{\sum_{j=1}^{n-2} t_{j+1}\varphi_{j+1}[\varphi_{j+1}e^{i\omega_K t_{j+1}} - \varphi_{0,j+1}e^{i\omega_{0,K} t_{j+1}}] + \ldots\right. \\
+ \quad & \left.\sum_{j=1}^{n-r} t_{j+r-1}[\varphi_{j+r-1}e^{i\omega_K t_{j+r-1}} - \varphi_{0,j+r-1}e^{i\omega_{0,K} t_{j+r-1}}]\right\},
\end{aligned}$$

for an arbitrary $r \in \mathbb{N}, r < n$. This gives

$$\frac{2\tilde{K}}{n^3 h}\mathbb{E}_0\left[\sup_{\delta}|\xi_1(\delta)|\right] \leq \frac{2\tilde{K}}{n^3 h}\left\{O\Big(\max(n^2 T_n^2, n T_n^2)\Big)\right\}^{\frac{1}{2}},$$

and together with $\mathbb{E}_0[\sup_\delta|\xi_1(\delta)|]$, which can be obtained similarly to $\mathbb{E}_0[\sup_\delta|\xi_1(\delta)|]$, therefore, we can find that

$$\mathbb{E}_0\left[\sup_{\delta}\left|\partial_\delta \tilde{f}_n(\delta)\right|\right] \leq O\left(\frac{1}{n}\right),$$

and obviously (3.79) is holds.

All Lemma in Sections 3.2 and 3.1 are the original finding of the thesis. The difference with the one provided in [Kundu and Nandi, 2012] and [Mangulis, 2012] is the continuous-time signal with $k$th harmonic of the components $\cos(\omega_k t)$ and $\sin(\omega_k t)$; that is included in the process observed at a high-frequency sampling setting. From Sections 3.1 and 3.2, we have shown the consistency of the estimates. This is not the new one, but the anomalous behavior of the frequency component caused the complexity in showing the consistency of the estimates, that is, we establish a two-step strategy for proving the consistency of the LSE of $(\lambda, A, B)$ and $\delta$. Since the periodic continuous-time sinusoidal signal processing in a time-inhomogeneous Ornstein–Uhlenbeck process is under a high-frequency sampling setting, then it needs complicated technical details.

## 3.3 Asymptotic Normality

To proceed the asymptotic normality of the LSE of $\theta$, we need the following Lemmas.

**Lemma 3.11.** *We have*

$$\mathbf{D}_n^{-1}\left[\partial_\theta^2 \mathbf{Q}_n\left(\tilde{\theta}_n\right) - \partial_\theta^2 \mathbf{Q}_n(\theta_0)\right]\mathbf{D}_n^{-1} \xrightarrow{p} 0 \tag{3.84}$$

*for any consistent estimator* $\tilde{\theta}_n$ *of* $\theta_0$.

*Proof.* Let $\mathbf{D}_n$ denote the $(2K+2)\times(2K+2)$ diagonal matrix

$$\mathbf{D}_n := \mathrm{diag}\Big(\sqrt{nh}, \sqrt{nh}\mathbb{I}_K, \sqrt{nh}\mathbb{I}_K, \sqrt{n^3 h^3}\Big). \tag{3.85}$$

Observe $\mathbb{D}_n^{-1}$ with $\mathbb{D}_n$ as in (3.85). That is, for the diagonal element $\sqrt{T_n}$,

$$\begin{aligned}
&\frac{1}{T_n}\left\{\left\{\sum_{j=1}^{n}\Big([\Delta_j Y - a_{j-1}(\tilde{\theta}_n)h]\partial_\theta^2 a_{j-1}(\tilde{\theta}_n) - h[\partial_\theta a_{j-1}(\tilde{\theta}_n)]^2\Big)\right\}\right. \\
&\left.-\left\{\sum_{j=1}^{n}\Big([\Delta_j Y - a_{j-1}(\theta_0)h]\partial_\theta^2 a_{j-1}(\theta_0) - h[\partial_\theta a_{j-1}(\theta_0)]^2\Big)\right\}\right\} \\
&= \frac{1}{T_n}\sum_{j=1}^{n}\Delta_j Y[\partial_\theta^2 a_{j-1}(\tilde{\theta}_n) - \partial_\theta^2 a_{j-1}(\theta_0)] - \frac{h}{T_n}\sum_{j=1}^{n}\Big[a_{j-1}(\tilde{\theta}_n)\partial_\theta^2 a_{j-1}(\tilde{\theta}_n) - a_{j-1}(\theta_0)\partial_\theta^2 a_{j-1}(\theta_0)\Big]
\end{aligned}$$

$$-\frac{h}{T_n}\sum_{j=1}^{n}\Big([\partial_\theta a_{j-1}(\tilde{\theta}_n)]^2-[\partial_\theta a_{j-1}(\theta_0)]^2\Big). \tag{3.86}$$

To prove Lemma 3.11, let us take a brief look at the last term in the right-hand side of (3.86). Since we have

$$\begin{aligned}\mathbb{E}_0\left[\left|\frac{1}{n}\sum_{j=1}^{n}\Big(a_{j-1}(\tilde{\theta}_n)-a_{j-1}(\theta_0)\Big)\right|\right] &\leq \frac{1}{n}\left\{\mathbb{E}_0\left[\left|\sum_{j=1}^{n}\Big(a_{j-1}(\tilde{\theta}_n)-a_{j-1}(\theta_0)\Big)\right|^2\right]\right\}^{\frac{1}{2}}\\ &= \frac{1}{n}\Big\{\mathbb{E}_0[\iota_{1,n}+\iota_{2,n}+\iota_{3,n}]\Big\}^{\frac{1}{2}},\end{aligned} \tag{3.87}$$

where

$$\begin{aligned}\iota_{1,n}&=\left(-\sum_{j=1}^{n}(\tilde{\lambda}-\lambda_0)Y_{t_{j-1}}\right)^2;\\ \iota_{2,n}&=\left(\sum_{j=1}^{n}\Big[h_{j-1}(\tilde{\beta})-h_{j-1}(\beta_0)\Big]\right)^2;\\ \iota_{3,n}&=-2(\tilde{\lambda}-\lambda_0)\sum_{j=1}^{n}Y_{t_{j-1}}\sum_{j=1}^{n}\Big[h_{j-1}(\tilde{\beta})-h_{j-1}(\beta_0)\Big].\end{aligned}$$

Using (3.35) and Lemma 3.3, it follows that

$$\iota_{1,n}=(\tilde{\lambda}-\lambda_0)^2 o_p(n). \tag{3.88}$$

We use Lemma 3.1 and the result of it, that is,

$$\frac{1}{n}\sum_{j=1}^{n}\cos(\tilde{\omega}t_{j-1}+\omega t_j)=\frac{1}{2n}+o\left(\frac{1}{T_n}\right),$$

to obtain that

$$\iota_{2,n}=n\left\{q^K(\tilde{A},\tilde{B})+\frac{1}{2}+o\left(\frac{1}{T_n}\right)\right\}, \tag{3.89}$$

where $q^K(\tilde{A},\tilde{B})$ is defined in (3.33). By Lemma 3.3, using the fact that

$$\sup_{\omega}\left|\frac{1}{n-1}\sum_{j=1}^{n-1}Y_{t_j}\cos(\omega t_{j+1})\right|\xrightarrow{p}0,$$

we find that

$$\iota_{3,n}=-2(\tilde{\lambda}-\lambda_0)o_p(\sqrt{n}). \tag{3.90}$$

Therefore, plugging (3.88), (3.89), and (3.90) to (3.87), we can deduce

$$\frac{1}{n}\left\{\mathbb{E}_0\left[\left|\sum_{j=1}^n\Big(a_{j-1}(\tilde{\theta}_n)-a_{j-1}(\theta_0)\Big)\right|^2\right]\right\}^{\frac{1}{2}}\leq O\Big(\frac{1}{\sqrt{n}}\Big).$$

Now, let us look at the first term in the right-hand side of (3.86). In a quite similar manner as above, for the diagonal element $\sqrt{T_n}$, and recalling (3.3), we have

$$\begin{aligned}
&\mathbb{E}_0\left[\left|\frac{1}{T_n}\sum_{j=1}^n\Delta_j Y\Big(\partial_\theta^2 a_{j-1}(\tilde{\theta}_n)-\partial_\theta^2 a_{j-1}(\theta_0)\Big)\right|\right]\\
&\leq\frac{1}{T_n}\left\{\mathbb{E}_0\left[\left|\sum_{j=1}^n\left\{\int_j a_s(\tilde{\theta}_n)ds+\sigma\Delta_j w\right\}\Big(\partial_\theta^2 a_{j-1}(\tilde{\theta}_n)-\partial_\theta^2 a_{j-1}(\theta_0)\Big)\right|^2\right]\right\}^{\frac{1}{2}}\\
&\leq\frac{1}{T_n}\left\{\mathbb{E}_0\left[\left|\int_j(1+|y_s|)ds\right|^2\right]\right\}^{\frac{1}{2}}O(\sqrt{n})=\frac{h}{T_n}\Big\{1+\sup_{s\leq T_n}\mathbb{E}_0[|y_s|^2]\Big\}^{\frac{1}{2}}O(\sqrt{n})\lesssim O\Big(\frac{1}{\sqrt{n}}\Big).
\end{aligned}$$

We can obtain similarly for the case of the diagonal element $\sqrt{T_n}$ with $\sqrt{T_n^3}$; $\sqrt{T_n^3}$, so this completes the proof.

□

**Lemma 3.12.** *We have*

$$\frac{1}{\sqrt{T_n}}\sum_{j=1}^n[\Delta_j Y-a_{j-1}(\theta_0)h]\partial_\theta a_{j-1}(\theta_0)-\frac{\sigma}{\sqrt{T_n}}\int_0^{T_n}\partial_\theta a_t(\theta_0)dw_t\xrightarrow{p}0. \tag{3.91}$$

*Proof.* First, concerning the diagonal element $\sqrt{T_n}$, we have

$$\begin{aligned}
&\frac{1}{\sqrt{T_n}}\sum_{j=1}^n[\Delta_j Y-a_{j-1}(\theta_0)h-\sigma\Delta_j w+\sigma\Delta_j w]\partial_\theta a_{j-1}(\theta_0)-\frac{\sigma}{\sqrt{T_n}}\int_0^{T_n}\partial_\theta a_t(\theta_0)dw_t\\
&=\frac{1}{\sqrt{T_n}}\sum_{j=1}^n[\Delta_j Y-a_{j-1}(\theta_0)h-\sigma\Delta_j w]\partial_\theta a_{j-1}(\theta_0)+\frac{\sigma}{\sqrt{T_n}}\left\{\sum_{j=1}^n\Delta_j w\partial_\theta a_{j-1}(\theta_0)-\int_0^{T_n}\partial_\theta a_t(\theta_0)dw_t\right\}.
\end{aligned} \tag{3.92}$$

We observe the first term of the right-hand side of (3.92). Again, recall (3.3). Then

$$\begin{aligned}
&\frac{1}{\sqrt{T_n}}\mathbb{E}_0\left[\left|\sum_{j=1}^n(\Delta_j Y-\sigma\Delta_j w-a_{j-1}(\theta_0)h)\partial_\theta a_{j-1}(\theta_0)\right|\right]\\
&\leq\frac{1}{\sqrt{T_n}}\left\{\mathbb{E}_0\left[\left|\sum_{j=1}^n\left[\int_j a_s(\theta_0)ds-a_{j-1}(\theta_0)h\right]\partial_\theta a_{j-1}(\theta_0)\right|^2\right]\right\}^{\frac{1}{2}}.
\end{aligned}$$

For $r$ is an arbitrary element of $\mathbb{N}$ with $r<n$, we have

$$
\begin{aligned}
&\left|\sum_{j=1}^{n}\int_j a_s(\theta_0)ds-a_{j-1}(\theta_0)h\right|^2\\
&\le\sum_{j=1}^{n}\left[\int_j a_s(\theta_0)ds-a_{j-1}(\theta_0)h\right]^2+2\left\{\sum_{j=1}^{n-1}\left[\int_j a_s(\theta_0)ds-a_{j-1}(\theta_0)h\right]\left[\int_{j+1}a_s(\theta_0)ds-a_j(\theta_0)h\right]\right.\\
&\left.+\cdots+\sum_{j=1}^{n-r}\left[\int_j a_s(\theta_0)ds-a_{j-1}(\theta_0)h\right]\left[\int_{j+r}a_s(\theta_0)ds-a_{j+r}(\theta_0)h\right]\right\},
\end{aligned}
$$

thus we obtain

$$
\begin{aligned}
&\frac{1}{\sqrt{T_n}}\mathbb{E}_0\left[\left|\sum_{j=1}^{n}(\Delta_jY-\sigma\Delta_jw-a_{j-1}(\theta_0)h)\partial_\theta a_{j-1}(\theta_0)\right|\right]\\
&\le\frac{1}{\sqrt{T_n}}\left\{O(\max\{nh^3,(n-1)h^3,(n-2)h^3+\cdots+(n-r)h^3\})\right\}^{\frac{1}{2}}O(\sqrt{n})=O\left(\sqrt{nh^2}\right).
\end{aligned}
\tag{3.93}
$$

Result (3.93) indicates that condition (1.9) is necessary in the study. Similarly, for the second term of the right-hand side of (3.92), we get

$$
\begin{aligned}
&\frac{\sigma}{\sqrt{T_n}}\mathbb{E}_0\left[\left|\sum_{j=1}^{n}\Delta_jw\partial_\theta a_{j-1}(\theta_0)-\int_0^{T_n}\partial_\theta a_t(\theta_0)dw_t\right|\right]\\
&\le\frac{\sigma}{\sqrt{T_n}}\left\{\mathbb{E}_0\left[\left|\int_0^{T_n}\partial_\theta a_s(\theta_0)dw_s-\int_0^{T_n}\partial_\theta a_t(\theta_0)dw_t\right|^2\right]\right\}^{\frac{1}{2}}\\
&\le\frac{\sigma}{\sqrt{T_n}}\left\{\mathbb{E}_0\left[\left|C^0\int_0^{T_n}dw_u\right|^2\right]\mathbb{E}_0\left[|Y_s-Y_t|^2\right]\right\}^{\frac{1}{2}}\lesssim O(\sqrt{h}),
\end{aligned}
\tag{3.94}
$$

with $C^0>0$. Having (3.93) and (3.94), we obtain Lemma 3.12.

□

The result is true for the diagonal element $\sqrt{T_n^3}$.

**Lemma 3.13.** *We have*

$$
\frac{1}{T_n}\sum_{j=1}^{n}[\Delta_jY-a_{j-1}(\theta_0)h]\partial_\theta^2a_{j-1}(\theta_0)-\frac{\sigma}{T_n}\int_0^{T_n}\partial_\theta^2a_t(\theta_0)dw_t\xrightarrow{p}0.
$$

*Proof.* We show Lemma 3.13 in a similar manner to Lemma 3.12. Note that

$$
\mathbb{E}_0\left[\left|\frac{1}{T_n}\sum_{j=1}^{n}[\Delta_jY-a_{j-1}(\theta_0)h-\sigma\Delta_jw]\partial_\theta^2a_{j-1}(\theta_0)\right|\right]\le O\left(\sqrt{h}\right),\tag{3.95}
$$

$$
\mathbb{E}_0\left[\left|\frac{\sigma}{T_n}\left\{\sum_{j=1}^{n}\Delta_jw\partial_\theta^2a_{j-1}(\theta_0)-\int_0^{T_n}\partial_\theta^2a_t(\theta_0)dw_t\right\}\right|\right]\le O\left(\frac{1}{\sqrt{n}}\right),\tag{3.96}
$$

then the proof is complete. $\square$

The result is true for the diagonal element $\sqrt{T_n}$ with $\sqrt{T_n^3}$; $\sqrt{T_n^3}$.

The asymptotic behavior of the LSE of $\theta$ is given in the following Theorem.

**Theorem 3.14.** *We have*

$$\mathbf{D}_n\Big(\hat{\theta}_n-\theta_0\Big)\xrightarrow{\mathcal{L}}\mathcal{N}_{2K+2}\Big(\mathbf{0},\sigma^2\mathbf{M}_0(\theta_0)^{-1}\Big), \tag{3.97}$$

*where*

- *we recalled $\theta$ with order $\theta=(\lambda,A_1,B_1,...,A_K,B_K,\delta)$;*
- $\mathbf{D}_n$ *is defined in* (3.85)*;*
- $\mathbf{M}_0(\theta_0)$ *is a* $(2K+2)\times(2K+2)$ *matrix, with general form as follows:*

$$\mathbf{M}_0(\theta_0):=\begin{pmatrix} C & 0 & 0 & 0 & 0 & \dots & 0 & 0 & 0 \\ & \frac{1}{2} & 0 & 0 & 0 & \dots & 0 & 0 & \frac{2\pi B_{0,1}}{4} \\ & & \frac{1}{2} & 0 & 0 & \dots & 0 & 0 & -\frac{2\pi A_{0,1}}{4} \\ & & & \frac{1}{2} & 0 & \dots & 0 & 0 & \frac{4\pi B_{0,2}}{4} \\ & & & & \frac{1}{2} & \dots & 0 & 0 & -\frac{4\pi A_{0,2}}{4} \\ & & & & & \ddots & \vdots & \vdots & \vdots \\ & & & & & & \frac{1}{2} & 0 & \frac{2K\pi B_{0,K}}{4} \\ & & & & & & & \frac{1}{2} & -\frac{2K\pi A_{0,K}}{4} \\ Sym. & & & & & & & & \frac{4\pi^2K^2(A_{0,K}^2+B_{0,K}^2)}{6} \end{pmatrix}, \tag{3.98}$$

*with $C$* (3.36).

*Proof.* We will follow the route of the Central Limit Theorem of a stochastic process of Theorem 5.5.1 of [Fuller, 2009]. First of all, we denote by $\partial_\theta\mathbf{Q}_n(\theta_0)$ a $(2K+2)\times 1$ vector of the first derivative,

$$\partial_\theta\mathbf{Q}_n(\theta_0):=(\partial_\lambda\mathbb{Q}_n(\theta_0),\partial_{A_1}\mathbb{Q}_n(\theta_0),\partial_{B_1}\mathbb{Q}_n(\theta_0),...,\partial_{A_K}\mathbb{Q}_n(\theta_0),\partial_{B_K}\mathbb{Q}_n(\theta_0),\partial_\delta\mathbb{Q}_n(\theta_0))^\top, \tag{3.99}$$

and $\partial_\theta^2\mathbf{Q}_n(\theta_0)$ the $(2K+2)\times(2K+2)$ matrix,

$$\partial_\theta^2\mathbf{Q}_n(\theta_0):=\begin{pmatrix} \partial^2_{\lambda^2}\mathbb{Q}_n & \partial^2_{\lambda A_1}\mathbb{Q}_n & \partial^2_{\lambda B_1}\mathbb{Q}_n & \dots & \partial^2_{\lambda A_K}\mathbb{Q}_n & \partial^2_{\lambda B_K}\mathbb{Q}_n & \partial^2_{\lambda\delta}\mathbb{Q}_n \\ \partial^2_{A_1\lambda}\mathbb{Q}_n & \partial^2_{A_1^2}\mathbb{Q}_n & \partial^2_{A_1B_1}\mathbb{Q}_n & \dots & \partial^2_{A_1A_K}\mathbb{Q}_n & \partial^2_{A_1B_K}\mathbb{Q}_n & \partial^2_{A_1\delta}\mathbb{Q}_n \\ \partial^2_{B_1\lambda}\mathbb{Q}_n & \partial^2_{B_1A_1}\mathbb{Q}_n & \partial^2_{B_1^2}\mathbb{Q}_n & \dots & \partial^2_{B_1A_K}\mathbb{Q}_n & \partial^2_{B_1B_K}\mathbb{Q}_n & \partial^2_{B_1\delta}\mathbb{Q}_n \\ \vdots & \vdots & \vdots & \ddots & \vdots & \vdots & \vdots \\ \partial^2_{A_K\lambda}\mathbb{Q}_n & \partial^2_{A_KA_1}\mathbb{Q}_n & \partial^2_{A_KB_1}\mathbb{Q}_n & \dots & \partial^2_{A_K^2}\mathbb{Q}_n & \partial^2_{A_KB_K}\mathbb{Q}_n & \partial^2_{A_K\delta}\mathbb{Q}_n \\ \partial^2_{B_K\lambda}\mathbb{Q}_n & \partial^2_{B_KA_1}\mathbb{Q}_n & \partial^2_{B_KB_1}\mathbb{Q}_n & \dots & \partial^2_{B_KA_K}\mathbb{Q}_n & \partial^2_{B_K^2}\mathbb{Q}_n & \partial^2_{B_K\delta}\mathbb{Q}_n \\ \partial^2_{\delta\lambda}\mathbb{Q}_n & \partial^2_{\delta A_1}\mathbb{Q}_n & \partial^2_{\delta B_1}\mathbb{Q}_n & \dots & \partial^2_{\delta A_K}\mathbb{Q}_n & \partial^2_{\delta B_K}\mathbb{Q}_n & \partial^2_{\delta^2}\mathbb{Q}_n \end{pmatrix} \tag{3.100}$$

By utilizing Taylor series expansions about $\theta_0$, it can be shown that

$$\mathbf{D}_n^{-1}\partial_\theta\mathbf{Q}_n(\theta_0)=\Big[-\mathbf{D}_n^{-1}\partial_\theta^2\mathbf{Q}_n\Big(\tilde{\theta}_n\Big)\mathbf{D}_n^{-1}\Big]\Big[\mathbf{D}_n\Big(\hat{\theta}_n-\theta_0\Big)\Big], \tag{3.101}$$

where $\tilde{\theta}_n$ is on the line joining $\hat{\theta}_n$ and $\theta_0$. Set

$$\mathbf{M}_n(\theta_0):=\Big[-\mathbf{D}_n^{-1}\partial_\theta^2\mathbf{Q}_n(\theta_0)\mathbf{D}_n^{-1}\Big], \tag{3.102}$$

then by (3.101), Lemma 3.11, Lemma 3.13 and Lemma 3.12, it suffices to show that there exists a fixed matrix $\mathbf{M}_0(\theta_0)$ such that

$$\mathbf{M}_n(\theta_0)\xrightarrow{p}\mathbf{M}_0(\theta_0), \tag{3.103}$$

and

$$\Big[\mathbf{D}_n^{-1}\partial_\theta\mathbf{Q}_n(\theta_0)\Big]\xrightarrow{\mathcal{L}}\mathcal{N}_{2K+2}\Big(\mathbf{0},\sigma^2\mathbf{M}_0(\theta_0)\Big). \tag{3.104}$$

To prove (3.103), we define the following.

$$z_{1,j}^n(\theta_0):=\frac{h}{T_n}[\partial_{\lambda,A,B}a_{j-1}(\theta_0)]^2; \tag{3.105}$$

$$z_{2,j}^n(\theta_0):=\frac{h}{T_n^2}[\partial_{\lambda,A,B}a_{j-1}(\theta_0)][\partial_\delta a_{j-1}(\theta_0)]; \tag{3.106}$$

$$z_{3,j}^n(\theta_0):=\frac{h}{T_n^3}[\partial_\delta a_{j-1}(\theta_0)]^2. \tag{3.107}$$

Here and in the sequel, $\partial_{\theta_i,\theta_l,\theta_m}a$ denotes the first derivative of $a$ with respect to $\theta_i$, $\theta_l$, and $\theta_m$, respectively. First, we observe (3.105). We find

$$\sum_{j=1}^n\mathbb{E}_0^{j-1}\left[\frac{1}{n}[\partial_\lambda a_{j-1}(\theta_0)]^2\right]=\frac{1}{n}\sum_{j=1}^n Y_{t_{j-1}}^2, \tag{3.108}$$

and also,

$$\sum_{j=1}^n\mathbb{E}_0^{j-1}\left[\left(\frac{h}{T_n}[\partial_\lambda a_{j-1}(\theta_0)]^2\right)^2\right]=\frac{1}{n^2}\sum_{j=1}^n[\partial_\lambda a_{j-1}(\theta_0)]^4=\frac{1}{n}\left\{\frac{1}{n}\sum_{j=1}^n Y_{j-1}^4\right\}. \tag{3.109}$$

Since we have (3.42) then we obtain

$$\sum_{j=1}^n\mathbb{E}_0^{j-1}\left[\left(\frac{h}{T_n}[\partial_\lambda a_{j-1}]^2\right)^2\right]\xrightarrow{p}0. \tag{3.110}$$

Having (3.108) with (3.35) and (3.36); (3.109) in hand, then we have

$$\frac{1}{n}\sum_{j=1}^n[\partial_\lambda a_{j-1}(\theta_0)]^2\xrightarrow{p}C, \tag{3.111}$$

with $C$ (3.36).

Observe that

$$\sum_{j=1}^{n}\mathbb{E}_0^{j-1}\left[\frac{1}{n}[\partial_\lambda a_{j-1}(\theta_0)][\partial_{A_K}a_{j-1}(\theta_0)]\right]=-\frac{1}{n}\sum_{j=1}^{n}Y_{t_{j-1}}\cos(\omega_{0,K}t_{j-1}). \tag{3.112}$$

By applying Lemma 3.3 to (3.112), and using the fact

$$\sum_{j=1}^{n}\mathbb{E}_0^{j-1}\left[\left(\frac{h}{T_n}[\partial_\lambda a_{j-1}(\theta_0)][\partial_{A_K}a_{j-1}(\theta_0)]\right)^2\right]=\frac{1}{n}\left\{\frac{1}{2n}\sum_{j=1}^{n}Y_{t_{j-1}}^2\cos(\omega_{0,K}t_{j-1})+\frac{1}{2n}\sum_{j=1}^{n}Y_{t_{j-1}}^2\right\};$$

by using Lemma 3.4, (3.35), (3.36) , then $\sum_{j=1}^{n}\mathbb{E}_0^{j-1}\left[\left(\frac{h}{T_n}[\partial_\lambda a_{j-1}(\theta_0)][\partial_{A_K}a_{j-1}(\theta_0)]\right)^2\right]\xrightarrow{p}0$. Thus

$$\frac{1}{n}\sum_{j=1}^{n}[\partial_\lambda a_{j-1}(\theta_0)][\partial_{A_K}a_{j-1}(\theta_0)]\xrightarrow{p}0. \tag{3.113}$$

Quite similar to (3.113), we get

$$\frac{1}{n}\sum_{j=1}^{n}[\partial_\lambda a_{j-1}(\theta_0)][\partial_{B_K}a_{j-1}(\theta_0)]\xrightarrow{p}0, \tag{3.114}$$

and

$$\frac{1}{n}\sum_{j=1}^{n}[\partial_{A_K}a_{j-1}(\theta_0)][\partial_{B_L}a_{j-1}(\theta_0)]\xrightarrow{p}0, \tag{3.115}$$

for any $L\in\mathbb{N}$.

By Lemma 3.1, furthermore, it is easy to find that

$$\sum_{j=1}^{n}\mathbb{E}_0^{j-1}\left[\frac{1}{n}[\partial_{A_K}a_{j-1}(\theta_0)]^2\right]=\frac{1}{n}\sum_{j=1}^{n}\cos^2(\omega_{0,K}t_{j-1})=\frac{1}{2}+o\left(\frac{1}{T_n}\right);$$

and

$$\sum_{j=1}^{n}\mathbb{E}_0^{j-1}\left[\left(\frac{1}{n}[\partial_{A_K}a_{j-1}(\theta_0)]^2\right)^2\right]=\frac{1}{n^2}\sum_{j=1}^{n}\cos^4(\omega_{0,K}t_{j-1})=\frac{1}{n}\left\{\frac{3}{8}+o\left(\frac{1}{T_n}\right)\right\},$$

therefore,

$$\frac{1}{n}\sum_{j=1}^{n}[\partial_{A_K}a_{j-1}(\theta_0)]^2\xrightarrow{p}\frac{1}{2}. \tag{3.116}$$

In a quite similar manner to (3.116), we obtain

$$\frac{1}{n}\sum_{j=1}^{n}[\partial_{B_K}a_{j-1}(\theta_0)]^2\xrightarrow{p}\frac{1}{2}. \tag{3.117}$$

Using Lemma 3.1, in the same way as (3.111)-(3.117), we find

$$\frac{1}{n}\sum_{j=1}^{n}[\partial_{A_K}a_{j-1}(\theta_0)][\partial_{A_L}a_{j-1}(\theta_0)]\xrightarrow{p}0, \tag{3.118}$$

and

$$\frac{1}{n}\sum_{j=1}^{n}[\partial_{B_K}a_{j-1}(\theta_0)][\partial_{B_L}a_{j-1}(\theta_0)]\xrightarrow{p}0, \tag{3.119}$$

where $K\neq L$.

We are done with (3.105). Now, we turn to (3.106). Recalling (3.80), we find that

$$\sum_{j=1}^{n}\mathbb{E}_0^{j-1}\left[\frac{h}{T_n^2}[\partial_\lambda a_{j-1}(\theta_0)][\partial_\delta a_{j-1}(\theta_0)]\right]=\tilde{K}\frac{h}{T_n^2}\sum_{j=1}^{n}Y_{t_{j-1}}t_{j-1}\Big\{A_{0,K}\sin(\omega_{0,K}t_{j-1})-B_{0,K}\cos(\omega_{0,K}t_{j-1})\Big\},$$

applying Corollary 3.5, we have

$$\sum_{j=1}^{n}\mathbb{E}_0^{j-1}\left[\frac{h}{T_n^2}[\partial_\lambda a_{j-1}(\theta_0)][\partial_\delta a_{j-1}(\theta_0)]\right]\xrightarrow{p}0. \tag{3.120}$$

Also, we can obtain

$$\begin{aligned}&\sum_{j=1}^{n}\mathbb{E}_0^{j-1}\left[\left(\frac{h}{T_n^2}[\partial_\lambda a_{j-1}(\theta_0)][\partial_\delta a_{j-1}(\theta_0)]\right)^2\right]\\&=\frac{h^2}{T_n^4}\sum_{j=1}^{n}Y_{t_{j-1}}^2t_{j-1}^2\left\{A_{0,K}^2\sin^2(\omega_{0,K}t_{j-1})+B_{0,K}^2\cos^2(\omega_{0,K}t_{j-1})+2A_{0,K}B_{0,K}\sin(\omega_{0,K}t_{j-1})\cos(\omega_{0,K}t_{j-1})\right\},\end{aligned} \tag{3.121}$$

Applying (3.35) for the first and the second term of the right hand side of (3.121); Corollary 3.5 for the last term of the right hand side of (3.121), we get

$$\sum_{j=1}^{n}\mathbb{E}_0^{j-1}\left[\left(\frac{h}{T_n^2}[\partial_\lambda a_{j-1}(\theta_0)][\partial_\delta a_{j-1}(\theta_0)]\right)^2\right]\xrightarrow{p}0,$$

therefore, together with (3.120), we have

$$\frac{h}{T_n^2}\sum_{j=1}^{n}[\partial_\lambda a_{j-1}(\theta_0)][\partial_\delta a_{j-1}(\theta_0)]\xrightarrow{p}0. \tag{3.122}$$

Next, we observe

$$\begin{aligned}&\sum_{j=1}^{n}\mathbb{E}_0^{j-1}\left[\frac{h}{T_n^2}[\partial_{A_K}a_{j-1}(\theta_0)][\partial_\delta a_{j-1}(\theta_0)]\right]\\&=-\frac{h}{T_n^2}\left\{\tilde{K}A_{0,K}\sum_{j=1}^{n}t_{j-1}\cos(\omega_{0,K}t_{j-1})\sin(\omega_{0,K}t_{j-1})-\tilde{K}B_{0,K}\sum_{j=1}^{n}t_{j-1}\cos^2(\omega_{0,K}t_{j-1})\right\}.\end{aligned} \tag{3.123}$$

Applying Corollary 3.2, Lemma 3.1 to the first term and the last term of the right hand side of (3.123), respectively; using the fact

$$\sum_{j=1}^{n}\mathbb{E}_0^{j-1}\left[\left(\frac{h}{T_n^2}[\partial_{A_K}a_{j-1}(\theta_0)][\partial_\delta a_{j-1}(\theta_0)]\right)^2\right]\xrightarrow{p}0,$$

we thus find

$$\frac{h}{T_n^2}\sum_{j=1}^{n}[\partial_{A_K} a_{j-1}(\theta_0)][\partial_\delta a_{j-1}(\theta_0)] \xrightarrow{p} \frac{\tilde{K}B_{0,K}}{4}. \tag{3.124}$$

Quite similarly to (3.124), we can obtain

$$\frac{h}{T_n^2}\sum_{j=1}^{n}[\partial_{B_K} a_{j-1}(\theta_0)][\partial_\delta a_{j-1}(\theta_0)] \xrightarrow{p} -\frac{\tilde{K}A_{0,K}}{4}. \tag{3.125}$$

Last, we look at case (3.107):

$$\begin{aligned}\sum_{j=1}^{n}\mathbb{E}_0^{j-1}\left[\frac{h}{n^3h^3}[\partial_\delta a_{j-1}(\theta_0)]^2\right] &= \frac{h}{T_n^3}\sum_{j=1}^{n}\Big[-t_{j-1}\tilde{K}(A_{0,K}\sin(\omega_{0,K}t_{j-1})-B_{0,K}\cos(\omega_{0,K}t_{j-1}))\Big]^2\\ &= \frac{h}{T_n^3}\sum_{j=1}^{n}t_{j-1}^2\tilde{K}^2\Big(A_{0,K}^2\sin^2(\omega_{0,K}t_{j-1})+B_{0,K}^2\cos^2(\omega_{0,K}t_{j-1})\Big)\\ &- 2A_{0,K}B_{0,K}\frac{h}{T_n^3}\sum_{j=1}^{n}t_{j-1}^2\tilde{K}^2\sin(\omega_{0,K}t_{j-1})\cos(\omega_{0,K}t_{j-1}).\end{aligned} \tag{3.126}$$

By Lemma 3.1 to the first and the second term of the right hand side of (3.126); Corollary 3.2 to the last term of the right hand side of (3.126); also, together with

$$\sum_{j=1}^{n}\mathbb{E}_0^{j-1}\left[\left(\frac{h}{n^3h^3}[\partial_\delta a_{j-1}(\theta_0)]^2\right)^2\right] \xrightarrow{p} 0,$$

then we can deduce that

$$\frac{h}{n^3h^3}\sum_{j=1}^{n}[\partial_\delta a_{j-1}(\theta_0)]^2 \xrightarrow{p} \frac{\tilde{K}^2}{6}\Big[A_{0,K}^2+B_{0,K}^2\Big]. \tag{3.127}$$

From (3.111)-(3.127), (3.102), with (3.85) and (3.100), we can deduce that there exists $\mathbf{M}_0(\theta_0)$ (3.98) such that (3.103) holds (see Appendix C for the positive semi-definite of the matrix).

Now, we turn to the proof of

$$\sup_\theta|\mathbf{M}_n(\theta)-\mathbf{M}_0(\theta)| \xrightarrow{p} 0 \quad as \quad n\to\infty. \tag{3.128}$$

Let

$$\mathbb{M}_{1,n}(\theta) := -\frac{1}{T_n}\sum_{j=1}^{n}\Big\{[\Delta_j Y - a_{j-1}(\theta)h]\partial_\theta^2 a_{j-1}(\theta) - h[\partial_\theta a_{j-1}(\theta)]^2\Big\}. \tag{3.129}$$

From (3.129), we get

$$\sup_\lambda|m_{1,n}(\theta)| \xrightarrow{p} 0, \tag{3.130}$$

where

$$m_{1,n}(\theta)=-\frac{1}{T_n}\sum_{j=1}^{n}\left\{[\Delta_j Y-a_{j-1}(\theta_0)h]\partial_\lambda^2 a_{j-1}(\theta_0)-h[\partial_\lambda a_{j-1}(\theta_0)]^2\right\}+\partial_\lambda\mathbb{M}_{1,n}(\tilde{\lambda})(\lambda-\lambda_0)-C.$$

Using Lemma 3.13; (3.111), and $\partial_\lambda\mathbb{M}_{1,n}(\tilde{\lambda})=o_p(1)$, then we have

$$\begin{aligned}
&\sup_\lambda|m_{1,n}(\theta)|\\
&\le\sup_\lambda\left\{\left|-\frac{1}{T_n}\sum_{j=1}^{n}[\Delta_j Y-a_{j-1}(\theta_0)h]\partial_\lambda^2 a_{j-1}(\theta_0)\right|+\left|\frac{h}{T_n}\sum_{j=1}^{n}[\partial_\lambda a_{j-1}(\theta_0)]^2-C\right|+\left|\partial_\lambda\mathbb{M}_{1,n}(\tilde{\lambda})(\lambda-\lambda_0)\right|\right\}\\
&=o_p(1).
\end{aligned}$$

Quite similarly to above and using (3.116), we get

$$\sup_{A_K}|m_{2,n}(\theta)|\xrightarrow{p}0, \tag{3.131}$$

where

$$\begin{aligned}
m_{2,n}(\theta) &= -\frac{1}{T_n}\sum_{j=1}^{n}\left\{[\Delta_j Y-a_{j-1}(\theta_0)h]\partial_{A_K}^2 a_{j-1}(\theta_0)-h[\partial_{A_K} a_{j-1}(\theta_0)]^2\right\}\\
&+ \partial_{A_K}\mathbb{M}_{1,n}(\tilde{A}_K)(A_K-A_{0,K})-\frac{1}{2}.
\end{aligned}$$

And by using(3.117),

$$\sup_{B_K}|m_{3,n}(\theta)|\xrightarrow{p}0, \tag{3.132}$$

where

$$\begin{aligned}
m_{3,n}(\theta) &= -\frac{1}{T_n}\sum_{j=1}^{n}\left\{[\Delta_j Y-a_{j-1}(\theta_0)h]\partial_{B_K}^2 a_{j-1}(\theta_0)-h[\partial_{B_K} a_{j-1}(\theta_0)]^2\right\}\\
&+ \partial_{B_K}\mathbb{M}_{1,n}(\tilde{B}_K)(B_K-B_{0,K})-\frac{1}{2}.
\end{aligned}$$

Following the same lines as (3.130)-(3.132), by applying (3.113)-(3.115), (3.118), and (3.119), respectively, we obtain

$$\begin{aligned}
&\sup_{A_K}|m_{4,n}(\theta)|\xrightarrow{p}0, \quad \sup_{B_K}|m_{5,n}(\theta)|\xrightarrow{p}0,\\
&\sup_{A_K}|m_{6,n}(\theta)|\xrightarrow{p}0, \quad \sup_{A_K}|m_{7,n}(\theta)|\xrightarrow{p}0, \quad \sup_{B_K}|m_{8,n}(\theta)|\xrightarrow{p}0,
\end{aligned} \tag{3.133}$$

where

$$m_{4,n}(\theta) = -\frac{1}{T_n}\sum_{j=1}^{n}\left\{[\Delta_j Y-a_{j-1}(\theta_0)h]\partial_{\lambda A_K}^2 a_{j-1}(\theta_0)-h[\partial_\lambda a_{j-1}(\theta_0)][\partial_{A_K} a_{j-1}(\theta_0)]\right\}$$

$$
\begin{aligned}
&+\quad \partial_{A_K}\mathbb{M}_{1,n}(\tilde{A}_K)(A_K-A_{0,K}),\\
m_{5,n}(\theta) &= -\frac{1}{T_n}\sum_{j=1}^{n}\Big\{[\Delta_j Y-a_{j-1}(\theta_0)h]\partial^2_{\lambda B_K}a_{j-1}(\theta_0)-h[\partial_\lambda a_{j-1}(\theta_0)][\partial_{B_K}a_{j-1}(\theta_0)]\Big\}\\
&+\quad \partial_{B_K}\mathbb{M}_{1,n}(\tilde{B}_K)(B_K-B_{0,K}),\\
m_{6,n}(\theta) &= -\frac{1}{T_n}\sum_{j=1}^{n}\Big\{[\Delta_j Y-a_{j-1}(\theta_0)h]\partial^2_{A_K B_L}a_{j-1}(\theta_0)-h[\partial_{A_K} a_{j-1}(\theta_0)][\partial_{B_L}a_{j-1}(\theta_0)]\Big\}\\
&+\quad \partial_{A_K}\mathbb{M}_{1,n}(\tilde{A}_K)(A_K-A_{0,K}),\quad L\in\mathbb{N},\\
m_{7,n}(\theta) &= -\frac{1}{T_n}\sum_{j=1}^{n}\Big\{[\Delta_j Y-a_{j-1}(\theta_0)h]\partial^2_{A_K A_L}a_{j-1}(\theta_0)-h[\partial_{A_K} a_{j-1}(\theta_0)][\partial_{A_L}a_{j-1}(\theta_0)]\Big\}\\
&+\quad \partial_{A_K}\mathbb{M}_{1,n}(\tilde{A}_K)(A_K-A_{0,K}),\quad K\neq L,\\
m_{8,n}(\theta) &= -\frac{1}{T_n}\sum_{j=1}^{n}\Big\{[\Delta_j Y-a_{j-1}(\theta_0)h]\partial^2_{B_K B_L}a_{j-1}(\theta_0)-h[\partial_{B_K} a_{j-1}(\theta_0)][\partial_{B_L}a_{j-1}(\theta_0)]\Big\}\\
&+\quad \partial_{B_K}\mathbb{M}_{1,n}(\tilde{B}_K)(B_K-B_{0,K}),\quad K\neq L.
\end{aligned}
$$

We move to the following

$$
\mathbb{M}_{2,n}(\theta):=-\frac{1}{T_n^3}\sum_{j=1}^{n}\Big\{[\Delta_j Y-a_{j-1}(\theta)h]\partial^2_{\theta}a_{j-1}(\theta)-h[\partial_\theta a_{j-1}(\theta)]^2\Big\}. \tag{3.134}
$$

Using (3.134) and (3.127), with similar proof to (3.129)-(3.133), we find

$$
\sup_{\delta}|m_{9,n}(\theta)|\xrightarrow{p}0, \tag{3.135}
$$

where

$$
\begin{aligned}
m_{9,n}(\theta) &= -\frac{1}{T_n^3}\sum_{j=1}^{n}\Big\{[\Delta_j Y-a_{j-1}(\theta_0)h]\partial^2_{\delta}a_{j-1}(\theta_0)-h[\partial_\delta a_{j-1}(\theta_0)]^2\Big\}\\
&+\quad \partial_{\delta}\mathbb{M}_{2,n}(\tilde{\delta})(\delta-\delta_0)-\frac{\tilde{K}^2}{6}[A^2_{0,K}+B^2_{0,K}].
\end{aligned}
$$

At last, we define

$$
\mathbb{M}_{3,n}(\theta):=-\frac{1}{T_n^2}\sum_{j=1}^{n}\Big\{[\Delta_j Y-a_{j-1}(\theta)h]\partial^2_{\theta}a_{j-1}(\theta)-h[\partial_\theta a_{j-1}(\theta)]^2\Big\}. \tag{3.136}
$$

Based on (3.136), together with (3.122), (3.124), and (3.125), respectively, we get

$$
\sup_{\lambda}|m_{10,n}(\theta)|\xrightarrow{p}0,\quad \sup_{A_K}|m_{11,n}(\theta)|\xrightarrow{p}0,\quad \sup_{B_K}|m_{12,n}(\theta)|\xrightarrow{p}0, \tag{3.137}
$$

where

$$
m_{10,n}(\theta) = -\frac{1}{T_n^2}\sum_{j=1}^{n}\Big\{[\Delta_j Y-a_{j-1}(\theta_0)h]\partial^2_{\lambda\delta}a_{j-1}(\theta_0)-h[\partial_\lambda a_{j-1}(\theta_0)][\partial_\delta a_{j-1}(\theta_0)]\Big\}
$$

$$
\begin{aligned}
&+ \quad \partial_\lambda \mathbb{M}_{3,n}(\tilde{\lambda})(\lambda-\lambda_0),\\
m_{11,n}(\theta) \quad &= \quad -\frac{1}{T_n^2}\sum_{j=1}^{n}\left\{[\Delta_j Y - a_{j-1}(\theta_0)h]\partial^2_{A_K\delta}a_{j-1}(\theta_0) - h[\partial_{A_K}a_{j-1}(\theta_0)][\partial_\delta a_{j-1}(\theta_0)]\right\}\\
&+ \quad \partial_{A_K}\mathbb{M}_{3,n}(\tilde{A}_K)(A_K - A_{0,K}) - \frac{\tilde{K}B_{0,K}}{4},\\
m_{12,n}(\theta) \quad &= \quad -\frac{1}{T_n^2}\sum_{j=1}^{n}\left\{[\Delta_j Y - a_{j-1}(\theta_0)h]\partial^2_{B_K\delta}a_{j-1}(\theta_0) - h[\partial_{B_K}a_{j-1}(\theta_0)][\partial_\delta a_{j-1}(\theta_0)]\right\}\\
&+ \quad \partial_{B_K}\mathbb{M}_{3,n}(\tilde{B}_K)(B_K - B_{0,K}) - \left(-\frac{\tilde{K}A_{0,K}}{4}\right).
\end{aligned}
$$

Finally, (3.128) holds through (3.130)-(3.137).

We turn to prove (3.104) with define

$$
\begin{aligned}
S^n_{1,j}(\theta_0) &:= \frac{\sigma}{\sqrt{T_n}}\Delta_j w \partial_\lambda a_{j-1}(\theta_0),\\
S^n_{2,K,j}(\theta_0) &:= \frac{\sigma}{\sqrt{T_n}}\Delta_j w \partial_{A_K} a_{j-1}(\theta_0),\\
S^n_{3,K,j}(\theta_0) &:= \frac{\sigma}{\sqrt{T_n}}\Delta_j w \partial_{B_K} a_{j-1}(\theta_0),\\
S^n_{4,j}(\theta_0) &:= \frac{\sigma}{\sqrt{T_n^3}}\Delta_j w \partial_\delta a_{j-1}(\theta_0).
\end{aligned}
$$

Observe that

$$
\sum_{j=1}^{n}\mathbb{E}_0^{j-1}\left[\left(S^n_{1,j}(\theta_0)\right)^2\right] = \sigma^2\frac{h}{T_n}\sum_{j=1}^{n}[\partial_\lambda a_{j-1}(\theta_0)]^2,
$$

and by plugging (3.111), we get

$$
\sum_{j=1}^{n}\mathbb{E}_0^{j-1}\left[\left(S^n_{1,j}(\theta_0)\right)^2\right] \xrightarrow{p} \sigma^2 C, \tag{3.138}
$$

with $C$ (3.36). Using a similar way to (3.138), by (3.116), (3.117), we obtain

$$
\sum_{j=1}^{n}\mathbb{E}_0^{j-1}\left[\left(S^n_{2,K,j}(\theta_0)\right)^2\right] \xrightarrow{p} \sigma^2\frac{1}{2}, \tag{3.139}
$$

and

$$
\sum_{j=1}^{n}\mathbb{E}_0^{j-1}\left[\left(S^n_{3,K,j}(\theta_0)\right)^2\right] \xrightarrow{p} \sigma^2\frac{1}{2}. \tag{3.140}
$$

Using (3.127), (3.113), (3.114), (3.122), (3.124), and (3.125) we have

$$
\sum_{j=1}^{n}\mathbb{E}_0^{j-1}\left[\left(S^n_{4,j}(\theta)\right)^2\right] \xrightarrow{p} \sigma^2\frac{\tilde{K}^2}{6}\left[A^2_{0,K}+B^2_{0,K}\right], \tag{3.141}
$$

$$
\sum_{j=1}^{n}\mathbb{E}_0^{j-1}\left[S^n_{1,j}(\theta_0)S^n_{2,K,j}(\theta_0)\right] \xrightarrow{p} 0, \tag{3.142}
$$

$$\sum_{j=1}^{n}\mathbb{E}_0^{j-1}\Big[S_{1,j}^n(\theta_0)S_{3,K,j}^n(\theta_0)\Big]\xrightarrow{p}0, \tag{3.143}$$

$$\sum_{j=1}^{n}\mathbb{E}_0^{j-1}\Big[S_{1,j}^n(\theta_0)S_{4,j}^n(\theta_0)\Big]\xrightarrow{p}0, \tag{3.144}$$

$$\sum_{j=1}^{n}\mathbb{E}_0^{j-1}\Big[S_{2,K,j}^n(\theta_0)S_{4,j}^n(\theta_0)\Big]\xrightarrow{p}\sigma^2\frac{\tilde{K}B_{0,K}}{4}, \tag{3.145}$$

$$\sum_{j=1}^{n}\mathbb{E}_0^{j-1}\Big[S_{3,K,j}^n(\theta_0)S_{4,j}^n(\theta_0)\Big]\xrightarrow{p}-\sigma^2\frac{\tilde{K}A_{0,K}}{4}. \tag{3.146}$$

Since we have (3.118), (3.119), then we obtain

$$\sum_{j=1}^{n}\mathbb{E}_0^{j-1}\Big[S_{2,K,j}^n(\theta_0)S_{2,L,j}^n(\theta_0)\Big]\xrightarrow{p}0, \tag{3.147}$$

$$\sum_{j=1}^{n}\mathbb{E}_0^{j-1}\Big[S_{3,K,j}^n(\theta_0)S_{3,L,j}^n(\theta_0)\Big]\xrightarrow{p}0, \tag{3.148}$$

with $K \neq L$. Also, using (3.115),

$$\sum_{j=1}^{n}\mathbb{E}_0^{j-1}\Big[S_{2,K,j}^n(\theta_0)S_{3,L,j}^n(\theta_0)\Big]\xrightarrow{p}0, \tag{3.149}$$

with $L \in \mathbb{N}$. From the properties of (3.138)-(3.149), and

$$\sum_{j=1}^{n}\mathbb{E}_0^{j-1}\Big[S_{i,\cdot,j}^n(\theta_0)\Big]\xrightarrow{p}0,$$

then we find (3.104). This completes the proof. □

All Lemma and Theorem in Section 3.3 are the original finding of the thesis. The difference with the one provided in [Fuller, 2009], [Kundu and Nandi, 2012], [Rao and Rubin, 1979] is the presence of the continuous-time signal in the SDE (2.1). This function should be treated with specific techniques in detail (e.g., A/D signal conversion). From the findings, we claim the rate convergence of $(\lambda, A, B)$ at $\sqrt{nh}$, while the rate convergence of $\delta$ at $\sqrt{n^3h^3}$.

# Chapter 4

# Numerical Experiments

[Gross and Galiana, 1987] defined electric power systems' short-term load forecasting as dealing with the prediction of the order of minutes, hours, and half hours up to 168 hours or a few weeks for the short-term problem. Whereas [Abu-Shikhah and Elkarmi, 2011] classified forecasting frames into long-term forecasting (1-20 years), medium-term (1-12 months), short-term (1-4 weeks), and very short-term (1-7 days ahead).

The numerical examples are presented to verify our theoretical findings in the previous section. We do a simulation study in Section 4.1, and we illustrate the proposed model (2.1) by describing the electric power and energy systems, namely: electricity load from Tokyo Electric Power Company (TEPCO), the energy consumption of light fixtures in one Belgium household, France household electric power, and a case study of Tetouan city's power consumption in Section 4.2. All calculations in the empirical results have been performed in the R program.

## 4.1 Simulation Study

Consider the cases of diffusion $\sigma = 1$. The simulation consists of the following steps:

1. Set a particular number of sinusoidal signals $K$, and step size $h$, we approximate $n$ elements $\{(Y_{t_j})_{j=0}^{n}\}$ of (3.1) with $\theta_0$, following the model setting in (2.1) and (1.4).

2. We estimate $\{\hat{\theta}_n^i\}_{i=1}^{L}$ by the optim function to be minimized is given by

$$\sum_{j=1}^{n} \frac{1}{h} \Big\{ Y_{t_j} - \Big( Y_{t_{j-1}} - \lambda h Y_{t_{j-1}} + h \quad h_{j-1}(\beta) \Big) \Big\}^2, \tag{4.1}$$

   where $L$ denotes the number of replicated runs.

3. Using the result in step 2, we calculate the mean and standard deviation of their estimates (*stdev*), then graph the histogram. The mean of their estimates and standard deviation of $\{\hat{\lambda}^i\}_{i=1}^{L}$,

$$\bar{\hat{\lambda}} = \frac{1}{L} \sum_{i=1}^{L} \hat{\lambda}^i$$

Table 4.1: The performance of the estimates concerning model (2.1), for $K=2$, and considered $n$ and $h$. The mean estimates is given with their standard deviation in parenthesis

| | $T_n=10$ $nh^2=1$ | $T_n=12.248$ $nh^2=0.5$ | $T_n=14.491$ $nh^2=0.3$ |
|---|---|---|---|
| $\lambda_0=1$ | 1.821 | 1.252 | 1.006 |
| | (0.207) | (0.057) | (0.028) |
| $A_{0,1}=1.5$ | 1.179 | 1.608 | 1.520 |
| | (0.211) | (0.052) | (0.028) |
| $B_{0,1}=1.5$ | 1.731 | 1.476 | 1.466 |
| | (0.179) | (0.066) | (0.032) |
| $A_{0,2}=1.5$ | 1.279 | 1.579 | 1.594 |
| | (0.401) | (0.104) | (0.062) |
| $B_{0,2}=1.5$ | 1.717 | 1.287 | 1.430 |
| | (0.344) | (0.117) | (0.063) |
| $\delta_0=0.785$ | 0.784 | 0.783 | 0.784 |
| | (0.002) | (0.0006) | (0.0005) |

and

$$stdev\left(\hat{\lambda}\right)=\sqrt{\frac{1}{L-1}\sum_{i=1}^{L}\left(\hat{\lambda}^i-\bar{\hat{\lambda}}\right)^2},$$

respectively. Similar arguments on the mean estimates and the standard deviation of the other estimates.

We perform simulations for $K=2$ and $K=3$. The mean of their estimates and their standard deviation are reported in Table 4.1, for $K=2$ over $L=2000$, and considered $(n,h)$, namely (100,0.1);(300,0.041), and (700,0.021). Whereas Table 4.2, for $K=3$ over $L=1000$, and considered $(n,h)$, namely (100,0.1);(300,0.045), and (800,0.019). The histogram of both simulations is shown in Figure 4.1 and Figure 4.2. Note that in the theoretical view, we have set $T_n\to\infty$ and $nh^2\to 0$. In our simulation, $T_n$ and $nh^2$ are set as mentioned in Table 4.1 and Table 4.2. It follows from Table 4.2 and Table4.1, the estimates seem better, in which $nh^2$ decreases and $T_n$ increases as well. This evidence is consistent with our theoretical findings in the previous section. From Figure 4.1 and Figure 4.2, we can see the histograms are approximately normal distributed.

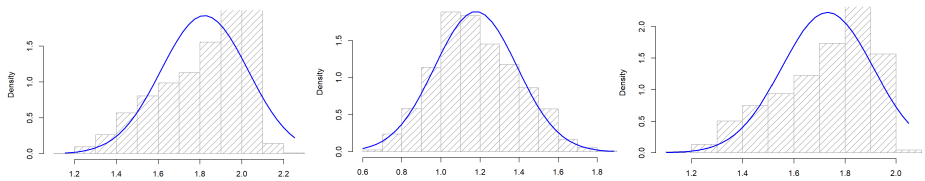

(a) $\hat{\lambda}$ (b) $\hat{A}_1$ (c) $\hat{B}_1$

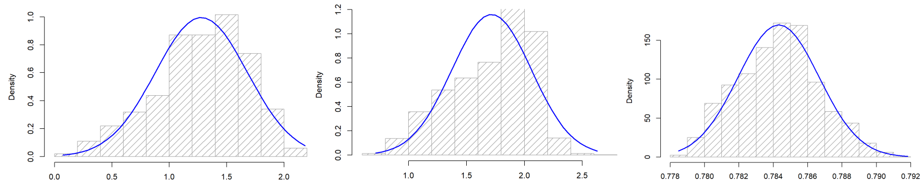

(d) $\hat{A}_2$ (e) $\hat{B}_2$ (f) $\hat{\delta}$

The histogram for $(n,h)=(100,0.1)$, with $\theta_0=(1,1.5,1.5,1.5,1.5,0.785)$.

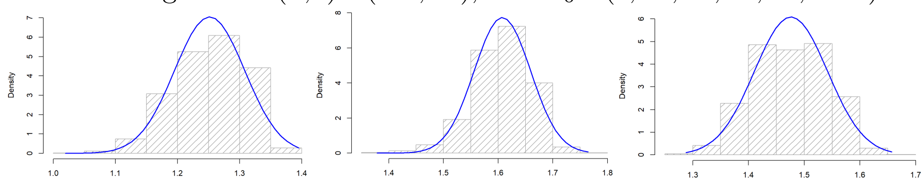

(g) $\hat{\lambda}$ (h) $\hat{A}_1$ (i) $\hat{B}_1$

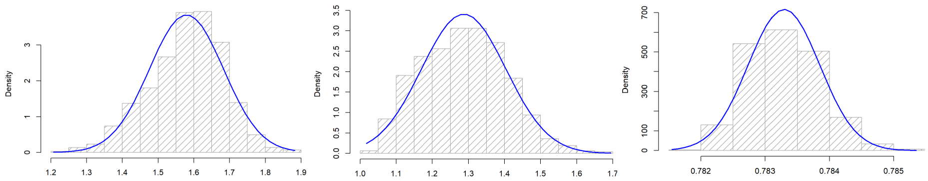

(j) $\hat{A}_2$ (k) $\hat{B}_2$ (l) $\hat{\delta}$

The histogram for $(n,h)=(300,0.041)$, with $\theta_0=(1,1.5,1.5,1.5,1.5,0.785)$.

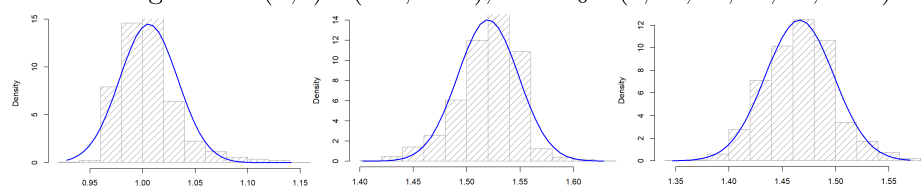

(m) $\hat{\lambda}$ (n) $\hat{A}_1$ (o) $\hat{B}_1$

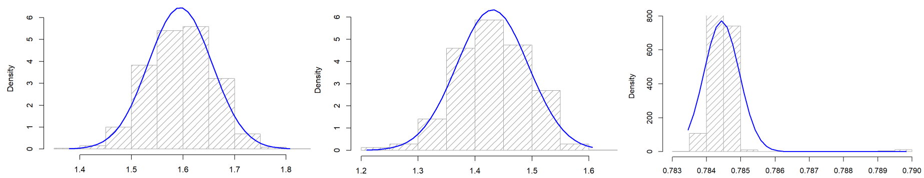

(p) $\hat{A}_2$ (q) $\hat{B}_2$ (r) $\hat{\delta}$

The histogram for $(n,h)=(700,0.021)$, with $\theta_0=(1,1.5,1.5,1.5,1.5,0.785)$.

Figure 4.1: Histogram of $\{\hat{\theta}_n^i\}_{i=1}^L$ with $L=2000$. The normal curve (solid blue line) is superimposed on the histogram.

Table 4.2: The performance of the estimates concerning model (2.1), for $K=3$, and considered $n$ and $h$. The mean estimates is given with their standard deviation in parenthesis

| | $T_n=10$ $nh^2=1$ | $T_n=13.416$ $nh^2=0.6$ | $T_n=15.492$ $nh^2=0.3$ |
|---|---|---|---|
| $\lambda_0=1$ | 1.876 | 1.324 | 0.972 |
| | (0.170) | (0.061) | (0.043) |
| $A_{0,1}=2$ | 1.544 | 1.894 | 2.085 |
| | (0.171) | (0.063) | (0.051) |
| $B_{0,1}=2$ | 2.349 | 2.279 | 1.940 |
| | (0.147) | (0.073) | (0.058) |
| $A_{0,2}=2$ | 1.396 | 2.056 | 2.112 |
| | (0.246) | (0.089) | (0.088) |
| $B_{0,2}=2$ | 2.268 | 1.912 | 1.884 |
| | (0.226) | (0.086) | (0.093) |
| $A_{0,3}=2$ | 1.766 | 2.057 | 2.082 |
| | (0.312) | (0.124) | (0.117) |
| $B_{0,3}=2$ | 2.041 | 1.855 | 1.850 |
| | (0.322) | (0.119) | (0.137) |
| $\delta_0=0.8$ | 0.801 | 0.800 | 0.780 |
| | (0.001) | (0.0003) | (0.0003) |

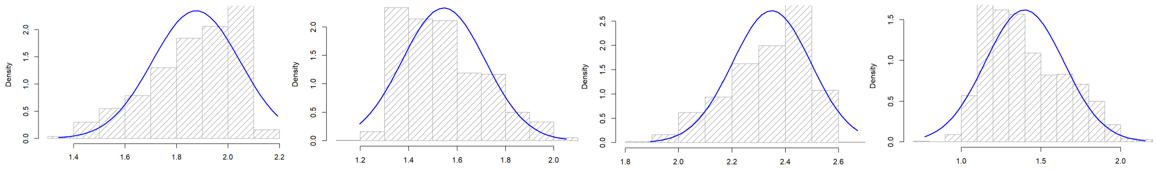

(a) $\hat{\lambda}$ (b) $\hat{A}_1$ (c) $\hat{B}_1$ (d) $\hat{A}_2$

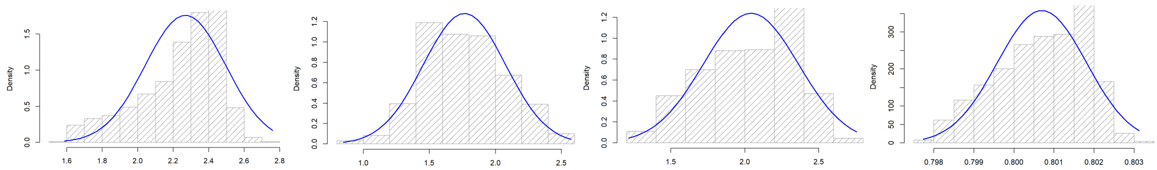

(e) $\hat{B}_2$ (f) $\hat{A}_3$ (g) $\hat{B}_3$ (h) $\hat{\delta}$

The histogram for $(n,h)=(100,0.1)$, with $\theta_0=(1,2,2,2,2,2,2,0.8)$.

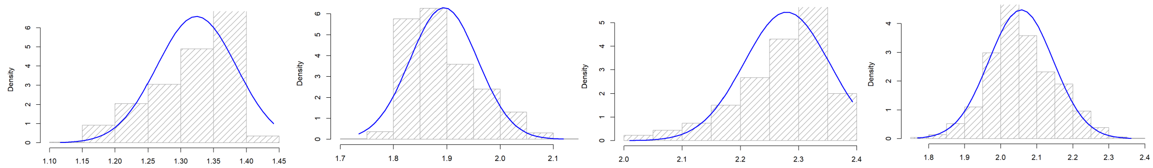

(i) $\hat{\lambda}$ (j) $\hat{A}_1$ (k) $\hat{B}_1$ (l) $\hat{A}_2$

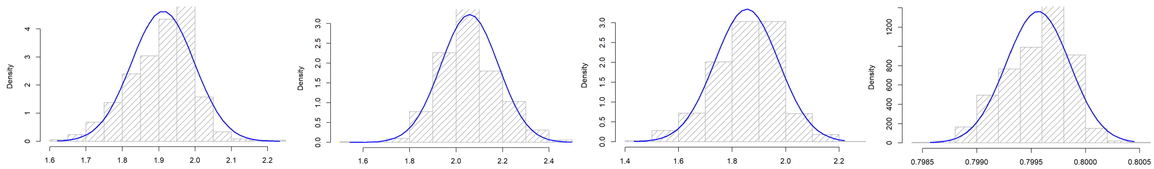

(m) $\hat{B}_2$ (n) $\hat{A}_3$ (o) $\hat{B}_3$ (p) $\hat{\delta}$

The histogram for $(n,h)=(300,0.045)$, with $\theta_0=(1,2,2,2,2,2,2,0.8)$.

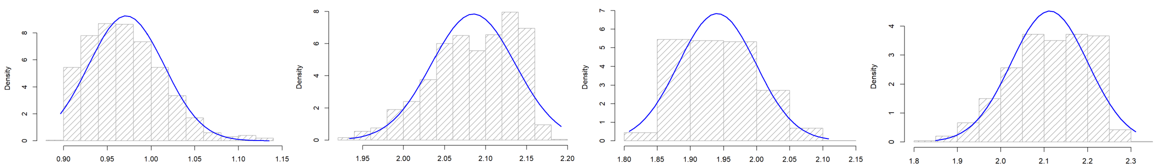

(q) $\hat{\lambda}$ (r) $\hat{A}_1$ (s) $\hat{B}_1$ (t) $\hat{A}_2$

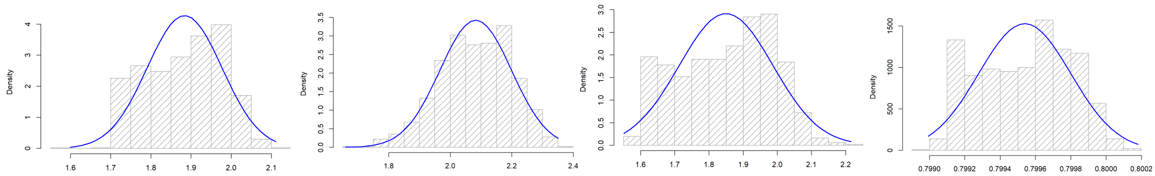

(u) $\hat{B}_2$ (v) $\hat{A}_3$ (w) $\hat{B}_3$ (x) $\hat{\delta}$

The histogram for $(n,h)=(800,0.019)$, with $\theta_0=(1,2,2,2,2,2,2,0.8)$.

Figure 4.2: Histogram of $\{\hat{\theta}_n^i\}_{i=1}^L$ with $L=1000$. The normal curve (solid blue line) is superimposed on the histogram.

## 4.2 Application to electric power and energy systems

The following is a list of the methodology's components considering the cases of diffusion $\sigma = 1$:

1. Set a particular number of sinusoidal signals $K$, and step size $h$ for $n$ samples of the real dataset as $(Y_{t_j})_{j=0}^{n}$ .
2. We set an initial of $\theta$ of (3.1), following the model setting in (2.1) and (1.4).
3. We estimate $\hat{\theta}_n$ of $(Y_{t_j})_{j=0}^{n_{tr}}$ by the `optim` function; recall that the objective function to be minimized is
$$\sum_{j=1}^{n_{tr}} \frac{1}{h}\Big\{Y_{t_j} - \Big(Y_{t_{j-1}} - \lambda h Y_{t_{j-1}} + h \quad h_{j-1}(\beta)\Big)\Big\}^2, \tag{4.2}$$
(see Appendix D for the convexity of the function).
4. Using the result in step 3, we calculate the Root Mean Squares Error (RMSE) of $(Y_{t_j})_{j=0}^{n_{tr}}$ and $(Y_{t_j})_{n_{tr}+1}^{n}$, that is,
$$\sqrt{\frac{1}{n_{tr}} \sum_{j=1}^{n_{tr}} \Big\{Y_{t_j} - \Big(Y_{t_{j-1}} - \lambda h Y_{t_{j-1}} + h \quad h_{j-1}(\beta)\Big)\Big\}^2},$$
$$\sqrt{\frac{1}{n_{ts}} \sum_{n_{tr}+1}^{n} \Big\{Y_{t_j} - \Big(Y_{t_{j-1}} - \lambda h Y_{t_{j-1}} + h \quad h_{j-1}(\beta)\Big)\Big\}^2},$$
where $n_{ts}$ is the number of test samples, and then observe the measurement in different configurations of $h$,$n$ and $K$.

We need to set an initial of $\theta$ to the equation in terms of the parenthesis of (4.2). This term is used to perform the initial least-squares error. It returns a least-squares object. Then the objective function is called to be optimized.

In this study, we implement a train-test split to evaluate the model that consists of splitting the dataset into training and testing sets; namely, we select an arbitrary split point: all records up to the split points are taken as the training dataset, and all the records from the split point to the end of observations is taken as the test set. One set was then used to train the model, and the testing dataset was used to evaluate the model (see, e.g., in [Igual and Seguí, 2017] and [Brownlee, 2016]).

### 4.2.1 Electricity load from TEPCO

In this Section, we analyze the empirical performance of $\hat{\theta}_n$ of the past electricity demand data with the theoretical values provided by the proposed model (2.1). A short-term dataset was obtained from TEPCO Holdings's files [TEPCO, 2016], and consisted of twenty-four-time series, one for each hour during a day, of hourly power demand system electricity consumption, with three decimal points.

The twenty-four electricity consumption time series, for the seven years, starting April 1, 2016, and ending June 9, 2022, as a first casual look at the hourly system electricity ($Y$ represents the electricity load, in kW) time series in Figure 4.3, which exhibits a seasonal and periodicity pattern. A repeating pattern within any fixed period is known as seasonal variation ([Metcalfe and Cowpertwait, 2009]), while a periodicity is a pattern in a time series that occurs at regular time intervals ([Puech et al., 2019]). Figure 4.3 also shows a trend of mean reversion, that is, when the load is high, its demand tends to increase, putting downforce on the load. Conversely, when the load is low, the electricity demand tends to decrease, providing an uplift to the load.

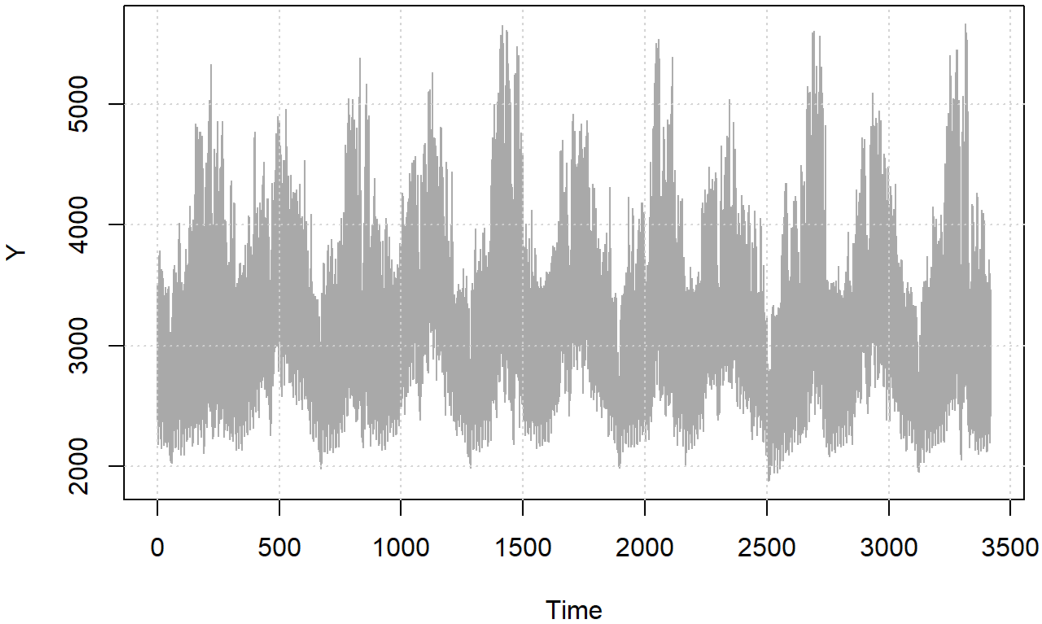


Figure 4.3: Hourly System Electricity Time Series (2016-2022)

Table 4.3-4.5 summarizes the overall results of performance of $\hat{\theta}_n$ concerning model (2.1) corresponding to different $n$ and $h$ for 2017, 2018, and 2019 loads; with their RMSE. We took the past electricity demand data in the period January 17, 2017, to July 11, 2017; January 27 to December 8, 2018; February 11 to June 16, 2019. From Table 4.3 and Table 4.5, it seems that the models are overfitting. A model is overfitting if there exists a less complex model with a lower test RMSE [Alshboul et al., 2022]. Overfitting indicates that the model fits the data very well, but due to the complexity of the pattern of the seasonality for any particular time series, we should care to predict the new data of the same system. Table 4.4 for $n = 7500$ reports the results that the models are relatively underfitting. A model is underfitting if there exists a more complex model with lower test RMSE [Alshboul et al., 2022]. Further, the models seem underfitting.

In this case, and the sequel, we compare the performance of $\hat{\theta}_n$ with the least absolute deviation-estimators (LADE), $\check{\theta}_n$; just for computationally comparisons. With the same methodology step in Section 4.2, excluding step 3, and change the objective function (4.2) with

Table 4.3: The performance of $\hat{\theta}_n$ concerning model (2.1), for electricity load in 2017, and considered $n$ and $h$; just for comparison. The RMSE of the train is given with the RMSE of the test in parenthesis

| $\hat{\theta}_n$ | $h=0.03$ | | $n=4000$ | | |
|---|---|---|---|---|---|
| | $n=4100$ | $n=4200$ | $h=0.03$ | $h=0.09$ | $h=0.3$ |
| $\hat{\lambda}$ | 0.005 | 0.005 | 0.005 | 0.002 | 0.0005 |
| $\hat{A}_1$ | 1.513 | 1.524 | 1.529 | 1.374 | 1.523 |
| $\hat{B}_1$ | 1.782 | 1.787 | 1.780 | 1.810 | 1.674 |
| $\hat{A}_2$ | 1.528 | 1.492 | 1.499 | 1.528 | 1.442 |
| $\hat{B}_2$ | 1.754 | 1.753 | 1.756 | 1.801 | 1.619 |
| $\hat{\delta}$ | 1.530 | 1.546 | 1.526 | 1.523 | 1.829 |
| RMSE | 528.936 | 541.560 | 527.781 | 527.764 | 527.790 |
| | (1058.368) | (1168.052) | (838.256) | (838.063) | (838.160) |

Table 4.4: The performance of $\hat{\theta}_n$ concerning model (2.1), for electricity load in 2018, and considered $n$ and $h$; just for comparison. The RMSE of the train is given with the RMSE of the test in parenthesis

| $\hat{\theta}_n$ | $h=0.07$ | | $n=7500$ | | |
|---|---|---|---|---|---|
| | $n=7450$ | $n=7550$ | $h=0.7$ | $h=0.1$ | $h=0.07$ |
| $\hat{\lambda}$ | 0.0007 | 0.0007 | 0.00007 | 0.0005 | 0.0007 |
| $\hat{A}_1$ | 1.517 | 1.516 | 1.431 | 1.481 | 1.538 |
| $\hat{B}_1$ | 1.798 | 1.791 | 1.916 | 1.873 | 1.799 |
| $\hat{A}_2$ | 1.497 | 1.506 | 1.498 | 1.439 | 1.497 |
| $\hat{B}_2$ | 1.765 | 1.762 | 1.734 | 1.794 | 1.754 |
| $\hat{\delta}$ | 1.517 | 1.531 | 1.500 | 1.506 | 1.522 |
| RMSE | 779.218 | 775.608 | 778.058 | 777.130 | 777.139 |
| | (451.756) | (480.421) | (463.496) | (462.103) | (462.057) |

Table 4.5: The performance of $\hat{\theta}_n$ concerning model (2.1), for $n=3000$ of electricity load in 2019, and considered $h$; just for comparison. The RMSE of the train is given with the RMSE of the test in parenthesis

| | | $n=3000$ | |
|---|---|---|---|
| $\hat{\theta}_n$ | $h=0.05$ | $h=0.065$ | $h=0.071$ |
| $\hat{\lambda}$ | 0.005 | 0.004 | 0.004 |
| $\hat{A}_1$ | 0.693 | 0.681 | 0.699 |
| $\hat{B}_1$ | 0.960 | 0.974 | 0.977 |
| $\hat{A}_2$ | 0.608 | 0.605 | 0.596 |
| $\hat{B}_2$ | 0.846 | 0.836 | 0.838 |
| $\hat{\delta}$ | 0.575 | 0.568 | 0.567 |
| RMSE | 610.483 (921.875) | 610.486 (921.974) | 610.479(921.990) |

the LADE, that is,

$$\check{\theta}_n \in \underset{\theta}{\operatorname{argmin}} \sum_{j=1}^{n} \left| Y_{t_j} - \left( Y_{t_{j-1}} - \lambda h Y_{t_{j-1}} + h h_{j-1}(\beta) \right) \right|.$$

It can be seen from Table 4.4; for electricity load in 2018, $n=7500; h=0.1, 0.07$, and Table 4.6, that the performance of the LSE is better than the LADE.

Table 4.6: The performance of the $\check{\theta}_n$ concerning model (2.1), for electricity load in 2018, and considered $n$ and $h$; just for comparisons. The RMSE of the train is given with the RMSE of the test in parenthesis

| $n=7500$ | $\check{\theta}_n$ | RMSE |
|---|---|---|
| $h=0.1$ | (0.001, 1.375, 1.842, 1.559, 1.840, 1.433) | 781.582 (534.095) |
| $h=0.07$ | (0.001, 1.595, 1.543, 1.610, 1.726, 1.701) | 781.570 (533.819) |

### 4.2.2 Belgium household appliances energy

This study was applied to real data for the energy consumption of light fixtures in one Belgium household. These data are available at [UCI Machine Learning Repository, 2017] and the relevant paper at [Candanedo et al., 2017]. The dataset contains 19737 energy uses in the household with a ten-minute sampling rate over a period from January 11, to May 27, 2016. We use a train-test split of 67% to visualize the energy use plotted in Figure 4.4 which shows $(Y_{t_j})_{j=0}^{n}$ and

$$\left( Y_{t_{j-1}} - \lambda h Y_{t_{j-1}} + h \quad h_{j-1}(\beta) \right), \quad j=1,\ldots,n \tag{4.3}$$

of energy. We can see that the periodicity of $h_t(\beta)$ (see (1.2), (1.4) and (1.5)) can be seen from its repeated pattern over identical subsequent periods, which is finally shown in (4.3); it seems that the sample path $(Y_{t_j})_{j=0}^{n}$ can be approximated by a sinusoidal signal processing $h_{j-1}(\beta)$ in (4.3).

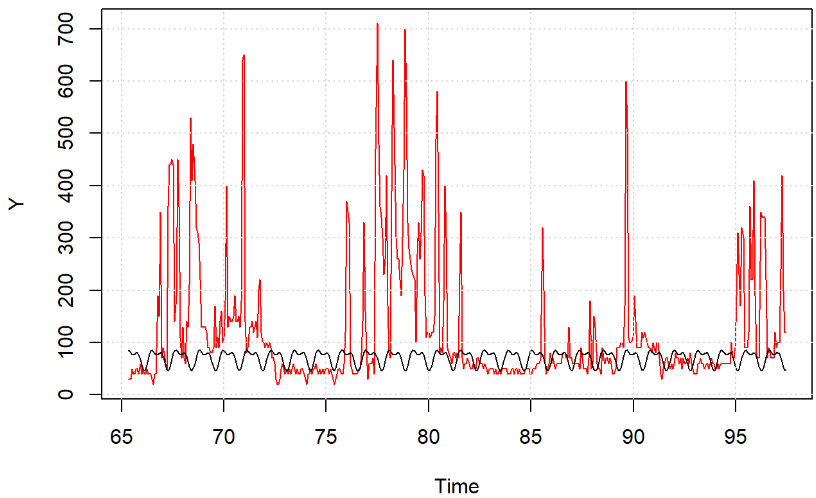


Figure 4.4: $(Y_{t_j})_{j=1006}^{1500}$ (red) and (4.3) (black) curves for 67% split test 1500 sample set (period from January 31, to February 3, 2016). $Y$ in Watt-hour of active energy; time in hours.

Table 4.7: The performance of $\hat{\theta}_n$ concerning model (2.1), for $h = 0.7$, and considered $n$; just for comparison. The performance of $\check{\theta}_n$ is given in the square. The RMSE of the training is given with the RMSE of the test in parenthesis

| $\hat{\theta}_n$ | $n = 18675$ | $n = 18700$ | $n = 18800$ |
|---|---|---|---|
| $\hat{\lambda}$ | 0.184 [-5.6e-05] | 0.229 [0.227] | 0.090 [-2.8e-05] |
| $\hat{A}_1$ | 1.510 [1.538] | 1.457 [1.483] | 1.506 [1.528] |
| $\hat{B}_1$ | 1.680 [1.760] | 1.758 [1.595] | 1.855 [1.752] |
| $\hat{A}_2$ | 1.517 [1.460] | 1.478 [1.553] | 1.506 [1.464] |
| $\hat{B}_2$ | 1.726 [1.746] | 1.764 [1.639] | 1.706 [1.755] |
| $\hat{\delta}$ | 1.597 [1.687] | 1.549 [1.754] | 1.573 [1.690] |
| RMSE of the LSE | 139.327 (136.860) | 139.242 (136.946) | 139.572(138.083) |
| RMSE of the LADE | 108.699 (95.626) | 139.257 (136.820) | 107.737 (99.137) |

When a train-test split of 90%, the results of the performance of the estimators and the RMSE of the training and testing are given in Table 4.7. From the training and testing of RMSE, the model is relatively underfitting. It follows that the forecast results obtained from the proposed model (2.1) with the LSE listed in Table 4.7 can be used in a ten-minute sampling of appliances' energy consumption with a large number of observations (period of measurement: January 18 to May 27, 2016). From Table 4.7 we can analyze that the LSE is better than the LADE.

### 4.2.3 France household electric power consumption

The time series is composed of a one-minute sampling rate of electric power consumption in a house located in Sceaux, Paris, France, between December 16, 2006, and ending December 13, 2008. The data set available at the [UCI Machine Learning Repository, 2012] is made available under the "Creative Commons Attribution 4.0 International (CC BY 4.0)" license. We considered four data of the energy consumed, namely:

- GAP represents the active energy consumed (in Wh) in the household by electrical equipment not measured in SM1 and SM2;
- GRP represents the reactive energy consumed (in Wh) in the household by electrical equipment not measured in SM1 and SM2;
- SM1 represents energy sub-metering no 1 (in Wh of active energy) corresponds to the kitchen, containing mainly a dishwasher, an oven, and a microwave;
- SM2 represents energy sub-metering no 2 (in Wh of active energy) corresponds to the laundry room, containing a washing machine, a tumble-drier, a refrigerator, and a light.

We analyze the empirical performance of $\hat{\theta}_n$ of the GAP and GRP; SM1 and SM2 with a train-test split of 90%. The performance of $\hat{\theta}_n$ and the RMSE is reported in Tables 4.8 and 4.9. From Table 4.8, the test RMSE of GAP is greater than the train RMSE. Whereas, for

Table 4.8: The performance of $\hat{\theta}_n$ concerning model (2.1) with $n$=900 of GAP and GRP, and considered $h$; just for comparison. The RMSE of the train is given with the RMSE of the test in parenthesis

| $\hat{\theta}_n$ | GAP | | GRP | |
|---|---|---|---|---|
| | $h$=0.7 | $h$=0.8 | $h$=0.7 | $h$=0.8 |
| $\hat{\lambda}$ | 0.002 | 0.002 | 0.053 | 0.067 |
| $\hat{A}_1$ | 0.485 | 0.487 | 0.510 | 0.539 |
| $\hat{B}_1$ | 0.528 | 0.495 | 1.036 | 0.979 |
| $\hat{A}_2$ | 0.731 | 0.713 | 1.027 | 1.052 |
| $\hat{B}_2$ | 0.360 | 0.464 | 0.812 | 3.527 |
| $\hat{\delta}$ | 0.848 | 0.761 | 0.694 | 0.643 |
| RMSE | 500.603 | 500.629 | 41.609 | 40.554 |
| | (506.358) | (506.705) | (27.995) | (25.345) |

Table 4.9: The performance of $\hat{\theta}_n$ concerning model (2.1), for SM1 and SM2, and considered $n$ and $h$; just for comparison. The RMSE of the train is given with the RMSE of the test in parenthesis

| $\hat{\theta}_n$ | SM1, $n$=2100 | | SM2, $h$=0.73 | | |
|---|---|---|---|---|---|
| | $h$=0.73 | $h$=0.83 | $n$=2100 | $n$=5100 | $n$=6100 |
| $\hat{\lambda}$ | 0.399 | 0.265 | −0.001 | 0.404 | 0.398 |
| $\hat{A}_1$ | 0.100 | 0.314 | 0.185 | 0.164 | 0.097 |
| $\hat{B}_1$ | 0.500 | 0.193 | 0.021 | 0.489 | 0.499 |
| $\hat{A}_2$ | 0.699 | 0.744 | 0.570 | 0.719 | 0.712 |
| $\hat{B}_2$ | 0.100 | 0.278 | 0.508 | 0.117 | 0.136 |
| $\hat{\delta}$ | 1.100 | 1.014 | 1.000 | 0.975 | 0.974 |
| RMSE | 6.738 | 6.742 | 9.546 | 12.220 | 12.021 |
| | (2.021) | (2.051) | (5.216) | (6.653) | (4.062) |

GRP, the test RMSE decreases as the train RMSE. The results indicate the model of GAP is overfitting, while the model of GRP is relatively underfitting.

As can be seen in Table 4.9, we can find out the fact that the test RMSE is less than the train RMSE. The model of SM1 and SM2 tends to be underfitting. The seasonality of the one-minute sampling rate of electric power consumption in the kitchen (period from December 16, to December 18, 2006) and laundry room (period from December 16, to December 20, 2006), can be approximated by (2.1) with the same periodic sinusoidal signal that its estimator listed in Table 4.9. This evidence indicates that the consumption of electric power in both rooms has the same pattern of periodicity in the given periods. Further, we also deduce that the performance of the LSE in Table 4.9 is better than the LADE in Table 4.10.

### 4.2.4 Power consumption of Tetouan city

According to reference [Salam and El Hibaoui, 2018], the data set that is available at [UCI Machine Learning Repository, 2021] comprises the power consumption data (in kWh) in

Table 4.10: The performance of $\check{\theta}_n$ concerning model (2.1), for SM1 and SM2, and considered $n$ and $h$; just for comparison. The RMSE of the train is given with the RMSE of the test in parenthesis

| $\check{\theta}_n$ | SM1, $n=2100$ | | SM2, $h=0.73$ | | |
|---|---|---|---|---|---|
| | $h=0.73$ | $h=0.83$ | $n=2100$ | $n=5100$ | $n=6100$ |
| $\hat{\lambda}$ | $-0.0003$ | $-0.0003$ | 0.0001 | $5.3e-05$ | $4.6e-05$ |
| $\hat{A}_1$ | 0.158 | 0.250 | 0.314 | 0.176 | 0.175 |
| $\hat{B}_1$ | 0.587 | 0.643 | 0.536 | 0.617 | 0.621 |
| $\hat{A}_2$ | 0.811 | 0.754 | 0.515 | 0.736 | 0.740 |
| $\hat{B}_2$ | 0.303 | 0.344 | 0.370 | 0.340 | 0.346 |
| $\hat{\delta}$ | 0.977 | 0.834 | 0.974 | 0.944 | 0.932 |
| RMSE | 6.083 | 6.077 | 9.837 | 11.206 | 10.993 |
| | (0.681) | (0.899) | (5.216) | (5.538) | (3.015) |

Table 4.11: The performance of $\hat{\theta}_n$ concerning model (2.1), and considered $n$ and $h$; just for comparison. The RMSE of the train is given with the RMSE of the test in parenthesis

| $\hat{\theta}_n$ | Quads, $n=3000$ | | Smir, $n=4000$ | | Boussafou, $n=4000$ | |
|---|---|---|---|---|---|---|
| | $h=0.002$ | $h=0.003$ | $h=0.002$ | $h=0.003$ | $h=0.002$ | $h=0.003$ |
| $\hat{\lambda}$ | 0.070 | 0.047 | 0.013 | 0.009 | 0.055 | 0.036 |
| $\hat{A}_1$ | 0.191 | 0.192 | 0.186 | 0.184 | 0.147 | 0.184 |
| $\hat{B}_1$ | 0.156 | 0.160 | 0.177 | 0.156 | 0.162 | 0.154 |
| $\hat{A}_2$ | 0.681 | 0.708 | 0.721 | 0.692 | 0.702 | 0.698 |
| $\hat{B}_2$ | 0.412 | 0.432 | 0.454 | 0.441 | 0.457 | 0.423 |
| $\hat{\delta}$ | 0.145 | 0.095 | 0.102 | 0.152 | 0.110 | 0.166 |
| RMSE | 8817.515 | 8817.581 | 4492.407 | 4492.372 | 5144.363 | 5144.285 |
| | (7755.679) | (7756.834) | (4505.368) | (4505.327) | (4443.826) | (4443.972) |

Tetouan city, collected every ten minutes from the supervisory control and data acquisition system of Amendis company which is distributed the energy to the three different source stations located in northern Morocco, namely Quads, Smir and Boussafou. We considered three data of their power consumption. To conclude this Section, the performance of the LSE of the power consumption of Quads, Smir, and Boussafou was analyzed with a train-test split of 90%.

We took the power consumption of Quads in the period January 14, to February 4, 2017; Smir in the period February 11, to March 11, 2017, and Boussafou in the period January 7, to February 4, 2017. Table 4.11 summarizes the results of the performance of $\hat{\theta}_n$ and the RMSE. The test RMSE of Quads increases as the train RMSE; the test RMSE of Smir decreases as the train RMSE; the test RMSE of Boussafou increases as the train RMSE decreases. The model of Quads and Boussafou tend to be underfitting. For Quads and Boussafou; $h=0.003$, we can see from Table 4.12 that the performance of the estimates of both is better than the LADE.

Table 4.12: The performance of $\check{\theta}_n$ concerning model (2.1). The RMSE of the train is given with the RMSE of the test in parenthesis

| $h=0.003$ | $\check{\theta}_n$ | RMSE |
|---|---|---|
| Quads | (0.046, -0.146, 0.335, 0.461, 0.361, 0.226) | 8817.986 (7670.666) |
| Boussafou | (0.043, 0.201, 0.115, 0.686, 0.331, 0.156) | 5194.563 (5041.249) |

## 4.3 Summary of the numerical experiments

From Subsection 4.2.1-4.2.4 we can summarize the following.

1. The salient feature of electricity consumption is seasonality. The hourly electricity load of TEPCO (Subsection 4.2.1) shows that the seasonality of the past electricity demand in the period January 27 to December 8, 2018, can be approximated by a periodic sinusoidal signal processing model $h_t(\beta)$ in the drift of (1.1). Further, the proposed model (2.1) can be used for medium-term forecasting using hour-by-hour Japan electricity load data.

2. A ten-minute sampling of appliances' energy consumption has been used in Belgium households (Subsection 4.2.2). The results identify the seasonal energy use of appliances in a low-energy house for a medium-term problem, say, the period January 18 to May 27, 2016. We suspect that the impressive performance of the periodicity of $h_t(\beta)$ is improved with the use of a large dataset. Our results confirm the findings in references [Taylor et al., 2006] and [Gould et al., 2008], that is, the use of the periodic model needed a longer time series to estimate the periodicity in the parameter, in our case, particularly in view of a ten-minute sampling dataset measurement in medium-term forecasting problems.

3. The results of electric power in Subsection 4.2.3 indicate that the seasonality of the one-minute sampling rate of the reactive energy consumed for December 16 to December 17, 2006, can be approximated by a periodic sinusoidal signal. Whereas, the seasonality of the one-minute sampling rate of electric power consumption in the kitchen and laundry room in the periods December 16 to December 20, 2006, can be approximated by (2.1) with the same periodicity. Seasonality identification to manage building electrification also has mentioned in [Buonocore et al., 2022], that is, the study proposed renewable energy and seasonal energy storage by identifying the building electrification seasonality of the electricity demand. The numerical studies confirm that the seasonality of a time-inhomogeneous Ornstein–Uhlenbeck process led to a good result for very short-term forecasting using minute-by-minute data.

4. In the given periods, the seasonality of power consumption of Quads and Boussafou (Subsection 4.2.4) has similarities. This evidence is supported by the seasonality of ten minutes of power consumption can be approximated by (2.1) with the same periodic sinusoidal signal processing model. Furthermore, [Salam and El Hibaoui, 2018] confirms the similarities because of the hot weather and vacation time. The results also confirm that the seasonality of a time-inhomogeneous Ornstein–Uhlenbeck process can be used for short-term forecasting with ten-minute-by-ten-minute data.

From the numerical experiments, we can deduce the following.

- In the computational comparisons, the performance of the LSE is better than the LADE;
- The proposed model (2.1) can capture the seasonal variation in very short-term to medium-term horizon forecasts. The performance of the estimates is very satisfactory for very short-term problems. We presume this happens because of the sensitivity of the periodic sinusoidal signal processing model in approaching the process, therefore, we should take care in applying the model to the new systems in each term horizon forecast.

# Chapter 5

# Summary and Future Works

In this thesis, we began by briefly discussing the difficulties in performing least-squares inference of $\theta=(\lambda,A,B,\delta)$ for observations modeled by the time-inhomogeneous signal processing model in the drift of Ornstein–Uhlenbeck process. Many of these difficulties are caused by the fact that, although the models exist in continuous time, the data are necessarily observed discretely in time in practice. Since $h_t(\beta)$ is a periodic sinusoidal signal, we use quantization to process a continuous-time sinusoidal signal into a sequence of numbers, and Euler–Maruyama discretization of the model. The sinusoidal processing model has been used in analyzing seasonal phenomena. We consider a periodic sinusoidal signal whose is modeled by the $k$th harmonic of components $\cos(\omega_k t)$ and $\sin(\omega_k t)$ to have the same periodicity for $\omega_k\equiv 2\pi k\delta$. By the periodicity, we can find $(\tilde{Y}_t)_{t\in\mathbb{R}}$ as a stationary solution of $(Y_t)_{t\in\mathbb{R}_+}$. The stationarity is easily relaxed since we employ that the sinusoidal signal is periodic. However, it is straightforward to generalize the model set, so it applies to the model where the continuous-time sinusoidal signal model is non-periodic.

The presence of frequency component with other parameters, namely $(\lambda,A,B)$ adds to the complexity of providing evidence of consistency. One of the research results that reveal this uniqueness is in [Kundu and Nandi, 2012], which shows the consistency $(A,B,\omega)$ in separate ways; say, Lemma 4.1 for consistency $(A,B)$ and Lemma 4.3 for consistency $\omega$. We obtain the convergence of the parameters at rate $\sqrt{nh}$, except for the frequency $\delta$ at $\sqrt{n^3h^3}$. Ibragimov and Has'minskii [Ibragimov and Hasâ€™minskii, 1981] treated $dY_t=\sin(\theta t)dt+dW_t$ when the sample path is continuously observed on $[0,T]$, and it is proved that the rate of estimation for $\theta$ is $\sqrt{T^3}$. This result is the same for discrete-time sinusoidal signal (see [Kundu, 1993]). We presume the rate convergence of frequency is the same under the same condition, that is, the noise term [Ziskind and Wax, 1988] has mean zero and finite variance; the sinusoidal processing model $\sum_{k=1}^{K}[A_k\cos(\omega_k t)+B_k\sin(\omega_k t)]$ is a periodic continuous-time signal. In this respect, it is interesting to study further that the rate for $\delta$ is the same as in the problem of frequency estimation without mean-reversion assumption with periodic or non-periodic sinusoidal signal, say,

$$dY_t=\sum_{k=1}^{K}[A_k\cos(\omega_k t)+B_k\sin(\omega_k t)]dt+dw_t.$$

Also, we can set other drift functions as a part of the one-factor mean-reverting model, such as

$$dY_t = \Big(-\lambda Y_t + \lambda h_t(\beta) + \frac{d}{dt} h_t(\beta)\Big) dt + dw_t,$$

with (1.2); and

$$X_t = \exp(f_t + Y_t),$$

with the deterministic function

$$f_t = \gamma_0 + \gamma_1 H_t + \gamma_2 P_t + \gamma_3 S_t,$$

where

- $H_t = 1$, if the % relative humidity (r.h) is between $30-60\%$, $H_t = 0$ otherwise;
- $P_t = 1$, if the temperature is between $15^0$C-$24^0$C, $P_t = 0$ otherwise;
- $S_t = 1$, if the wind speed is between $2-10.5$ m/s, $S_t = 0$ otherwise,

and $Y_t$ is defined in (2.1).

The least-squares methods only infer the estimators of the drift, therefore, one can extend the procedure proposed by [Katsamaki and Skiadas, 1995] to estimate the parameters of the diffusion. In all the development of the thesis assumed that the number of components $K$ is known in advance. Moreover, the estimation of the number of components $K$ can be considered a model selection problem. In some literature studies, several approaches can be done to estimate the number of components, namely the likelihood ratio approach, and information-theoretic criterion (see[Kundu and Nandi, 2005, Kundu and Mitra, 2000] for references to the number of components of a discrete-time sinusoidal signal).

A special case of interest is when the process is in the state-space form (e.g., [Hamilton, 2020], [Shumway et al., 2000]), that is,

$$Y_t = y_0 + \int_0^t (-\lambda Y_s + h_s(\beta)) ds + A_t \alpha_t + \sigma w_t, \tag{5.1}$$

with an unobserved process

$$\alpha_t = \Psi \alpha_{t-1} + \zeta_t, \tag{5.2}$$

where $\zeta_t \sim \mathcal{NID}(0, Q_t)$, and initial state distribution $\alpha_1 \sim \mathcal{N}(a_1, P_1)$, $a_1, P_1$ are fixed and known but can be generalized. Concerning seasonality, it is interesting to study further that (5.1) can capture the seasonality in the periodicity representation and non-periodic seasonal components in the state equation (5.2). Moreover, we can compare the performance of SDE (2.1) and (5.1) in the electric power and energy systems forecast.

A class of models that can capture a time variation is the periodic model, while the features of seasonality that appear as a periodic pattern are common at least with daily and weekly series (see [El-Hawary, 2017], [Heston and Sadka, 2008], and [Kundu and Nandi, 2012]). Further, the behavior of an electric power system load depends on time, weather, or other random disturbances.

Time factors include weekly periodicity and seasonal variations. In this thesis, practical experiments were conducted in Section 4.2 which confirms that the proposed model (2.1) with the periodic continuous-time sinusoidal signal can be used to capture the seasonal variation in very short to medium-term problems. We feel sure that our proposed model is appropriate for long-term forecasting (e.g., in-stock exchange problems). In this view, in addition to the model of [Hirose, 2021] for medium and short-term forecasting, our model (2.1) as a periodic time-inhomogeneous Ornstein–Uhlenbeck process can be used to identify a seasonal variation that appears in a periodicity pattern in all-time horizon forecasts, excluding the long short-term problems.

Interestingly, an important point to note regarding the non-periodic sinusoidal signal capturing irregular (or non-linearity) components that are caused by irregular patterns (see [Djuric and Kay, 1990, Kundu and Nandi, 2008, Lahiri et al., 2012] in the case of discrete-time chirp signal), is that we can consider non-periodic time-inhomogeneous Ornstein–Uhlenbeck model as paving the way to a massive solar energy supply and wind power generation in very short-term forecasting due to the existence of high non-linearity in the systems (e.g., [Hossain et al., 2021], [Dambreville et al., 2014] for references).

In other fields than electric power and energy system, we can apply the Gompertzian model

$$dY_t = (-\lambda \log Y_t + g_t(\alpha))Y_t dt + \sigma Y_t dw_t$$

approach to predicting virus, bacterial, and cancer cell growths (e.g., [Harvey and Kattuman, 2020]). Exogenous factors that affect virus, bacterial, and cancer cell growths, e.g., moisture, pH level, oxygen level, and cell deformability; are included in a time-dependent function $g_t(\alpha) = \alpha_0 + \sum_{i=1}^{q} \alpha_i q_i(t)$.

# Appendix A

# Stationarity

Recall (2.2). We will look for $\{\tilde{Y}_t, t \in \mathbb{R}\}$ as a stationary solution of (2.2). Let us define

$$\tilde{Y}_t = \tilde{q}_t + \tilde{L}_t, \quad t \in \mathbb{R}, \tag{A.1}$$

where

$$\begin{aligned}
\tilde{q}_t &= e^{-\lambda t} \sum_{k=1}^{K} \int_{-\infty}^{t} e^{\lambda \tau} [A_k \cos(\omega_k \tau) + B_k \sin(\omega_k \tau)] d\tau, \\
\tilde{L}_t &= \sigma e^{-\lambda t} \int_{-\infty}^{t} e^{\lambda \tau} d\tilde{w}_\tau.
\end{aligned}$$

Here, $\tilde{w} = \{\tilde{w}_\tau\}_\tau$ is a (bilateral) Wiener process that is defined as in [Peyre, 2017], that is, the increment is adapted to $(\mathcal{F}_\tau)_{\tau \in \mathbb{R}}$, which means, for all $\tau \in \mathbb{R}$,

- for all $u \leq 0$ then $(\tilde{w}_{\tau+u} - \tilde{w}_\tau)$ is $\mathcal{F}_\tau$-measurable;
- for all $v \geq 0$ then $(\tilde{w}_{\tau+v} - \tilde{w}_\tau)$ is independent from $\mathcal{F}_\tau$.

*Proof of Lemma 2.1.* Let us denote

$$\tilde{Y}_{s-1+t} = \tilde{q}_{s-1+t} + \tilde{L}_{s-1+t}, \quad t \in [0,T], s \in \mathbb{N},$$

where

$$\tilde{q}_{s-1+t} = e^{-\lambda(s-1+t)} \sum_{k=1}^{K} \int_{-\infty}^{s-1+t} e^{\lambda \tau} [A_k \cos(\omega_k \tau) + B_k \sin(\omega_k \tau)] d\tau, \tag{A.2}$$

$$\tilde{L}_{s-1+t} = \sigma e^{-\lambda(s-1+t)} \int_{-\infty}^{s-1+t} e^{\lambda \tau} d\tilde{w}_\tau. \tag{A.3}$$

First, we observe (A.2).

- For $s = 1$, we have $\tilde{q}_t = \int_0^t e^{-\lambda t} e^{\lambda \tau} h_\tau(\beta) d\tau$. A periodic signal is fully identified by its behavior in a single period $[\upsilon_0, \upsilon_0 + T_0]$, where $\upsilon_0$ is arbitrary. The area of periodic signal $S_t$ given by $area(S) = \int_{t_0}^{t_0+T_0} S_t dt$ [Cariolaro, 2011a]. Since we have (1.4), there exists $T > 0$

such that the signal $h_t(\beta)$ in (1.3) is periodic (1.5). Therefore, by using (2.4), we obtain

$$\tilde{q}_T = \int_0^T e^{-\lambda T} e^{\lambda\tau} h_\tau(\beta) d\tau =: S_T^0(\theta) = \mu_T(\theta),$$

where

$$\mu_T(\theta) = \sum_{k=1}^{K} \left[\frac{\omega_k}{\omega_k^2 + \lambda^2}\right] \left\{ \sin(\omega_k T) \left[\frac{\lambda B_k}{\omega_k} + A_k\right] + \cos(\omega_k T) \left[\frac{\lambda A_k}{\omega_k} - B_k\right] - e^{-\lambda T} \left[\frac{\lambda A_k}{\omega_k} - B_k\right] \right\}.$$

- For $s = 2$,

$$\tilde{q}_{1+t} \;=\; e^{-\lambda(1+t)} \int_0^1 e^{\lambda\tau} h_\tau(\beta) d\tau + e^{-\lambda} \int_1^{1+t} e^{-\lambda t} e^{\lambda\tau} h_\tau(\beta) d\tau.$$

  Further, there exists $T > 0$, such that

$$\tilde{q}_{1+T} \;=\; e^{-\lambda(1+T)} \int_0^1 e^{\lambda\tau} h_\tau(\beta) d\tau + e^{-\lambda} S_T^1(\theta),$$

  where $S_T^1(\theta) := \int_1^{1+T} e^{-\lambda T} e^{\lambda\tau} h_\tau(\beta) d\tau$.

  Thus, for $s \in \mathbb{N}$, $t \in [0,T]$, there exists $T > 0$ such that

$$\begin{aligned} \tilde{q}_{s-1+T} &= e^{-\lambda(s-1+T)} \int_0^{s-1} e^{\lambda\tau} h_\tau(\beta) d\tau + \int_{s-1}^{s-1+T} e^{-\lambda(s-1+T)} e^{\lambda\tau} h_\tau(\beta) d\tau \\ &= e^{-\lambda(s-1+T)} \int_0^{s-1} e^{\lambda\tau} h_\tau(\beta) d\tau + e^{-\lambda(s-1)} S_T^{s-1}(\theta), \end{aligned} \quad \text{(A.4)}$$

  where $S_T^{s-1}(\theta) := \int_{s-1}^{s-1+T} e^{-\lambda T} e^{\lambda\tau} h_\tau(\beta) d\tau$; it assures that (A.2) is stationary.

We now turn to (A.3). Denote

$$\tilde{L}_{s-1+t} = \tilde{L}_{1,s-1+t} + \tilde{L}_{2,s-1+t},$$

where

$$\begin{aligned} \tilde{L}_{1,s-1+t} &= \sigma e^{-\lambda(s-1+t)} \int_{-\infty}^{s-1} e^{\lambda\tau} d\tilde{w}_\tau, \\ \tilde{L}_{2,s-1+t} &= \sigma e^{-\lambda(s-1+t)} \int_{s-1}^{s-1+t} e^{\lambda\tau} d\tilde{w}_\tau. \end{aligned}$$

Observe that

- $$\tilde{L}_{1,s-1+t} = \sigma e^{-\lambda(s-1+t)} \int_{-\infty}^{s-1} e^{\lambda\tau} d\tilde{w}_\tau = \sigma \sum_{i=-\infty}^{0} e^{-\lambda((1-i)+t)} \int_0^1 e^{\lambda\tau} d\tilde{w}_\tau. \quad \text{(A.5)}$$

If $C[0,T]$ denotes the space of all continuous functions from $[0,T]$ to $\mathbb{R}$, then

$$\tau:[0,T]\mapsto C[0,T]; \quad \tau\mapsto\left\{\tilde{w}_{(1-i)+\tau}\Big(u\mapsto\tilde{Y}_{(1-i)+\tau}(u), i\in(-\infty,0]\Big)-\tilde{w}_{\tau}\Big(u\mapsto\tilde{Y}_{\tau}(u)\Big)\right\}.$$

Hence, for all $\tau\in[0,T]$, there exists a stationary increment $\tilde{w}=\{\tilde{w}_{\tau}\}_{\tau\in[0,T]}$ whose increments are adapted to $\mathcal{F}_{\tau}$, namely

- for all $(1-i)\leq 0$ then $\{\tilde{w}_{(1-i)+\tau}-\tilde{w}_{\tau}\}$ is $\mathcal{F}_{\tau}$-measurable;
- for all $(1-i)\geq 0$ then $\{\tilde{w}_{(1-i)+\tau}-\tilde{w}_{\tau}\}$ is independent from $\mathcal{F}_{\tau}$.

- Further, observe that

$$\tilde{L}_{2,s-1+t}=\sigma e^{-\lambda(s-1+t)}\int_{s-1}^{s-1+t}e^{\lambda\tau}d\tilde{w}_{\tau}=\sigma e^{-\lambda t}\int_{0}^{t}e^{\lambda\tau}d\tilde{w}_{\tau}. \tag{A.6}$$

We have

$$\tau:[0,T]\mapsto C[0,T]; \quad \tau\mapsto\left\{\tilde{w}_{(s-1)+\tau}\Big(u\mapsto\tilde{Y}_{(s-1)+\tau}(u); s\geq 1, s\in\mathbb{N}\Big)-\tilde{\omega}_{\tau}(u\mapsto\tilde{Y}_{\tau}(u))\right\}.$$

Therefore, for all $\tau\in[0,T]$, there exists a stationary increment $\tilde{w}=\{\tilde{w}_{\tau}\}_{\tau\in[0,T]}$ which is adapted to $\mathcal{F}_{\tau}$, that is, for all $s\geq 1, s\in\mathbb{N}$ then $\{\tilde{w}_{(s-1)+\tau}-\tilde{w}_{\tau}\}$ is independent from $\mathcal{F}_{\tau}$. Hence, it follows that for all $t\in[0,T]$, the sequence $\{\tilde{Y}_{s-1+t}\}_{t\in[0,T],s\in\mathbb{N}}$ is stationary.

□

From Lemma 2.1, it follows that for any continuous real-valued function $\phi(.)$ with polynomial growth, satisfying $\mathbb{E}_0[|\phi(y_0)|]<\infty$,

$$\frac{1}{T}\int_{0}^{T}\phi(\tilde{Y}_t)dt\xrightarrow{p}\mathbb{E}_0[\phi(y_0)].$$

Obviously, because of the periodicity of $h_t(\beta)$ and Lemma 2.1 imply that

$$\frac{1}{T_n}\int_{0}^{T_n}\phi(\tilde{Y}_t)dt\xrightarrow{p}\mathbb{E}_0[\phi(y_0)]. \tag{A.7}$$

*Proof of Lemma 2.2.* Recalling $\tilde{Y}_t$ and $Y_t$,

$$\begin{aligned}&|\tilde{Y}_t-Y_t|\\&=\left|\tilde{q}_t+\tilde{L}_t-\left(e^{-\lambda t}y_0+e^{-\lambda t}\int_{0}^{t}e^{\lambda\tau}h_t(\beta)d\tau+\sigma e^{-\lambda t}\int_{0}^{t}e^{\lambda\tau}dw_{\tau}\right)\right|\\&\leq\left|\frac{y_0}{e^{\lambda t}}\right|+\left|e^{-\lambda t}\left(\int_{-\infty}^{t}e^{\lambda\tau}h_{\tau}(\beta)d\tau-\int_{0}^{t}e^{\lambda\tau}h_{\tau}(\beta)d\tau\right)\right|+\left|\sigma e^{-\lambda t}\left(\int_{-\infty}^{t}e^{\lambda\tau}d\tilde{w}_{\tau}-\int_{0}^{t}e^{\lambda\tau}dw_{\tau}\right)\right|.\end{aligned}$$

Therefore, we have $|\tilde{Y}_t-Y_t|\xrightarrow{a.s.}0$ as $t\to\infty$ (see Lemma 4.3 and Lemma 4.4 of [Dehling et al., 2010] for reference). □

Since we have

$$\int_0^{T_n} \phi(\tilde{Y}_t)dt = \lim_{h\to 0}\sum_{j=1}^{n}\phi(\tilde{Y}_{t_j})h$$

that implies

$$\frac{h}{T_n}\sum_{j=1}^{n}\phi(\tilde{Y}_{t_j}) \xrightarrow{p} \frac{1}{T_n}\int_0^{T_n}\phi(\tilde{Y}_t)dt,$$

then by (A.7), we get

$$\frac{1}{n}\sum_{j=1}^{n}\phi(\tilde{Y}_{t_j}) \xrightarrow{p} \mathbb{E}_0[\phi(y_0)]. \tag{A.8}$$

Together with Lemma 2.2 and (A.8), the expression (2.6) follows.

# Appendix B

# Supplement of Section 3.2

Minimizing (3.4) with respect to $(\lambda,A,B)$ yields the LSE of $(\lambda,A,B)$. We first compute the explicit form of the LSE. By the first derivative of (3.4) and Lemma 3.1, we have

$$-\sum_{j=1}^{n}(\Delta_j Y+h\hat{\lambda}Y_{t_{j-1}})\cos(\omega_K t_{j-1})+h\sum_{j=1}^{n}\sum_{k=1}^{K}\Big[\hat{A}_k\cos(\omega_k t_{j-1})+\hat{B}_k\sin(\omega_k t_{j-1})\Big]\cos(\omega_K t_{j-1})=0$$
$$-\sum_{j=1}^{n}(\Delta_j Y+h\hat{\lambda}Y_{t_{j-1}})\cos(\omega_K t_{j-1})+\frac{nh}{2}\hat{A}_K=0,$$

Hence

$$\hat{A}_{K,n}=\frac{2}{T_n}\sum_{j=1}^{n}(\Delta_j Y+h\hat{\lambda}Y_{t_{j-1}})\cos(\omega_K t_{j-1}). \tag{B.1}$$

Similarly, we find

$$\hat{B}_{K,n}=\frac{2}{T_n}\sum_{j=1}^{n}(\Delta_j Y+h\hat{\lambda}Y_{t_{j-1}})\sin(\omega_K t_{j-1}). \tag{B.2}$$

Now, we turn to $\hat{\lambda}_n$. We have

$$\sum_{j=1}^{n}\Delta_j YY_{t_{j-1}}+h\hat{\lambda}\sum_{j=1}^{n}Y_{t_{j-1}}^2-h\sum_{j=1}^{n}\sum_{k=1}^{K}[\hat{A}_k\cos(\omega_k t_{j-1})+\hat{B}_k\sin(\omega_k t_{j-1})]Y_{t_{j-1}}=0$$
$$\sum_{j=1}^{n}\Delta_j YY_{t_{j-1}}+h\hat{\lambda}\sum_{j=1}^{n}Y_{t_{j-1}}^2-h\sum_{j=1}^{n}\Bigg\{\frac{2}{T_n}\sum_{j=1}^{n}(\Delta_j Y+\hat{\lambda}hY_{t_{j-1}})\cos^2(\omega_1 t_{j-1})+\frac{2}{T_n}\sum_{j=1}^{n}(\Delta_j Y+\hat{\lambda}hY_{t_{j-1}})\sin^2(\omega_1 t_{j-1})$$
$$+\cdots+\frac{2}{T_n}\sum_{j=1}^{n}(\Delta_j Y+\hat{\lambda}hY_{t_{j-1}})\cos^2(\omega_K t_{j-1})+\frac{2}{T_n}\sum_{j=1}^{n}(\Delta_j Y+\hat{\lambda}hY_{t_{j-1}})\sin^2(\omega_K t_{j-1})\Bigg\}Y_{t_{j-1}}=0,$$

therefore,

$$\hat{\lambda}_n=D\frac{\sum_{j=1}^{n}(\Delta_j Y)Y_{t_{j-1}}}{h\sum_{j=1}^{n}Y_{t_{j-1}}^2}, \tag{B.3}$$

where $D=\frac{2K-1}{1-2K}$, $K\in\mathbb{N}$. Inserting (B.1), (B.2) and (B.3) into (3.4); applying Lemma 3.1, leads to (3.61), that is,

$$\begin{aligned}\mathbb{Q}_n^*(\delta) &= \frac{1}{h}\sum_{j=1}^{n}\left\{\left(\Delta_j Y+\hat{\lambda}hY_{t_{j-1}}\right)-\left(h\sum_{k=1}^{K}\left[\hat{A}_k\cos(\omega_k t_{j-1})+\hat{B}_k\sin(\omega_k t_{j-1})\right]\right)\right\}^2\\ &= \frac{1}{h}\sum_{j=1}^{n}\left(\Delta_j Y+\hat{\lambda}hY_{t_{j-1}}\right)^2-2\frac{nh}{2}\sum_{k=1}^{K}\left[\hat{A}_k^2+\hat{B}_k^2\right]+\frac{nh}{2}\sum_{k=1}^{K}\left[\hat{A}_k^2+\hat{B}_k^2\right]\\ &= \frac{1}{h}\sum_{j=1}^{n}\left(\Delta_j Y+\hat{\lambda}hY_{t_{j-1}}\right)^2-I_n(\delta). \qquad \text{(B.4)}\end{aligned}$$

Therefore, we get (3.62). The function $I_n(\delta)$ (3.64) known as periodogram (see [Stoica and Moses, 1997] for reference). We can see that the LSE of $(\lambda,A,B)$ is obtained by minimizing (3.4) which is equivalent to maximizing (3.64).

Next, we turn to the expression of (3.70) and (3.71). Recall (3.69), and observe (for e.g., the cosine term),

$$\frac{1}{n^3h}\sum_{k=1}^{K}\left[\sum_{j=1}^{n}\varphi_{j-1}\cos(\omega_k t_{j-1})\right]^2=\frac{1}{n^3h}\sum_{k=1}^{K}\sum_{j=1}^{n}\varphi_{j-1}^2\cos^2(\omega_k t_{j-1})+\varphi_n^*(\omega).$$

By applying Lemma 3.3, and $\psi_i:=\varphi_i\varphi_{i-1}$, we obtain the term $\varphi_n^*(\omega)$ as

$$\begin{aligned}&\varphi_n^*(\omega)\\ &=\frac{2}{n^3h}\sum_{k=1}^{K}\left\{\sum_{j=1}^{n-1}\psi_j\cos(\omega_k t_j)\cos(\omega_k t_{j-1})+\cdots+\sum_{j=1}^{n-r}\psi_{j+r-1}\cos(\omega_k t_{j+r-1})\cos(\omega_k t_{j-1})\right\}\\ &=\frac{1}{n^3h}\sum_{k=1}^{K}\left\{\sum_{j=1}^{n-1}\psi_j(\cos(\omega_k[t_j-t_{j-1}])+\cos(\omega_k[t_j+t_{j-1}]))+\ldots\right.\\ &\left.+\sum_{j=1}^{n-r}\psi_{j+r-1}(\cos(\omega_k[t_{j-1}-t_{j+r-1}])+\cos(\omega_k[t_{j-1}+t_{j-1}]))\right\}\\ &=\frac{1}{n^3h}\sum_{k=1}^{K}\left\{(n-1)\left(\cos(\omega_k h)\frac{1}{n-1}\sum_{j=1}^{n-1}\psi_j\right)+(n-1)\frac{1}{n-1}\sum_{j=1}^{n-1}\psi_j\cos(\omega_k[t_j+t_{j-1}])\right.\\ &\left.+\cdots+(n-r)\left(\cos(\omega_k h)\frac{1}{n-r}\sum_{j=1}^{n-r}\psi_{j+r-1}\right)+(n-r)\frac{1}{n-r}\sum_{j=1}^{n-r}\psi_{j+r-1}\cos(\omega_k[t_{j+r-1}+t_{j-1}])\right\}.\end{aligned}$$

There exists $\psi(.)$ that satisfying $\mathbb{E}_0[|\psi(y_0)|]<\infty$, such that, for $r$ is an arbitrary element of $\mathbb{N}$ with $r<n$,

$$\frac{1}{n-r}\sum_{j=1}^{n-r}\psi_j\xrightarrow{p}\mathbb{E}_0[\psi(y_0)].$$

Also, with the following lemma that is proved in a similar way to Lemma 3.3, we get $\varphi_n^*(\omega)=o_p\left(\frac{1}{nT_n}\right)$.

**Lemma B.1.** *We have*

$$\sup_{\omega}\left|\frac{1}{n}\sum_{j=1}^{n}Y_{t_j}\cos(\omega[t_j+t_{j-1}])\right|\xrightarrow{p}0 \quad as \quad n\to\infty,$$

With similar arguments for the sine term, we have

$$\frac{1}{n^3h}\sum_{k=1}^{K}\left[\sum_{j=1}^{n}\varphi_{j-1}\sin(\omega_k t_{j-1})\right]^2=\frac{1}{n^3h}\sum_{k=1}^{K}\left[\sum_{j=1}^{n}\varphi_{j-1}^2\sin^2(\omega_k t_{j-1})\right]+o_p\left(\frac{1}{nT_n}\right).$$

Hence, we can obtain

$$\begin{aligned}\tilde{f}_n(\delta) &= \frac{1}{n^3h}\sum_{k=1}^{K}\sum_{j=1}^{n}\Big\{\Big(\varphi_{j-1}^2\cos^2(\omega_k t_{j-1})-\varphi_{0,j-1}^2\cos^2(\omega_{0,k}t_{j-1})\Big)\\ &+ \Big(\varphi_{j-1}^2\sin^2(\omega_k t_{j-1})-\varphi_{0,j-1}^2\sin^2(\omega_{0,k}t_{j-1})\Big)\Big\}+o_p\left(\frac{1}{nT_n}\right).\end{aligned}$$

Look for the cosine term; we have

$$\begin{aligned}&\frac{1}{n^3h}\sum_{k=1}^{K}\sum_{j=1}^{n}\Big\{\varphi_{j-1}^2\cos^2(\omega_k t_{j-1})-\varphi_{0,j-1}^2\cos^2(\omega_{0,k}t_{j-1})\Big\}\\ &=\frac{1}{n^3h}\sum_{k=1}^{K}\sum_{j=1}^{n}\Big\{\varphi_{j-1}\cos(\omega_k t_{j-1})-\varphi_{0,j-1}\cos(\omega_{0,k}t_{j-1})\Big\}^2-2\varphi_{0,j-1}^2\cos^2(\omega_{0,k}t_{j-1})\\ &+2\varphi_{j-1}\varphi_{0,j-1}\cos(\omega_k t_{j-1})\cos(\omega_{0,k}t_{j-1}),\end{aligned}$$

and then, combining with the sine term that has a similar form, we obtain

$$\begin{aligned}\tilde{f}_n(\delta) &= \frac{1}{n^3h}\sum_{k=1}^{K}\sum_{j=1}^{n}\Big\{[\varphi_{j-1}\cos(\omega_k t_{j-1})-\varphi_{0,j-1}\cos(\omega_{0,k}t_{j-1})]^2\\ &+ [\varphi_{j-1}\sin(\omega_k t_{j-1})-\varphi_{0,j-1}\sin(\omega_{0,k}t_{j-1})]^2\Big\}-\varsigma_{1,n}+\varsigma_{2,n},\end{aligned}$$

where

$$\varsigma_{1,n}=\frac{2}{n^3h}\sum_{k=1}^{K}\sum_{j=1}^{n}\varphi_{0,j-1}^2\Big[\cos^2(\omega_{0,k}t_{j-1})+\sin^2(\omega_{0,k}t_{j-1})\Big],$$

$$\varsigma_{2,n}=\frac{2}{n^3h}\sum_{k=1}^{K}\sum_{j=1}^{n}\varphi_{j-1}\varphi_{0,j-1}[\cos(\omega_k t_{j-1})\cos(\omega_{0,k}t_{j-1})+\sin(\omega_k t_{j-1})\sin(\omega_{0,k}t_{j-1})].$$

We find $\varsigma_{1,n}$ as follows:

$$\varsigma_{1,n}=\frac{2K}{nT_n}\frac{1}{n}\sum_{j=1}^{n}\varphi_{0,j-1}^2=o_p\left(\frac{1}{nT_n}\right).$$

Again, for $\varsigma_{2,n}$, similar to the discussion of $\psi_i$ above, and with the following Corollary

B.2, we get

$$\varsigma_{2,n} = o_p\left(\frac{1}{nT_n^2}\right).$$

**Corollary B.2.** *For $\omega \neq \omega_0$,*

$$\left|\frac{1}{n}\sum_{j=1}^{n}\varphi_j \cos(\omega t_j)\cos(\omega_0 t_j)\right| \xrightarrow{p} 0 \quad as \quad n \to \infty, \tag{B.5}$$

*Proof.* Using Lemma 3.1, we obtain

$$\mathbb{E}_0\left[\left|\frac{1}{n}\sum_{j=1}^{n}\varphi_j \cos(\omega t_j)\cos(\omega_0 t_j)\right|\right] \leq o\left(\frac{1}{T_n}\right)$$

□

Therefore, we can obtain (3.71).

Now, we turn to $\sum_{j=1}^{n}\mathbb{E}_0^{j-1}\left[\left(\tilde{f}_{1,j}^n(\delta)+\tilde{f}_{2,j}^n(\delta)\right)^2\right]$.

$$\sum_{j=1}^{n}\mathbb{E}_0^{j-1}\left[\left(\tilde{f}_{1,j}^n(\delta)+\tilde{f}_{2,j}^n(\delta)\right)^2\right] = \frac{1}{n^6h^2}\sum_{j=1}^{n}\left(q_{1,j}^K(\delta)+q_{2,j}^K(\delta)\right)^2, \tag{B.6}$$

where

$$q_{1,j}^K(\delta) = \sum_{k=1}^{K}[\varphi_{j-1}\cos(\omega_k t_{j-1}) - \varphi_{0,j-1}\cos(\omega_{0,k} t_{j-1})]^2, \tag{B.7}$$

$$q_{2,j}^K(\delta) = \sum_{k=1}^{K}[\varphi_{j-1}\sin(\omega_k t_{j-1}) - \varphi_{0,j-1}\sin(\omega_{0,k} t_{j-1})]^2. \tag{B.8}$$

We use the following results from Lemma 3.1, that is,

$$\frac{1}{n}\sum_{j=1}^{n}\cos^4(\omega t_j) = \frac{3}{2} + o\left(\frac{1}{T_n}\right),$$

$$\frac{1}{n}\sum_{j=1}^{n}\cos^3(\omega t_j)\cos(\omega_0 t_j) = o\left(\frac{1}{T_n^2}\right), \quad \omega \neq \omega_0.$$

Therefore, we obtain

$$\frac{1}{n^6h^2}\sum_{j=1}^{n}\left(q_{1,j}^K(\delta)\right)^2 = O\left(\frac{1}{n^2T_n^2}\right),$$

and

$$\frac{1}{n^6h^2}\sum_{j=1}^{n}\left(q_{2,j}^K(\delta)\right)^2 = O\left(\frac{1}{n^2T_n^2}\right).$$

Quite similar, we get

$$\frac{1}{n^6h^2}\sum_{j=1}^{n} q_{1,j}^K(\delta)q_{2,j}^K(\delta) = O\left(\max\left(\frac{1}{n^3T_n^2}, \frac{1}{n^2T_n^2}, \frac{1}{nT_n^4}\right)\right).$$

This provides (3.76).

# Appendix C

# Positive semi-definite matrix

We will show the fixed matrix $\mathbf{M}_0$ (3.98) is positive semi-definite, that is, if only if

- $\mathbf{M}_0$ is symmetric,
- $\mathbf{v}^T\mathbf{M}_0\mathbf{v} \geq 0$, for all non zero vector $\mathbf{v} \neq \mathbf{0}$

Since we have (3.98), obviously that $\mathbf{M}_0 = \mathbf{M}_0^T$. Therefore, $\mathbf{M}_0$ is symmetric. From the second-derivative of (3.4), and also Lemma 3.13, we can express $\partial_\theta^2 \mathbf{Q}_n(\theta_0)$ the $(2K+2)\times(2K+2)$ matrix as

$$\partial_\theta^2 \mathbf{Q}_n(\theta_0) = \Big[\partial_\theta \mathbf{a}^T(\theta_0)\partial_\theta \mathbf{a}(\theta_0)\Big].$$

For any non zero $(2K+2)\times 1$ vector $\mathbf{v}$,

$$\begin{aligned}
\mathbf{v}^T\mathbf{M}_0(\theta_0)\mathbf{v} &= \mathbf{v}^T\Big[\mathbf{D}_n^{-1}\partial_\theta^2\mathbf{Q}_n(\theta_0)\mathbf{D}_n^{-1}\Big]\mathbf{v} \\
&= \mathbf{v}^T\Big[\mathbf{D}_n^{-1}\partial_\theta\mathbf{a}^T(\theta_0)\partial_\theta\mathbf{a}(\theta_0)\mathbf{D}_n^{-1}\Big]\mathbf{v} \\
&= \Big[\mathbf{v}^T(\mathbf{D}_n^{-1})^T\partial_\theta\mathbf{a}^T(\theta_0)\Big]\Big[\partial_\theta\mathbf{a}(\theta_0)\mathbf{D}_n^{-1}\mathbf{v}\Big] \\
&= \Big[\partial_\theta\mathbf{a}(\theta_0)\mathbf{D}_n^{-1}\mathbf{v}\Big]^T\Big[\partial_\theta\mathbf{a}(\theta_0)\mathbf{D}_n^{-1}\mathbf{v}\Big] \geq 0.
\end{aligned}$$

Hence, $\mathbf{M}_0(\theta_0)$ is positive semi-definite.

Now, let $L$ is a eigenvalue of $\mathbf{M}_0$ then there exists eigenvector, say, $(2K+2)\times 1$ vector $\mathbf{v}$, $\mathbf{v} \neq \mathbf{0}$ such that

$$\begin{aligned}
\mathbf{M}_0(\theta_0)\mathbf{v} &= L\mathbf{v} \\
\mathbf{v}^T\mathbf{M}_0(\theta_0)\mathbf{v} &= \mathbf{v}^T L\mathbf{v}
\end{aligned}$$

Since $\mathbf{v}^T\mathbf{v} \geq 0$ for all $\mathbf{v}$, then $L$ is non-negative. Further, all the eigenvalues are non-negative.

# Appendix D

# Convexity

Recall (3.4), let us denote $f_j(\theta) := \Delta_j Y - a_{j-1}(\theta)h$. The function $f_j$ is convex if only if its Hessian matrix $\nabla^2 f(\theta)$ is positive definite, for all $\theta \in \Theta$. We will check the convexity of the function (3.4) with respect to $\theta$. Now, from (3.4), we can obtain the gradient and the second derivatives of $f(\theta)$, respectively, as follows

$$\nabla f(\theta) = \frac{2}{h}\sum_{j=1}^{n} f_j(\theta)\nabla f_j(\theta),$$

and

$$\nabla^2 f(\theta) = \frac{2}{h}\left\{\sum_{j=1}^{n} f_j(\theta)\nabla^2 f_j(\theta) + \sum_{j=1}^{n}\nabla f_j(\theta)\nabla f_j(\theta)^T\right\}. \tag{D.1}$$

Observe that the last term of the right-hand side of (D.1), $\sum_{j=1}^{n}\nabla f_j(\theta)\nabla f_j(\theta)^T \geq 0$, and leaving out the term $\sum_{j=1}^{n} f_j(\theta)\nabla^2 f_j(\theta)$ to be checked. For each $j$, we have

$$\partial^2_{A_K\delta} f_j(\theta) = h\tilde{K} t_{j-1}\sin(\omega_K t_{j-1}), \tag{D.2}$$

$$\partial^2_{B_K\delta} f_j(\theta) = -h\tilde{K} t_{j-1}\cos(\omega_K t_{j-1}), \tag{D.3}$$

and

$$\partial^2_{\delta^2} f_j(\theta) = h\tilde{K}^2 t_{j-1}^2[A_K\cos(\omega_K t_{j-1}) + B_K\sin(\omega_K t_{j-1})] \tag{D.4}$$

for any $K \in \mathbb{N}$. Since (D.2)-(D.4) is not always positive, then $\nabla^2 f(\theta)$ is not positive definite. Therefore, the function (3.4) is not convex with respect to $\theta$.

The initial values are sensitive in the simulation study (e.g., the fixed initial values). This is a generally inevitable issue in non-convex optimization, and further consideration of stabilizing the global optimization is beyond the scope of this study. This study does not present evidence that shows the instability of the function with respect to the initial values for numerical optimizations. The stabilizing of the global optimization with the evidence consideration would be interesting for future issues.

# Bibliography


[Abu-Shikhah and Elkarmi, 2011] Abu-Shikhah, N. and Elkarmi, F. (2011). Medium-term electric load forecasting using singular value decomposition. *Energy*, 36(7):4259–4271.

[Aït-Sahalia, 2002] Aït-Sahalia, Y. (2002). Maximum likelihood estimation of discretely sampled diffusions: a closed-form approximation approach. *Econometrica*, 70(1):223–262.

[Alshboul et al., 2022] Alshboul, O., Alzubaidi, M. A., Mamlook, R. E. A., Almasabha, G., Almuflih, A. S., and Shehadeh, A. (2022). Forecasting liquidated damages via machine learning-based modified regression models for highway construction projects. *Sustainability*, 14(10):5835.

[Billingsley, 2013] Billingsley, P. (2013). *Convergence of probability measures*. John Wiley & Sons.

[Brownlee, 2016] Brownlee, J. (2016). *Machine learning mastery with Python: understand your data, create accurate models, and work projects end-to-end*. Machine Learning Mastery.

[Buonocore et al., 2022] Buonocore, J. J., Salimifard, P., Magavi, Z., and Allen, J. G. (2022). Inefficient building electrification will require massive buildout of renewable energy and seasonal energy storage. *Scientific Reports*, 12(1):1–9.

[Candanedo et al., 2017] Candanedo, L. M., Feldheim, V., and Deramaix, D. (2017). Data driven prediction models of energy use of appliances in a low-energy house. *Energy and buildings*, 140:81–97.

[Cariolaro, 2011a] Cariolaro, G. (2011a). Classical signal theory. In *Unified Signal Theory*, pages 17–79. Springer.

[Cariolaro, 2011b] Cariolaro, G. (2011b). *Unified signal theory*. Springer Science & Business Media.

[Chanard et al., 2020] Chanard, K., Métois, M., Rebischung, P., and Avouac, J.-P. (2020). A warning against over-interpretation of seasonal signals measured by the global navigation satellite system. *Nature communications*, 11(1):1–4.

[Chen et al., 2017] Chen, F., Mamon, R., Davison, M., et al. (2017). Inference for a mean-reverting stochastic process with multiple change points. *Electronic Journal of Statistics*, 11(1):2199–2257.

[Dacunha-Castelle and Florens-Zmirou, 1986] Dacunha-Castelle, D. and Florens-Zmirou, D. (1986). Estimation of the coefficients of a diffusion from discrete observations. *Stochastics: An International Journal of Probability and Stochastic Processes*, 19(4):263–284.

[Dambreville et al., 2014] Dambreville, R., Blanc, P., Chanussot, J., and Boldo, D. (2014). Very short term forecasting of the global horizontal irradiance using a spatio-temporal autoregressive model. *Renewable Energy*, 72:291–300.

[Dehling et al., 2010] Dehling, H., Franke, B., and Kott, T. (2010). Drift estimation for a periodic mean reversion process. *Statistical Inference for Stochastic Processes*, 13(3):175–192.

[Djuric and Kay, 1990] Djuric, P. M. and Kay, S. M. (1990). Parameter estimation of chirp signals. *IEEE Transactions on Acoustics, Speech, and Signal Processing*, 38(12):2118–2126.

[El-Hawary, 2017] El-Hawary, M. E. (2017). *Advances in Electric Power and Energy Systems: Load and Price Forecasting*. John Wiley & Sons.

[Florens-Zmirou, 1993] Florens-Zmirou, D. (1993). On estimating the diffusion coefficient from discrete observations. *Journal of applied probability*, 30(4):790–804.

[Fuller, 2009] Fuller, W. A. (2009). *Introduction to statistical time series*, volume 428. John Wiley & Sons.

[Genon-Catalot and Jacod, 1993] Genon-Catalot, V. and Jacod, J. (1993). On the estimation of the diffusion coefficient for multi-dimensional diffusion processes. In *Annales de l'IHP Probabilités et statistiques*, volume 29, pages 119–151.

[Ghosh et al., 2018] Ghosh, H. et al. (2018). gompertz stochastic differential equation growth model with exogenous variables and time-dependent diffusion.

[Giorno et al., 2017] Giorno, V., Román-Román, P., Spina, S., and Torres-Ruiz, F. (2017). Estimating a non-homogeneous gompertz process with jumps as model of tumor dynamics. *Computational Statistics & Data Analysis*, 107:18–31.

[Gould et al., 2008] Gould, P. G., Koehler, A. B., Ord, J. K., Snyder, R. D., Hyndman, R. J., and Vahid-Araghi, F. (2008). Forecasting time series with multiple seasonal patterns. *European Journal of Operational Research*, 191(1):207–222.

[Gross and Galiana, 1987] Gross, G. and Galiana, F. D. (1987). Short-term load forecasting. *Proceedings of the IEEE*, 75(12):1558–1573.

[Gutiérrez et al., 2012] Gutiérrez, R., Gutiérrez-Sanchez, R., et al. (2012). A stochastic gompertz model with logarithmic therapy functions: Parameters estimation. *Applied Mathematics and Computation*, 219(8):3729–3739.

[Gutiérrez et al., 2006] Gutiérrez, R., Gutiérrez-Sánchez, R., and Nafidi, A. (2006). Electricity consumption in morocco: stochastic gompertz diffusion analysis with exogenous factors. *Applied Energy*, 83(10):1139–1151.

[Hamilton, 2020] Hamilton, J. D. (2020). *Time series analysis*. Princeton university press.

[Harvey and Kattuman, 2020] Harvey, A. and Kattuman, P. (2020). Time Series Models Based on Growth Curves With Applications to Forecasting Coronavirus. *Harvard Data Science Review*, (Special Issue 1). https://hdsr.mitpress.mit.edu/pub/ozgjx0yn.

[Heston and Sadka, 2008] Heston, S. L. and Sadka, R. (2008). Seasonality in the cross-section of stock returns. *Journal of Financial Economics*, 87(2):418–445.

[Hirose, 2021] Hirose, K. (2021). Interpretable modeling for short-and medium-term electricity demand forecasting. *Frontiers in Energy Research*, 9:724780.

[Hossain et al., 2021] Hossain, M. A., Chakrabortty, R. K., Elsawah, S., and Ryan, M. J. (2021). Very short-term forecasting of wind power generation using hybrid deep learning model. *Journal of Cleaner Production*, 296:126564.

[Ibragimov and Hasâ€™minskii, 1981] Ibragimov, I. and Hasâ€™minskii, R. (1981). Several estimation problems in a gaussian white noise. In *Statistical Estimation*, pages 321–361. Springer.

[Igual and Seguí, 2017] Igual, L. and Seguí, S. (2017). Introduction to data science. In *Introduction to Data Science*, pages 1–4. Springer.

[Katsamaki and Skiadas, 1995] Katsamaki, A. and Skiadas, C. (1995). Analytic solution and estimation of parameters on a stochastic exponential model for a technological diffusion process. *Applied stochastic models and data analysis*, 11(1):59–75.

[Kessler, 1997] Kessler, M. (1997). Estimation of an ergodic diffusion from discrete observations. *Scandinavian Journal of Statistics*, 24(2):211–229.

[Kundu, 1993] Kundu, D. (1993). Asymptotic theory of least squares estimator of a particular nonlinear regression model. *Statistics & probability letters*, 18(1):13–17.

[Kundu, 1997] Kundu, D. (1997). Asymptotic theory of the least squares estimators of sinusoidal signal. *Statistics: A Journal of Theoretical and Applied Statistics:*, 30(3):221–238.

[Kundu and Mitra, 2000] Kundu, D. and Mitra, A. (2000). Detecting the number of signals for an undamped exponential model using cross-validation approach. *Signal Processing*, 80(3):525–534.

[Kundu and Nandi, 2005] Kundu, D. and Nandi, S. (2005). Estimating the number of components of the fundamental frequency model. *Journal of the Japan Statistical Society*, 35(1):41–59.

[Kundu and Nandi, 2008] Kundu, D. and Nandi, S. (2008). Parameter estimation of chirp signals in presence of stationary noise. *Statistica Sinica*, pages 187–201.

[Kundu and Nandi, 2012] Kundu, D. and Nandi, S. (2012). *Statistical signal processing: frequency estimation*. Springer Science & Business Media.

[Lahiri et al., 2012] Lahiri, A., Kundu, D., and Mitra, A. (2012). Efficient algorithm for estimating the parameters of a chirp signal. *Journal of Multivariate Analysis*, 108:15–27.

[Mangulis, 2012] Mangulis, V. (2012). *Handbook of series for scientists and engineers*. Elsevier.

[Metcalfe and Cowpertwait, 2009] Metcalfe, A. V. and Cowpertwait, P. S. (2009). *Introductory time series with R*. Springer.

[Nichols et al., 2021] Nichols, G. L., Gillingham, E., Macintyre, H., Vardoulakis, S., Hajat, S., Sarran, C., Amankwaah, D., and Phalkey, R. (2021). Coronavirus seasonality, respiratory infections and weather. *BMC infectious diseases*, 21(1):1–15.

[Oppenheim et al., 1997] Oppenheim, A. V., Willsky, A. S., Nawab, S. H., Hernández, G. M., et al. (1997). *Signals & systems*. Pearson Educación.

[Pérez Monsalve and Marín Sanchez, 2017] Pérez Monsalve, J. P. and Marín Sanchez, F. H. (2017). Parameter estimation in mean reversion processes with periodic functional tendency. *arXiv e-prints*, pages arXiv–1710.

[Peyre, 2017] Peyre, R. (2017). Fractional brownian motion satisfies two-way crossing. *Bernoulli*, 23(4B):3571–3597.

[Plosser, 1978] Plosser, C. I. (1978). A time series analysis of seasonality in econometric models. In *Seasonal analysis of economic time series*, pages 365–408. NBER.

[Prakasa Rao, 1983] Prakasa Rao, B. (1983). Asymptotic theory for non-linear least squares estimator for diffusion processes. *Statistics: A Journal of Theoretical and Applied Statistics*, 14(2):195–209.

[Proakis, 2001] Proakis, J. G. (2001). *Digital signal processing: principles algorithms and applications*. Pearson Education India.

[Puech et al., 2019] Puech, T., Boussard, M., Dâ€™Amato, A., and Millerand, G. (2019). A fully automated periodicity detection in time series. In *International Workshop on Advanced Analysis and Learning on Temporal Data*, pages 43–54. Springer.

[Rao and Rubin, 1979] Rao, B. and Rubin, H. (1979). Asymptotic theory for process least squares estimators for diffusion processes. Technical report, PURDUE UNIV LAFAYETTE IND DEPT OF STATISTICS.

[Rice and Rosenblatt, 1988] Rice, J. A. and Rosenblatt, M. (1988). On frequency estimation. *Biometrika*, 75(3):477–484.

[Román-Román et al., 2018] Román-Román, P., Serrano-Pérez, J. J., and Torres-Ruiz, F. (2018). Some notes about inference for the lognormal diffusion process with exogenous factors. *Mathematics*, 6(5):85.

[Salam and El Hibaoui, 2018] Salam, A. and El Hibaoui, A. (2018). Comparison of machine learning algorithms for the power consumption prediction:-case study of tetouan city–. In *2018 6th International Renewable and Sustainable Energy Conference (IRSEC)*, pages 1–5. IEEE.

[Shumway et al., 2000] Shumway, R. H., Stoffer, D. S., and Stoffer, D. S. (2000). *Time series analysis and its applications*, volume 3. Springer.

[Song and Li, 2011] Song, K.-S. and Li, T.-H. (2011). Asymptotics of least squares for nonlinear harmonic regression. *Statistics*, 45(4):309–318.

[Stoica and Moses, 1997] Stoica, P. and Moses, R. L. (1997). *Introduction to spectral analysis*. Pearson Education.

[Taylor et al., 2006] Taylor, J. W., De Menezes, L. M., and McSharry, P. E. (2006). A comparison of univariate methods for forecasting electricity demand up to a day ahead. *International journal of forecasting*, 22(1):1–16.

[TEPCO, 2016] TEPCO (2016). *The electricity demand data on 2016-2022*. Available at `http://tepco.co.jp/en/forecast/html/download-e.html`.

[UCI Machine Learning Repository, 2012] UCI Machine Learning Repository (2012). Individual household electric power consumption data set. `https://archive.ics.uci.edu/ml/datasets/Individual+household+electric+power+consumption`.

[UCI Machine Learning Repository, 2017] UCI Machine Learning Repository (2017). Belgium household energy prediction. `https://archive.ics.uci.edu/ml/datasets/Appliances+energy+prediction`.

[UCI Machine Learning Repository, 2021] UCI Machine Learning Repository (2021). Power consumption of Tetouan city Data Set. `https://archive.ics.uci.edu/ml/datasets/Power+consumption+of+Tetouan+city`. Accessed: 2021-05-08.

[Wang et al., 2013] Wang, S., Feng, J., and Liu, G. (2013). Application of seasonal time series model in the precipitation forecast. *Mathematical and Computer modelling*, 58(3-4):677–683.

[Whittle, 1952] Whittle, P. (1952). The simultaneous estimation of a time series harmonic components and covariance structure. *Trabajos de estadística*, 3(1-2):43–57.

[Yoshida, 1992] Yoshida, N. (1992). Estimation for diffusion processes from discrete observation. *Journal of Multivariate Analysis*, 41(2):220–242.

[Ziskind and Wax, 1988] Ziskind, I. and Wax, M. (1988). Maximum likelihood localization of multiple sources by alternating projection. *IEEE Transactions on Acoustics, Speech, and Signal Processing*, 36(10):1553–1560.